Modeling Operating Speed for Geometric Design Consistency and Safety Assessment of a Two-lane Rural Highway located in Mountainous Terrain

A thesis submitted in partial fulfilment of the requirements

for the award of the degree of

Doctor of Philosophy

in

Civil Engineering

by

Regulus Dominic K Shallam

Under the supervision of

Prof. Mallikarjuna C.

Dr. Anjan Kumar S.

Department of Civil Engineering,

Indian Institute of Technology Guwahati,

Guwahati-781039, Assam, India

December, 2021

Department of Civil Engineering
Indian Institute of Technology Guwahati,
Guwahati-781039, Assam, India

Certificate

This is to certify that the work contained in this thesis entitled '**Modeling Operating Speed for Geometric Design Consistency and Safety Assessment of a Two-lane Rural Highway located in Mountainous Terrain'**, submitted by Regulus Dominic K Shallam (Roll no. 146104043) to the Indian Institute of Technology Guwahati, for the award of degree of Doctor of Philosophy in Civil Engineering, has been carried out under our supervision. The work has not been submitted anywhere for the award of any degree.

Prof. Mallikarjuna C.
Professor
Department of Civil Engineering
Indian Institute of Technology Guwahati,
Guwahati-781039, Assam, India
Date: 17/12/2021

Dr. Anjan Kumar S.
Associate Professor
Department of Civil Engineering
Indian Institute of Technology Guwahati,
Guwahati-781039, Assam, India
Date: 17/12/2021

Declaration

I, Regulus Dominic K Shallam, declare this thesis titled '**Modeling Operating Speed for Geometric Design Consistency and Safety Assessment of a Two-lane Rural Highway located in Mountainous Terrain'**, and the work presented in it has been carried out by me under the supervision of Prof. Mallikarjuna C. and Dr. Anjan Kumar S., Department of Civil Engineering, Indian Institute of Technology Guwahati. The work has not been submitted anywhere for the award of any degree.

Regulus Dominic K Shallam

Department of Civil Engineering

Indian Institute of Technology Guwahati,

Guwahati, Assam, India-781039

Date: 17/12/2021

Acknowledgement

I would like to express my appreciation and heartfelt thanks to my supervisor Prof. Mallikarjuna C., Professor, and my co-supervisor Dr. Anjan Kumar S., Associate Professor, Department of Civil Engineering, Indian Institute of Technology, Guwahati, Assam, India, for their constant supervision, direction, encouragement, and generous support during my research work. Their insightful feedback, enthusiastic cooperation, and motivating interactions served as a powerful motivator for completing this research project. Without their patience, encouragement, and unwavering commitment to this project, conducting research and writing this dissertation would not have been possible.

I am profoundly grateful to the chairman of doctoral committee, Prof. T.L. Ryntathiang, and the committee members Dr. Ravi K. and Dr. B. Deka for their guidance and suggestions on how to improve the quality of my work. I would also like to express my heartfelt gratitude to the Head, Department of Civil Engineering, IIT Guwahati, for his direct and indirect support and encouragement in carrying out my research. I would like to thank the staff for their assistance and support in different ways.

I would like to convey my thanks to all my fellow research scholars Suvin P.V., Pranab Kar, A.V.A. Bharat, and Koustabh Borah, and all my friends who have extended their support and encouragement.

I express my special thanks to my parents, siblings, cousins, and girlfriend for their unwavering love and encouragement.

Regulus Dominic K Shallam

Date: 17/12/2021

Abstract

Safety is one of the important aspects of the roadway design. Operating speed consistency, design speed consistency and driver workload are widely used to assess the geometric design consistency and safety of an alignment. Geometric design consistency can be defined as the conformance of the highway's geometric and operational features with the drivers' expectancy. Among the various measures, operating speed (V_{85}) based consistency measures are commonly used for evaluating a road alignment. A majority of the operating speed models were developed for the plain terrain and these models are not applicable for the roads located in mountainous terrain. Formulation of operating speed models (OSMs) for a complicated highway geometry is a challenging task. The complexity of the alignment due to the superimposition of the horizontal and vertical alignments and a huge variability in the associated geometric parameters create challenges in predicting the operating speed for mountainous terrain.

The objective of this study was to develop the operating speed models for evaluating the geometric design consistency of a two-lane rural highway passing through mountainous terrain. Speed data were collected from eighty-six horizontal curves of the Shillong bypass, located in Meghalaya, India. Data were collected using radar gun and V-Box equipped test vehicles. The data analysis showed that the operating speeds at the start, middle, and end of the curve were statistically the same at a majority of the sampled curves. However, the operating speed of passenger cars, empty and loaded trucks were found to be statistically different, hence separate models were developed for all the three vehicle types. The applicability of the existing operating speed models developed for the highways passing through mountainous terrains was investigated. It was found that, most of the important geometric variables related to these models were not statistically significant, and the MAPE values were high. This study hypothesised that a single model would be incapable of predicting the operating speed observed at the horizontal curves superimposed with the vertical alignment and a further understanding of the driver's perception was needed.

Drivers' speed choice on a curve depends on their perception of the safety offered by that particular geometric element. Perception is a latent variable and is difficult to measure from the field. This study assumed that the speed and path radius adopted by the drivers while traversing the curves reflected the perception. Analysis of the speed variability and the difference between path radius and curve radius showed that the curve direction and superimposed horizontal and vertical alignments significantly influence the driver's perception. Hence, this study proposed a clustering-based approach to deal with the drivers' perception of complex geometry. Curve direction and the type of superimposed vertical alignment were considered as the criteria for clustering the curves. Based on these two criteria, the curves were clustered into eight groups. For each cluster, the geometric variables influencing the operating speed were identified through correlation analysis. Post clustering, a significant improvement in the correlation between the geometric parameters and the operating speed was observed. The results support the assumption that, driver perception plays a significant role in the operating speed decisions.

The other important aspect that needs a due consideration in the OSM for mountainous terrain is the role of sharp curves and long tangents. Highways passing through mountainous terrain consist of a few geometric elements that differ from most elements because they are designed to tackle the topographical challenges. The existing practice for the development of OSMs cannot capture such distinctive elements as the data are significantly biased to the geometric elements constituting a major part of the alignment. The representation of these distinctive elements would be further lowered after clustering the horizontal curves. Hence, the present study develops the operating speed models considering the selection bias and heteroscedasticity in the sampled data through the Robust Weighted Least Square (RWLS) approach.

The findings from this study indicate that the consideration of curve clustering and selection bias resulted in improved operating speed models. Models developed in this study indicates that the characteristics of horizontal alignment and vertical alignment have varied impact on the operating speeds of all the three vehicle types and across the curve categories. The characteristics of horizontal alignment were found to be influencing the operating speed of all the vehicle types moving on the curves superimposed

with the downgrades. Length of the approach tangent (L_{at}) was found to be significant in the models related to five curve categories and for all the three vehicle types. Whereas the vertical alignment characteristics were found to be influencing the operating speed of vehicles moving on the horizontal curves superimposed with upgrades. Contrary to some of the earlier findings (Fitzpatrick et al. 2000b), the vertical alignment characteristics (gradient at the approach tangent and at start of the curve) affect the operating speed of passenger cars (on horizontal curves superimposed with upgrades and sag curves). It was also observed that, on right-turning curves superimposed with upgrade, gradient at the approach tangent has the highest negative impact on operating speed of loaded truck followed by operating speed of empty truck and passenger car. The findings from this study suggests the importance of considering the combination of horizontal and vertical alignment for modeling the operating speeds of vehicles on mountainous terrain. The categorisation of the horizontal curves for developing the operating speed models was able to identify the geometric variables accurately that were influencing the speed of the vehicles.

A comparison of design consistency (using the safety criteria I of Lamm et al. 1995) assessed using the models estimated using Ordinary Least Square (OLS) and RWLS was undertaken to confirm the adequacy of the proposed approach. It was found that the consistency measure derived using the OLS and RWLS approaches differ statistically, showing that the safety assessment may not be reliable if the OSM is not appropriate. The predicted geometric design consistency using OLS and RWLS was cross-checked with the number of reported crashes. This comparison also suggests that the OSM developed through the RWLS approach could capture the design inconsistency more accurately.

The results from the evaluation of safety criteria I and III suggest that the design consistency evaluation yields varying levels of consistency across vehicle categories. The endangerment of the trucks was showing a better agreement with the overall safety criteria (84-89 percent) than that of the passenger cars (57-61 percent). Since trucks have a higher proportion in the crash data, it is more accurate to use the truck endangerment for evaluating the design consistency. The findings from this study could be further improved by considering the curves superimposed with more than one vertical curve.

Contents

List of Figures

List of Tables

List of Symbols

A	Algebraic difference between the grades
CCR	Curvature change rate (others)
CCR_S	Curvature change rate (Lamm)
CCR_{SB}	Curvature change rate (Lamm), of the following curve B
C_{max}	Maximum curvature on segment following sag-curve
DC	Degree of Curvature
DC_A	Degree of Curvature, of the preceeding curve A
e	Superelevation
e_{pc}	Superelevation at the point of curvature
f_{RA}	Side friction assumed
f_{RD}	Side friction demand
G	Grade
G_1	Grade at approach tangent
G_{1B}	Grade at approach tangent, of the following curve B
G_2	Grade at point of the curve
G_{2B}	Grade at point of the curve, of the following curve B
G_3	Grade at the middle of the curve
G_{3A}	Grade at the middle, of the preceding curve A
G_4	Grade at the end of the curve
G_5	Grade of the exit tangent
G_{5B}	Grade of the exit tangent, of the following curve B
$G_{max,f}$	Maximum slope on segments following upslope-curves
G_{mean}	Mean slope of downslope-curves
G_U	Average grade of the positive gradient part within hog or sag segments
K	Rate of the vertical curve
L_{at}	Length of the approach tangent
$L_{at}\times R$	Length of approach tangent radius interaction
L_{atA}	Length of the approach tangent, of the preceding curve A
L_C	Length of Curve
L_D	Length of the negative gradient part within hog or sag segments
L_{et}	Length of exit tangent
LG_1	Length of the grade at approach tangent
$L_{LP\text{-}SP}$	Distance from limiting point to the summit point
L_O	Distance between point of intersection of horizontal curve and point of intersection of vertical curve
L_S	Length of downslope or upslope - curves
$L_{SP\text{-}PC}$	The length between the summit point and point of curvature
LSW	Left shoulder width
L_t	Transition length

$L_{U\text{-}D}$	The ratio of the length of the positive gradient part to the length of the negative gradient part within hog or sag segment
L_V	Length of vertical curve
LW	Single lane width
$OLMC$	Overlapping length up to mid-curve
Q_1	25th percentile speed
Q_2	75th percentile speed
R	Curve radius
$R \times LW$	Interaction between radius and lane width
R_A	Curve radius of the preceding curve A
R_a	Actual radius
R_B	Curve radius of the following curve B
R_p	Percieved radius
RSW	Right Shoulder width
SD	Sight distance
SW	Shoulder width
T_{ADT}	Average daily traffic
$Turn$	Curve direction (0 for a right turn and 1 for left turn)
V'	Dummy (0=hog, 1=sag)
V_{85}	The operating speed
V_{85AT}	The operating speed at approach tangent
V_{85C}	The operating speed of the passenger car
$V_{85C,\ Tan}$	The operating speed of the passenger car at approach tangent
V_{85i}	The operating speed at section *i*
V_{85LT}	The operating speed of the loaded truck
$V_{85LT,\ Tan}$	The operating speed of the loaded truck at approach tangent
V_{85MC}	The operating speed at middle of the curve
V_{85PC}	The operating speed at start of the curve
V_{85PT}	The operating speed at end of the curve
V_{85T}	The operating speed of the empty truck
$V_{85T,\ Tan}$	The operating speed of the empty truck at approach tangent
V_{85tan}	The operating speed at tangent
V_{85VMC}	The operating speed at the middle of the vertical curve
V_{avgC}	Average speed of car
V_{avgC}	Average speed of passenger car
V_{avgLT}	Average speed of loaded truck
V_{avgLT}	Average speed of loaded truck
V_{avgMC}	Average speed of at the middle of curve
V_{avgPC}	Average speed of at the point of start of curve
V_{avgPT}	Average speed of at the point of end of curve
V_{avgT}	Average speed of empty truck
V_D	The design speed
V_p	Posted speed
X	Shared portion of lengths of horizontal and vertical curves in the same combination

Δ	Deflection angle
Δ_1	Deflection angle of previous curve
Δ_2	Deflection angle of following curve
$\Delta_{85}V$	85^{th} percentile speed differential
ΔG	Difference between the grades of adjacent slopes on hog or sag segments
ΔV_{85}	Change in operating speed
ΔC_C	Curvature change between downslope-curves or crest-curves and following segments
ΔC_{CAT}	The rate of change of Circle Curve Curvature to Approach Transition Curve Curvature
ΔC_{CDT}	Rate of change of Circle Curve Curvature to Departure Transition Curve Curvature
$\Delta G'$	Differential of maximum and minimum slope on sag-curve
ΔL_{CH}	Rate of change of Circle Curve Length to Horizontal Length
ΔS_{CH}	The rate of change of Circle Curve Slope to Horizontal Curve Slope

List of Abbreviations

AT	Approach Tangent
ET	Exit tangent
GIS	Geographic information system
GPS	Global position system
IQR	Interquartile range
JU	Jowai to Umiam
LCV	Light commercial vehicle
MAD	Median absolute deviation
MAPE	Mean absolute percentage error
MAV	Multi-axle vehicle
MC	Middle of curve
OLS	Ordinary least square
OSM	Operating speed model
PC	Point of Curvature
PT	Point of Tangency
RMSE	Root mean square error
RWLS	Robust weighted least square
SC	Safety Criteria/Criterion
UJ	Umiam to Jowai
WLS	Weighted least square

Chapter 1

Introduction

1.1 Overview

Road safety is one of the major challenges faced by a majority of the low and middle income countries. Around 1.35 million people die, and 50 million are injured in road crashes every year (WHO, 2018). According to a report released by the ministry of road transport and highways, Govt. of India (MoRTH 2019a), over 151,000 people were killed in road crashes in India in 2019, and about 70 percent of these crashes involve the individuals of age group, 18-45 years. The country has about one percent of the global vehicle population but accounted for six percent of the world's road traffic crashes (WHO, 2018). As per the WHO Global Report on Road Safety 2018, India accounts for 11% of the global deaths related to road traffic crashes.

In India, among the National Highways, 48.76% of road length is covered by two-lane undivided roads, followed by 29.13% single or intermediate lane roads, and 22.11% of 4-8 lane divided highways (MoRTH 2019a). Highways (both National and State) accounted for about 5% of the total road network and witnessed a disproportionately large share of 55% crashes and 63% fatalities during the year 2018 (MoRTH 2019b). Crashes on these roads have been attributed to higher vehicle speeds and increasingly higher traffic volume. There were 190,800 crashes on two-lane rural roads in 2016, rendering them the most prone to crashes (Chatterjee and Mitra 2019). Two-lane rural roads located in plain and mountainous terrain differ significantly in terms of the alignment design, traffic characteristics, and the safety aspects. Specifically, the geometric design of the roads passing through mountainous terrain warrants a more careful assessment in terms of consistency and safety.

Several factors contribute to the road traffic crashes on the mountainous roads (Joshi et al. 2014). Manipur, Meghalaya, Mizoram, Nagaland, Sikkim, Tripura are small hill states with different traffic and fatality patterns than the other parts of India. Fatality rates per million population have increased in these

states in recent years. In terms of the fatalities per 100 crashes (crash severity), reported in 2018, Mizoram, a hill state, tops the list. Another four states, Uttarakhand, Arunachal Pradesh, Sikkim, and Meghalaya, are figured in the top 15.

Roadway geometric design needs to consider safety as an important aspect along with the efficient movement of people and cargo. To achieve this goal, designers strive to provide the best and most efficient design possible. One technique used to improve safety on the roadway is by examining the consistency of the geometric design. Design consistency can be defined as the conformance of the highway's geometric and operational features with the drivers' expectancy (Alexander 1986). Generally, drivers make minimum errors at geometric features that conform to or match with their expectations.

Drivers expectancy relates to a driver's readiness to respond to situations, events, and information in predictable and successful ways. It influences the speed and accuracy of information handling, and affects all aspects of highway design and operations, and information presentation (Alexander 1986). Drivers' expectancy depends on the amount of experience and the number of times a driver has driven on a particular road. It also depends on the road's similarity to the other roads the driver has experienced driving and how accurate her/his predictions are on that road (Fitzpatrick et al. 2000b). However, design inconsistencies arise when the road's geometry does not conform to the driver's expectancy. Design inconsistency results from the abrupt changes in the geometric features which might lead to more driver workload. To avoid the abrupt changes that might lead to crashes, the designers should ensure that the road geometry corresponds to the driver's expectations by evaluating the design consistency and redesigning the inconsistent locations.

Vehicle speed is an important criterion for identifying potentially dangerous roadway sections, thus it is also known as a surrogate safety measure) (Eluru et al. 2013). A roadway's geometric design is based on an the design speed; if vehicle operating speeds differ significantly from the design speeds considered, the geometric design may be inefficient and, in certain cases, unsafe. Lamm et al. (1986) have reported that half of all the crashes on two-lane rural highways are caused due to inadequate speed adaptation, which indicates that safety is related to design consistency. Inconsistency in design can be described as a geometric

feature or a combination of geometric features with extreme characteristics that lead to unsafe maneuvers. In this situation, speed errors may lead to inappropriate driving maneuvers and undesirable crashes (Fitzpatrick 2000; Gibreel et al. 1999; Hassan et al. 2000).

Most of the research and development of design consistency measures focuses on four main areas: speed, safety, alignment indices, and driver workload. Of all the speed-based measures, operating speed (V_{85}) is widely used for evaluating the geometric design consistency. This speed is the 85th percentile of a distribution of speeds chosen by drivers in free-flow conditions with no environmental constraints. Operating speed models are used to estimate this speed on a given road alignment.

1.2 Need for the study

Geometric design consistency evaluation considers various metrics formulated based on the parameters related to either vehicle operation, road geometry, or driver workload (Fitzpatrick et al. 2000c). However, the operating speed-based measure, reflecting the vehicle operations and road geometry, is commonly used for consistency evaluation. The operating speed is defined as the 85th percentile of the vehicles' free-flow speed (AASTHO 2018).

Several operating speed models have been developed across the world. However, the interdependency of speed and the geometric variables differ from model to model (Llopis-Castelló et al. 2018c; Misaghi and Hassan, 2005). A majority of the models were developed for the plain terrain (Lamm and Choueiri 1987; Misaghi and Hassan 2005; Shankar et al. 2013; Zuriaga et al. 2010). Several such operating speed models, for different vehicle types, were also developed for the Indian highways (Jacob and Anjaneyulu 2013; Maji et al. 2018). However, these OSMs are not applicable for the roads located in mountainous terrain. The challenges in modeling the operating speed for a mountainous terrain include the complexity of the alignment due to the superimposition of the horizontal and vertical alignments and a vast variability in the associated geometric parameters.

The gradient of a road passing through mountainous terrain ranges from 4 to 7%, and the tangents are expected to be relatively shorter. Design codes have mentioned that the vertical curves need to be longer,

and sharp horizontal curves should be avoided as far as possible. In the early 2000s, India's mountainous roads were designed as per IRC SP 48-1998 and IRC 52-2001 (2nd revision), where the ruling and the minimum design speeds were limited to 50km/h and 40km/h, respectively. Accordingly, the absolute minimum radii of horizontal curves were considered as 80m (ruling minimum) and 50m. However, as per the recent IRC SP 73-2015, the design speeds (V_D) range between 40-60 km/h, and the minimum radii range between 75 to 150m. IRC SP 48-1998 and IRC SP 73-2015 use different limiting superelevation rates but a constant side friction factor of 0.15, leading to the differences in the minimum radii. This shows that the design practice itself constrains the geometric variables' uniformity in the design of mountainous roads.

Similarly, a road alignment passing through mountainous terrain might have a few flat gradients, long tangents, and sharp horizontal curves. However, the number of such elements would be less, but they are critical for developing the operating speed models. In such a scenario, the representation of such features in the random sample used for developing the operating speed models would be less, leading to selection bias. To overcome this, data corresponding to less prevalent elements must be added to the sample by considering the range of geometric variables observed in the overall highway alignment. This addition might lead to the non-uniformity of sampling points used for OSM. Further, the operating speed models estimated using the ordinary least squares (OLS) technique fail to capture the effect of the under-represented geometric elements. Besides, for modeling the operating speeds on mountainous roads, many researchers have suggested categorizing horizontal curves based on the superimposed vertical alignment. This categorization might further aggravate the selection bias. In this case, also, the modeler needs to add the data corresponding to the missing range. Ordinary Least Square (OLS) may not yield reliable parameter estimates in both these cases since the data corresponding to the less prevalent geometric elements. These gaps motivate this study to develop the OSMs necessary for consistency evaluation, considering the issues related to the geometry of the highways passing through mountainous terrain.

1.3 Objective

The objective of this study is to develop operating speed models and evaluate the design consistency and safety aspects of two-lane rural roads passing through mountainous terrain. The following are the important tasks were identified to achieve this objective.

1. Analysis of the driver perception when traveling on a horizontal curve superimposed with vertical alignment and segregating the curves into various categories.
2. Developing and validating the OSMs for each curve category, considering the selection bias and heteroscedasticity.
3. Evaluating the geometric design consistency in terms of the operating speed consistency, design consistency, and safety.

1.4 Scope of the study

The scope of this study is limited to the two-lane undivided rural highways passing through mountainous terrain. Data used for the modeling reflect only fair weather and daylight conditions. Operating speed models were developed only for the horizontal curves (superimposed with only one vertical alignment) and the approach tangents. Verification of the applicability of various consistency indices is beyond the scope of this study.

1.5 Organization of the thesis

The thesis initially gives an "Introduction" of the importance of road safety and a brief description of design consistency followed by the study's objectives. The second chapter describes the "Literature review" of OSM and the design consistency methods. The third chapter "Data Collection and analysis" presents the speed data statistics and the applicability of the existing operating speed models. The fourth chapter "Curve clustering" presents the methodology adopted in clustering the horizontal curves based on the driver perception analysis. The fifth chapter "Modeling of operating speed" deals with the development of operating speed models for types of curves and tangents. The sixth chapter deals with the "Geometric Design consistency analysis," while the last chapter describes the "Conclusions" of the thesis.

Chapter 2

Literature Review

2.1 Introduction

Road safety is a major concern, specifically on the two-lane rural highways in India. Operating Speed Models (OSM) play a critical role in assessing and improving the roadway design which is closely linked to safety. Operating speed modeling for rural highways passing through rural areas is complicated due to complex road design. This chapter presents the review of all the relevant aspects in OSM for mountainous terrain. There are three major sections in this chapter, starting with the design consistency studies, demonstrating the key and common approaches. This is followed by the design consistency measurements based on operating speed. The final section presents the OSM developed for mountainous terrain. This section reviews several factors influencing the operating speed of various types of vehicles besides the studies related to the behavior of drivers while negotiating horizontal curves.

2.2 Design Consistency Studies

Design consistency implies that the roadway does not interrupt the driver's expectancy or hinder his/her ability to control the vehicle safely (Alexander 1986). Gibreel et al. (1999) have conducted a state-of-the-art review on highway geometric design and categorized the geometric design consistency studies into three types, namely speed consideration, performance consideration, and safety consideration, which are defined as follows.

Speed Consideration – It deals with the effect of geometric parameters on the operating speed. Also, it addresses the evaluation of the design consistency of the road elements based on the operating speed.

Safety Consideration – It deals with the safety of the vehicles operating on the different alignments of the highway. The geometric elements of the road have a significant effect on the safety of road users. The number of crashes corresponding to different geometric alignments has been studied by many researchers in the past and have evaluated the design consistency of the highway based on the crashes.

Performance Consideration – It deals with the driver's behavior and his/her workload when driving along the alignment of a highway. Since it was challenging to measure drivers' behavior and workload, a very few studies have used this consideration

Researchers have assessed the geometric design consistency using the measures such as speed, vehicle dynamics, alignment indices, and the driver workload (Gibreel et al. 1999; Wooldridge et al. 2003; Hassan 2004). Table 2.1 presents several such evaluation methods, categorized into four types, namely, speed consideration, safety consideration, driver workload and alignment indices. Each of these categories has used different types of information related to vehicle/driver and the road geometry to evaluate the consistency. Speed based indicators can be further categorized into operating speed and individual vehicle speed based approaches. Operating speed based approaches are used for evaluating the consistency of a single element, consistency of two consecutive elements, and the consistency of an entire alignment. In order to assess the consistency in the geometric design, different criteria and methodologies, strongly related to the level of crash rates have been developed, which in turn are based on the analysis of the evolution of the operating speeds (Wilches et al. 2020). Consistency assessment based on the individual vehicle speed has attracted a lot of attention and used for assessing the speed changes on tangent-curve or tangent-curve-tangent. Majority of these studies are based on speed data collected using instrumented vehicles (Zuriaga et al. 2010; Montella et al. 2014; Malaghan et al. 2020b) or using Lidar (Mcfadden and Elefteriadou 2000).

Cafiso and La Cava (2009) compared the Driving Performance Indicator (DPI) with the other theoretical design consistency criteria based on operating speed and geometric relation design, and found a statistically significant correlation between them. Authors found that the maximum driving speed differential between successive elements and between the average section speed and the minimum single element speed agreed statistically with accident history. Thus, confirming that it can be used for design consistency evaluation. In spite of the importance of driver workload in evaluating design consistency, analytical models are not readily available to quantify driver workload (Hassan et al. 2001). It is difficult

to measure such subjective estimates and, hence, to validate such models (Gibreel et al. 1999). The consistency evaluation criterion for vehicle stability is based on the formula in (2.1), which has been subject to considerable criticism (Hassan et al. 2001; Donnell et al. 2016). Furthermore, side friction is also not as easy to recognize and measure as the operating speed.

$$R = \frac{V^2}{127(e + f_R)} \tag{2.1}$$

Thus, the use of the non-speed based approaches as a measure of consistency was much more limited than the approaches based on operating speed. Section 2.3 presents a detailed review of operating speed-based design consistency studies.

Table 2.1 Various approaches available/used for the assessment of Geometric Design Consistency

Approach	Types		Authors
Speed consideration	Operating speed-based	Single element (V_{85}-V_D)	Leisch and Leisch (1977), Lamm et al. (1995), Fitzpatrick et al. (1997), Hassan et al. (2001), Richl et al. (2005), Antonio Martín-Jiménez et al. (2018)
		Successive element (ΔV_{85})	Lamm et al. (1995), Hassan et al. (2001), Fitzpatrick et al. (2000b), Cafiso and La Cava (2009), Montella and Imbriani (2015), Dhahir and Hassan (2019a)
		Inertial operating speed (V_i) profiles	García et al. (2013), Montella and Imbriani (2015), Llopis-Castelló et al. (2018b; a, 2019)
		Global consistency models	Polus and Mattar-Habib (2004), Garach et al. (2014), Camacho-Torregrosa et al. (2013)
	Single vehicle speed-based	85th percentile speed differential ($\Delta_{85}V$)	Hirsh (1987), McFadden and Elefteriadou (2000), Misaghi and Hassan (2005), Castro et al. (2011), Choudhari and Maji (2019) Dhahir and Hassan (2019a), Malaghan and Pawar (2020)
Safety-consideration	Vehicle stability		Lamm et al. (1995), Ng and Sayed (2004), Hassan et al. (2001), Hassan (2004), Montella and Imbriani (2015), Colonna et al. (2016), Antonio Martín-Jiménez et al. (2018)
	Traffic accidents		Wu et al. (2013a), Hassan et al. (2001); Montella et al. (2008)
Driver workload	Visual demand		Wooldridge et al. (2000), Fitzpatrick (2000), Krammes et al. (1995), Hassan et al. (2001), Easa and He (2006)
	Critical rating		Messer (1980), Taylor and Thompson (1977)
	Psychophysiological parameter analyses		Cafiso et al. (2004), Furedy et al. (1992), Heger (1995)
Alignment indices	Average radius		Lamm et al. (1986), Fitzpatrick (2000)
	Average rate of vertical curvature		Lamm et al. (1986), Fitzpatrick (2000)
	Ratio of curve radius to the average radius		Fitzpatrick (2000), Hassan et al. (2001)

Several authors have studied the influence of geometric design consistency on road safety (Cafiso et al. 2010; Wu et al. 2013a; Montella and Imbriani 2015; Garach et al. 2016) and concluded that there is a close relationship between the two. Among the various techniques, operating speed-based method has been the most commonly used measure to examine design consistency and its impact on safety (Gong 2007; Russo et al. 2016; Yan et al. 2017; Malaghan et al. 2020b). The operating speed profile analysis relates safety with the speed variability (Castro et al. 2013). A large portion of collisions have been attributed to improper speed adaptation (Al-Masaeid et al. 1995), hence operating speed can also be a good indicator of the level of safety on the road segment (Hassan et al. 2001). Fitzpatrick (2000) mentioned that the predicted speed reduction has the strongest relationship to crash frequency, hence the speed reduction should be the primary measure in any design consistency methodology.

Although the single vehicle speed-based geometric design consistency approach should be the highly desired method for evaluating the design consistency, collecting such speed data would be possible only through instrumented vehicles or identifying the individual vehicles traversing the curve. This is not always possible to collect such as dataset corresponding to several curves, covering adequate number of vehicles. The operating speed-based approaches (single, successive element speed consistency) are still predominantly used for geometric design consistency analysis (Montella and Imbriani 2015; Dhahir and Hassan 2019a; Nama et al. 2016).

2.3 Concept of Operating Speed

The operating speed is the speed at which motor vehicles generally operate on a road. The Manual on Uniform Traffic Control Devices (MUTCD) defines Operating Speed as “a speed at which a typical vehicle or the overall traffic operates.” American Association of State Highway and Transportation Officials (AASHTO, Green Book 1994), defined the operating speed as “the highest overall speed at which a driver can travel on a given highway under favorable weather conditions and prevailing traffic conditions without at any time exceeding the safe speed as determined by the design speed on a section-by-section basis." However, in July 2001, the AASHTO revised the definition as "the speed at which drivers are observed

operating their vehicles during free-flow conditions." It is important to note that the operating speed definition has evolved with time and research.

Researchers and practitioners frequently use the 85th percentile of the free-flow speed distribution (V_{85}) as the operating speed measure (AASHTO 2004). The 85th percentile speed is the speed at or below which 85 percent of the drivers operate without any restrictions and under favorable conditions. The assumption underlying the 85th percentile speed is that most drivers operate their vehicles at speeds they perceive to be safe.

2.3.1 Basic Formulation and Evolution of Operating Speed Modeling

Speed is one factor that can be used to assess the convenience and efficiency of a highway. Designers also use speed to evaluate the road consistency and driver expectations on roadways. In the US highway design guides, the highway elements consider a design speed that would be consistent with the anticipated operating speed (AASTHO 2018). This design speed is chosen based on the road class, topography, and land use (AASTHO 2018). Designers are generally encouraged to maintain a constant design speed over a considerable length of the roadway, to promote design consistency. However, studies have reported that the design speed concept is not enough to reduce the speed variations, exclusively. The reason is the presence of design elements, e.g., cross-section dimensions, which are not directly related to design speed but still significantly impact the operating speeds (Hassan and Sarhan 2011). Thus, including the concept of operating speed in the design phase has gained attention in the last two decades. The operating speed assessment can determine the anticipated speed changes of the individual vehicles negotiating successive road elements (Hassan and Sarhan 2011). By reducing such speed changes, there is a greater chance of improving safety performance. This reduction in speed changes may also reduce frequent changes in road configurations, thereby achieving a harmonious driving environment (Hassan and Sarhan 2011).

2.3.2 Applications of Operating Speed Models

The concept of operating speed was used in the highway design in Germany for the first time in the year 1973 (Lobo, 2017). It was used as a parameter in the evaluation of design consistency. Later, other countries like Australia, Austria, Canada, France, Portugal, Spain, Switzerland, and the UK have also incorporated the concept of operating speed in the design of highways. Operating speed was used in selecting the design speed, setting geometric parameters, defining speed limits, and evaluating the design consistency

The operating speed models are not transferable, even within the same country, due to driver behavior differences, and it highlights the fact that no single model is universally accepted (Misaghi and Hassan 2005). The driver behavior differences will exist from one country/locale to another (Chen et al., 2014), and the operating speed model format, the independent variables, and coefficients may differ substantially. Since the road conditions and the operating speed interpretations are diverse, following a standard operating speed model is impossible.

2.3.3 Application of Operating Speed in the assessment of Geometric Design Consistency and Road Safety

The consistency of a roadway's alignment is one of the most common road characteristics that affect the safety. Operating speed models are useful to assess the new and existing roads' consistency and to conduct safety analyses of two-lane rural roads. The actual difference between the value of the operating speed representing the drivers' speed behavior and the design speed is analysed to assess the safety and design consistency. Through this, it is possible to improve the alignment design where the variations in measured speed are unacceptable, thereby increasing the safety. The quantitative evaluation of safety levels could significantly improve road safety management. Many highway design standards provide rules for determining alignment accuracy (Fitzpatrick et al. 2000b).

As mentioned earlier, the most commonly used criteria are focused on operating speed to evaluate the consistency of a highway design. By comparing the design speed V_D and operating speed V_{85},

consistency is evaluated for a single element. And for successive geometric elements, design consistency is assessed based on the change in the operating speed.

2.3.3.1 Single Element Consistency (Design Speed Consistency)

The design speed (V_D) concept, which is defined as "a selected speed used to determine the various geometric design features of the roadway (AASHTO 2011)" explicitly relates to horizontal curve radius-superelevation design. An appropriate design speed should be uniformly applied to all the alignment elements of the roadway (Fitzpatrick et al. 2000b). The design speed consistency measure is based on the difference of design and operating speeds related to a single highway element. The greater the difference, the more is the inconsistency in the geometric design. It has also been reported that collisions involving high operating speeds frequently result in serious injury or death (Bhowmik et al. 2019). Leisch (1977) concluded that the difference between the operating and the design speed on a specific highway should not exceed 15 km/h. Furthermore, the operating speed difference between the passenger cars and trucks on a specified element should be less than 15km/h. Lamm et al. (1988, 1995) considered individual design elements along the observed roadway section to evaluate the design consistency. The absolute difference between the operating speed and the design speed was investigated, and concluded that this difference in speed was suggested as a criterion (Criteria I) to evaluate design consistency (Table 2.2).

Table 2.2 Safety criteria I (Lamm et al. 1995)

Design	Criteria	Recommendations
Good	V_{85} - $V_D \leq 10$ km/h	Consistency; No alignment correction required
Fair	10 km/h < V_{85}-$V_D \leq 20$ km/h	Minor inconsistency; Traffic warning devices required
Poor	V_{85} - V_D >20 km/h	Strong inconsistency; Redesign recommended

Fitzpatrick et al. (1997) studied the relationships between design speed, operating speed, and posted speed on two-lane rural highways and found that V_{85} on horizontal curves was less than V_D for all curves with V_D>70 km/h and, greater than V_D for most curves with V_D<70 km/h.

2.3.3.2 Successive Elements Consistency (Operating Speed Consistency)

The design speed used for a horizontal curve does not consider the speed of the motorists on the tangents. The design speed is frequently determined based on the geometric features of vertical and horizontal curves. Unfortunately, such a design strategy causes inconsistencies between subsequent roadway components, resulting in nonuniform driving performance, lower driver comfort, and an increased risk of collision (Thiessen et al. 2017). This might lead to some safety concerns when the driver operates her/his vehicle at a high speed on the long tangents and lowers the speed before reaching the horizontal curves. The speed difference between the curve and tangent (either approaching or exiting) was used to evaluate the consistency in the transition between two successive geometric elements, which is usually expressed as the difference in the operating speeds (ΔV_{85}) between the tangent and curve (Fitzpatrick et al. 2000c). This is one of the most widely used methods for evaluating the design consistency. Fitzpatrick et al. (2000c) hypothesised that, high speed variance indicates inconsistent design features, whereas low speed variance reveals the design features that are in line with driver expectations. Figure 2.1 illustrates this with a long tangent followed by horizontal curve of a smaller or larger radius of curvature. The design inconsistency can be detected by increased speed variance. High speed variance has been linked to an increased crash risk. This association could be linked to the road's geometry.

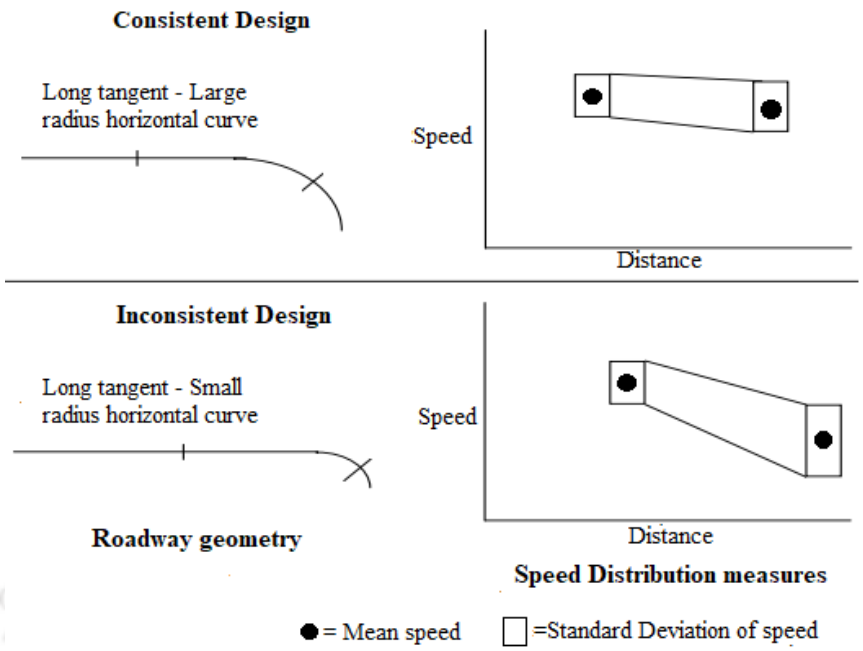

Fig. 2.1 Speed variation along the tangent and curve (Fitzpatrick et al. 2000c)

Different combinations of successive elements have been studied by Lamm et al. (1988) a long tangent accompanied by a horizontal curve and two consecutive horizontal curves with or without a short tangent. Based on the average crash rates, Lamm et al. (1995) suggested the following criterion (Criteria II) to evaluate design consistency between a tangent and the following curve (Table 2.3).

Table 2.3 Safety criteria II (Lamm et al. 1995)

Design	Criteria	Recommendations
Good	range of change in $V_{85} \leq 10$ km/h	Consistency; No alignment correction required
Fair	10 km/h < range of change in $V_{85} \leq 20$ km/h	Minor inconsistency; Traffic warning devices required
Poor	range of change in $V_{85} > 20$ km/h	Strong inconsistency; Redesign recommended

These safety criteria proposed by Lamm et al. (1995) were widely used by many researchers to evaluate the design consistency of two-lane rural highways (Hassan et al. 2001; Richl and Sayed 2005; Castro et al. 2008; Zilioniene and Vorobjovas 2011).

2.4 Review of Operating Speed Modeling

This section presents a comprehensive review of the literature on operating speed modeling. Details of the data collection locations, collection of speed data, and vehicle categories considered for V_{85} models are

discussed. Further, the operating speed studies are analyzed based on horizontal alignment and the cross-sectional elements. This section also presents a review of the studies related to the horizontal-vertical alignment combinations.

The Operational Effects of Geometrics Committee of the Transportation Research Board, through its circular E-C 151 (TRB Operational Effects of Geometrics Committee and others 2011), made a few remarks regarding the current research level on the OSM. Some criticisms and recommendations were made to improve the applicability of the model and speed predictability. As per this circular, most of the modeling focuses on passenger cars and predict the V_{85} on horizontal curves, assuming the vehicles maintain a constant speed throughout the curve. Many models contain the parameters such as radius, degree of curve, curve length, and deflection angle. A few models also include variables related to the vertical alignment like the gradient, K, and sight distance. EC-151 Circular suggests a further exploration of the impact of the geometric variables on the operating speed, especially on mountainous terrain. The 85th percentile speeds have been the subject of the majority of past research studies examining at vehicle speed as a function of a numerous exogenous variables (Eluru et al. 2013). The factors impacting drivers' speed selection behaviour can be observed from three perspectives: (1) driver characteristics, (2) vehicle characteristics, and (3) roadway characteristics (Afghari et al. 2018).

2.4.1 Data Collection for OSM

Speed data collection on the curve/tangent is governed by the application of this data in consistency assessment of a single element or two consecutive elements or a complete alignment. Spot speed data, speed of a vehicle at several locations on the tangent-curve-tangent segment, and vehicle trajectory data collected using GPS are widely used for geometric design consistency assessment. Spot speed data, collected at a single point on the curve or on a tangent, are used to develop the operating speed models corresponding to a curve or a tangent. Spot speed data collected at several locations on a tangent-curve combination are used for developing the speed differential models. Speed data collected at several locations or speed extracted from the trajectories are used for developing the speed reduction models.

Several researchers have used spot speed data collected using radar guns, pavement sensors, and similar other mechanisms, to develop the operating speed models for selected geometric elements, i.e., tangent or curve (Islam and Seneviratne 1994; Mcfadden and Elefteriadou 2000; Misaghi and Hassan 2005). These data collection methods assume a constant operating speed throughout the horizontal curve; acceleration and deceleration only happen on the tangents (Krammes et al. 1995, Fitzpatrick 2000; Lamm et al. 1999; Hassan and Sarhan 2011). According to these assumptions, spot speed data are collected at the center of the horizontal curve and at the midpoint of the preceding tangent to develop the corresponding operating speed models. Donnell et al. (2001) has collected speeds at three locations—the midpoint of the approach tangent, the midpoint of the horizontal curve, and the midpoint of the departure tangent, to develop operating speed profile models for trucks on two-lane highways. A few other researchers have also collected speed at the point of the curve (PC) and the point of tangent (PT) of the horizontal curve to develop operating speed models. For example, Islam and Seneviratne (1994) studied the changes in operating speed on two-lane rural highways. It was noticed that there were significant differences between the operating speed values on the same horizontal curve at the point of the curve (PC), the middle of the curve (MC), and the point of tangent (PT). These differences lead to different conclusions regarding the consistency of a design. Gibreel et al. (2001) collected operating speed data at five points on each site (PC, MC, PT, approach tangent AT and exit tangent ET) to establish the effect of the 3D alignment on the operating speed profile. Similarly, Gong (2007) also collected speed at PC, MC and PT, and employed a paired *t*-test and found that the difference was not significant at 95% confidence level.

To evaluate the operating speed consistency on tangent-curve combination, researchers have developed OSMs corresponding to the curve as well as tangents. Al-Masaeid et al. (1995) took measurements of different vehicle speeds on the central part of the curve and on the tangent, 250m away from the start of the curve. Fitzpatrick et al. (2000b, 2003) and Polus et al. (2000) have also used the speed data collected from the middle of the approach tangent for modeling the operating speed. Misaghi and Hassan (2005) focused on developing the operating speed and speed differential models for two-lane rural

highways and collected speed data at the approach and exit tangent and the middle of the curve. However, this study did not conduct any statistical test to differentiate the speed at these 3 points along the curve. A similar study was also conducted by Castro et al. (2011), who measured the speed using radar meters and developed operating speed models, at the beginning, midpoint, and end of curves. Besides this, the speed change experienced by drivers from tangent to curve was also studied, and a model was developed. Hence it can be concluded that operating speed data should be collected on the approach tangent as well as on the horizontal curve (PC, MC, or PT) so that the consistency of the curve can be analysed. Jacob and Anjaneyulu (2013) gave an illustration to use the OSMs developed for horizontal curve and tangent to improve the safety of highways by evaluating the consistency of geometric design through the consistency evaluation criterion developed by Lamm et al. (1995).

However, a few studies have checked the suitability of data collected at the middle of the curve for developing the operating speed models. Fitzpatrick et al. (2000a) reported that the minimum speeds occur between the mid and three-quarter point of the curve. Similarly, Mcfadden and Elefteriadou (2000) concluded that the location of maximum speed on the tangent would not occur at a specific location on the approach tangent, and the occurrence of the minimum operating speed on the curve might not coincide with the midpoint of the curve. Llopis-Castello et al. (2018c) conducted a hypothesis test based on the analysis of paired data was performed to determine whether the operating speed at mid-curve (V_{85MC}) could be considered similar to the minimum operating speed (V_{85min}) or not. They found that V_{85MC} could not be considered similar to V_{85min} at a 95% confidence level. Malaghan et al. (2021) showed that the operating speeds measured at the midpoint of the horizontal curves overestimate the actual minimum operating speeds measured over the entire curve length of horizontal curves between 1.2 and 1.9 km/h. However, Jacob and Anjaneyulu (2013) conducted a pilot study using Global Positioning System (GPS) to identify the speed variability on the curve. They found that the vehicles start decelerating well before the point of curvature. The vehicle's speed was found to be constant on the approach tangent up to a distance of 60 m ahead of the

point of curvature. Beyond that, vehicles were found to decelerate. Speed was found to be minimum within 10 m of the middle of the curve. Hence, speed on the curve was observed at the middle of the curve.

To overcome the limitations attributed to spot speed data, several researchers have used the driver simulator and GPS devices to trace the continuous speed variation on tangent-to-curve transitions (Malaghan et al. 2020a). Such data are useful in capturing 85th percentile speed differential ($\Delta_{85}V$) for individual vehicles from tangent-to-curve transition and to determine the actual speed reduction (Montella et al. 2014; Zuriaga et al. 2010; Malaghan et al. 2020b). Mcfadden and Elefteriadou (2000) used lidar guns for obtaining the speed at several points along the approach tangent and the curve, and found that the 85th percentile of maximum speed reduction (85 MSR) was, on an average, approximately two times greater than the speed differential obtained from the conventional ΔV_{85}. Montella et al. (2014) used an instrumented vehicle with GPS, to analyze the driver behavior in speed choice and deceleration or acceleration performance and develop operating speed and several other prediction models. Models were developed to predict operating speed on curves and tangents, deceleration and acceleration rates to be used in the operating speed profiles, starting and ending points of constant operating speed in a curve, 85th percentile of the deceleration and acceleration rates of individual drivers, and 85th percentile of the individual drivers' maximum speed reduction in the tangent-to-curve transition. Malaghan et al. (2020b) gave an experimental examination of the operating speed variation of the drivers on horizontal curves, tangents, and tangent-to-curve transitions using continuous speed profiles for two-lane rural highways in India.

For evaluating the design consistency of the alignment, it is necessary to collect speed data at the tangent and the successive curve for developing the operating speed models. Several studies have collected speed at specific locations or middle of the approach tangents, as well as PC, MC, and PT of the horizontal curve. Researchers have also argued that the speed of a vehicle is not the minimum at the middle of the curve. However, given the difficulties in collecting the speed data on the entire tangent-curve combination, a majority of the studies develop operating speed models based on the spot speed data collected at various points of the tangent and horizontal curve.

2.4.2 Vehicle type considered for OSM

According to AASHTO (2004) "in the design of any highway facility, the designer should consider the largest design vehicle that is likely to use that facility with considerable frequency". The effect of road geometry on vehicle maneuverability varies due to the inconsistency in road geometric design with respect to the requirements of different vehicle types (Malaghan et al. 2020b). Several studies have focused on passenger cars for developing OSM (Fitzpatrick et al. 2000b; Gibreel et al. 2001; Islam and Seneviratne 1994; Krammes et al. 1995; Misaghi and Hassan 2005). Misaghi and Hassan (2005) noted that the majority of the models (25 out of 27 studies considered in their study) were developed focussing on speed prediction for passenger cars, whereas the models that can predict the speed for light trucks or heavy trucks were very few. This was because, passenger cars were dominant in the two-lane highways, and the lack of field observed truck speeds was the biggest hurdle in the development of truck models (Adolini-Minnicino and Elefteriadou 2004). Leisch and Leisch (1977) made two special assumptions about trucks that differentiate truck speed modeling procedures from passenger car modeling procedures – (i) gradients causes trucks to have unusually high rates of deceleration and extremely low speeds on steep, sustained upgrades; (ii) truck operating speeds are determined primarily by the mechanical characteristics of the vehicles, whereas, passenger car speeds mostly depend on driver characteristics.

Donnell et al. (2001) have developed truck operating speed models for two-lane highways. They have mentioned that, on the highways where the truck proportion is high, and consideration of truck operating speed profiles is essential. Misaghi and Hassan (2005) observed statistically significant differences between the speeds of passenger cars and trucks, but not the difference in the speeds of passenger cars and light trucks. Boroujerdian et al. (2016) also found that the difference between the speeds of passenger cars and heavy vehicles is statistically significant at a significance level of 5%. Llopis-Castelló et al. (2018c) stated that not considering heavy vehicle in OSM might lead to inconsistent geometric designs. Moreover, speed difference between passenger cars and heavy vehicles might cause inconsistencies in vehicle operations along the upgrades (Harwood 2003). Most researchers concluded that,

while passenger car speeds are governed by the horizontal alignment, heavy vehicle speeds depend on both the horizontal and vertical alignment. Therefore, the analysis of the operating speeds of both the passenger cars and heavy vehicles should be carried out considering three-dimensional (3D) geometric effects. Llopis-Castelló et al. (2018c) found that, with upgrades greater than 3 percent, the vertical alignment significantly affects the speed of trucks. For loaded trucks, the effect of vertical alignment on the speed was greater than that for unloaded ones. Hence, the development of truck operating speed models is crucial to assess the geometric design consistency of the highways passing through mountainous terrain.

For the mixed traffic streams, researchers have investigated the variability in the operating speed across the vehicle types (e.g., Jacob and Anjaneyulu 2013; Morris and Donnell 2014; Schurr et al. 2005). Al-Masaeid et al. (1995) evaluated the consistency by using the speed reduction of passenger cars, light trucks, and trucks. Jacob and Anjaneyulu (2013) developed OSMs for different vehicles as the road geometry effect differs among the various types of vehicles. Most of these studies suggest considering a separate model-form for different vehicle types due to the vehicles' varying physical, mechanical and dynamical properties that lead to a different speed choice with the geometry.

2.5 OSM for mountainous terrain

Factors governing the vehicle operations on mountainous terrain are different when compared to the plain terrain. In plain terrain, the road geometry has a relatively less impact on the speeds of the free flowing vehicles. Mostly the drivers are able to travel at their desired speeds. However, the vehicle operations in mountainous terrain are significantly affected by the road geometry.

Most of the mountainous highways have overlapped horizontal and vertical alignments because of the terrain (Wang et al., 2014). The alignment characteristics have significant influence on the vehicle speed, especially in the segments with a combination of horizontal and vertical. Wang et al., (2014) mentioned that there is little research which has taken the vertical curve geometric features into the prediction model of vehicle speed, and also about combined horizontal and vertical curve highway design. Fitzpatrick et al. (2000b) reported that combined horizontal and vertical alignments increase the complexity of the driving

task and the driver's workload. For example, a horizontal curve combined with crest vertical curve could increase the driver's workload in two ways: by having a reduced sight distance and by having to control the vehicle in a three-dimensional space.

2.5.1 OSM without classifying the curves

Several studies have developed OSMs on horizontal curves without classifying the curves (Al-Masaeid et al. 1995; Donnell et al. 2001; Llopis-Castelló et al. 2018c). Considering the differential effect of the road geometry corresponding to mountainous terrain, several studies have developed separate operating speed models for passenger cars and trucks.

Al-Masaeid et al. (1995) developed operating speed reduction models for passenger cars, between the horizontal curves and tangents, and successive curves, for the mountainous, rolling and level terrain. They observed that the degree of curve, radius of the first and second curve are the important geometric characteristics that explain the operating speed reduction from tangent to curve, and from one curve to another. Also, the length of the common tangent between successive curves, deflection angles of preceding and following curve affect the 85^{th} percentile speed of passenger cars on tangents. Andueza (2000) developed the operating speed models of passenger cars, for curves and tangents, located in mountainous terrain. The 85^{th} percentile speed for the curves was estimated using the radius of the curve under consideration, the radius of the previous curve, sight distance on the curve, and length of the approach tangent. The 85^{th} percentile speed for the tangent was estimated using the radius of the curve under consideration, and length of the approach tangent. Several researchers (Morris and Donnell 2014; Wang et al. 2014) have studied the operating speeds on the horizontal curves combined with steep vertical grades. Morris and Donnell (2014) found that the radius, percent grade, superelevation, turning direction indicator and right shoulder width influence the operating speed of passenger cars. The radius of the horizontal curve tends to impact the operating speeds of passenger cars more rather than the speeds of trucks. Wang et al. (2014) studied the influence of the combination of the horizontal curve with the downslope on passenger cars speed using driving simulator. They found that the gradient, radius of curvature, and curve length have

a significant influence on passenger car speed. Jacob and Anjaneyulu (2015) developed OSMs for passenger car, on combined horizontal curve with hog vertical curves. They found that the radius (R), length of hog curve (L_V) and the distance between points of intersection of tangents to the vertical curve and that to the horizontal curve (L_O) were the variables that influence the operating speed of passenger cars on the horizontal curve.

Several authors have also developed the operating speed models for the trucks. Al-Masaeid et al. (1995) found that the degree of curve, radius of the first and second curve have significant impact on the reduction in operating speed of light trucks and trucks. Donnell et al. (2001) have developed the operating speed models for trucks on two-lane rural highways using a combination of field and simulated data on horizontal curves combined with vertical grades. On an average, 20 speed observations on trucks were collected at each site. They found that the vertical grades have a significant effect on truck speeds. The radius of curve, length of approach tangent, grade of approach tangent, and the length of approach tangent interacting with the curve radius were found to influence the operating speed of trucks. They have highlighted the need to study the operating speeds of trucks on sag and crest vertical curves. Morris and Donnell (2014) found that the radius, percent grade, turning direction, and lane width have a significant influence on the operating speed of trucks. They also found that the vertical grades tend to impact the trucks' operating speed more significantly than the passenger cars. Jacob and Anjaneyulu (2015) developed OSMs for truck on combined horizontal curve with hog vertical curves. They found that radius of the curve and length of ascending grade of the hog curve are some of the variables that influence the operating speed of trucks at the middle of horizontal curve. Llopis-Castelló et al. (2018c) developed speed prediction models for heavy vehicles on horizontal curves of two-lane rural roads. They have collected the speed profiles using Global Positioning System (GPS) tracking devices. They found that the radius of the horizontal curve and the grade at the point of curvature have a significant influence on the operating speeds of heavy vehicles. The operating speeds of heavy vehicles were significantly affected by the vertical alignment, i.e. upgrades greater than 3%. This influence of grade was larger for loaded trucks than for unloaded ones.

It can be observed from the literature surveyed that the radius of curvature is a common variable that affects the operating speed of passenger cars and trucks in mountainous terrain. However, the gradient of either the approach tangent or the curve controls the operating speed of trucks compared to the passenger cars. Table 2.4 summarizes some of the studies related to operating speed, for mountainous terrain.

Table 2.4 Summary of past studies of operating speeds on 3D alignments, without classifying curves

Authors & Year	Vehicle type	Right/ Left Driving	Data Collection	No. of curves	No. of observations per site	Parameters
Al-Masaeid et al. (1995)	Passenger Car, Light truck, Trucks	Right	40-m trap length	93	N/A	R_A, R_B, DC, L_{at}, Δ_1, Δ_2
Andueza (2000)	Passenger Cars	Right	Radar gun	21	30-64	R_A, R_B, SD, L_{at},
Donnell et al. (2001)	Trucks	Right	Lidar gun	17	At least 100	R, G_1, G_5, L_{at}, L_{et}, L_{at}*R
Morris and Donnell (2014)	Passenger Cars, trucks	Right	Laser gun	19	Approx. 75-100	R, G, e, *Turn*, *RSW*, *LW*
Wang et al. (2014)	Passenger Car	Right	Driving simulator	22	21 drivers	ΔS_{CH}, R, ΔC_{CAT}, ΔC_{CDT}, ΔL_{CH},
Jacob and Anjaneyulu (2015)	Passenger Car, Two-wheeler, Bus, Truck	Left	Trap length based	52	N/A	R, LG_1, L_o, L_V
Llopis-Castelló et al. (2018c)	Unloaded and Loaded truck	Right	GPS	105	80 drivers	R, G_2

2.5.2 Effect of 3D alignment on the driver's perception

Smith and Lamm (1994) have hypothesized that the perceived radius of a horizontal curve varies when overlapped with a crest or a sag curve. This may result in perspective views that make the horizontal curve appear flatter than it is in reality. In such situation, higher and excessive operating speeds cause higher crash risks. They also observed that the crash rate is higher at sag vertical curve than the crest curves. Their results supports the hypothesis that superimposed sag vertical curves may create a potential hazard by making the horizontal curve to appear flatter. Hassan and Easa (2003) and Smith and Lamm (1994) have found that the horizontal curve appears to be sharper when superimposed with a hog curve and flatter with a sag curve (Figure 2.2). Hassan and Easa (2003) tested the hypothesis that the overlapping vertical alignment affects the driver's perception of the horizontal curvature, using computer animations and field measurements.

Authors found that the trend of the change in operating speed on horizontal curves in sag combinations was consistently different from that of the horizontal curves in crest combinations.

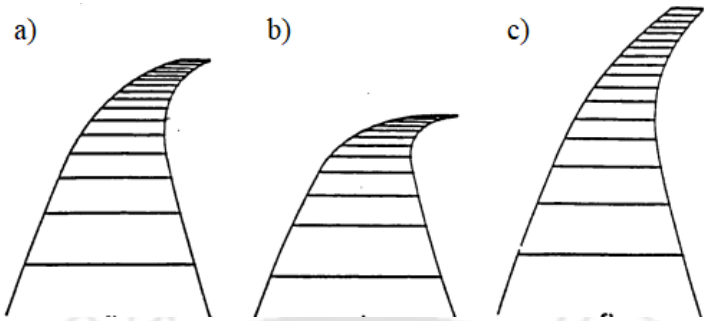

Fig. 2.2 3D view of Horizontal curve superimposed with a) no vertical curve b) hog c) sag (Smith & Lamm 1994)

Hassan et al. (1997) have identified that a 2D design may overestimate or underestimate the required radius depending on the vertical alignment. The radius of curvature for horizontal curves and K-value for vertical crest curves depend on other geometric elements. The interaction between these features cannot be ignored as it may lead to erroneous geometric design standards. They have proposed that a 3D-based design standard be developed and used in highway geometric design practices for a safe and consistent design of the geometric alignment. Based on the studies using computer animations, Hassan and Easa (2003) found that the direction of the horizontal curve and the algebraic difference in the grades do not influence the driver's perception about the curve radius. The field measurements of operating speed verified that the driver behavior on the approach to the horizontal curve varies with the type of overlapping vertical curve. Drivers consistently reduce the operating speed on the approach to horizontal curves combined with a crest curve and accelerate before the beginning of horizontal curves combined with sag curves. These trends were evident regardless of the value of the vertical grade of the approach tangent.

Bidulka et al. (2002) and Hassan et al. (2002) examined the hypothesis made by Smith and Lamm (1994) and found that the perceived radius of a horizontal curve varies when overlapped with a crest and a sag curve. They found the hypothesis to be valid. Hasan et al. (2005) have found that the misperception of the horizontal curve is directly proportional to the radius of the horizontal curve. They also found that the

offset between the midpoints of the horizontal and vertical curve does not affect the perception; however, as the positive offset (vertical curve following a horizontal curve) increases, the perception problem decreases. Bidulka et al. (2002), Hassan et al. (2002), and Richl and Sayed (2005) have also studied the "perceived radius" and quantified the influence of vertical curves on horizontal curve perception. They found a statistically significant difference between the actual and perceived radii. Hassan et al. (2002) developed a model for the perceived radius as a function of the actual radius which is shown below.

$$R_p = -51.28 + 0.935R_a + 132.11V' + 0.125R_aV' \quad (2.2)$$

where, R_p= Perceived radius, R_a=Actual radius, V'=Dummy (0=Hog, 1=Sag)

Richl and Sayed (2005) studied the effect of using actual and perceived radius on design consistency in terms of their operating speeds. They compared the number of horizontal curve sections falling as a "good" rating under the design consistency safety criteria I (difference between the operating speed for an alignment element and the design speed for the alignment) & II (difference in the operating speeds between successive alignment elements) defined by Lamm et al. (1995). When they used the perceived radii instead of the actual radius, a change in the difference between the operating speeds was observed. This in turn, changed the number of horizontal curve segments that received a "good" rating under criteria I and II. The use of perceived radii resulted in a higher disparity between the operating speeds on the alignment. As a result, more horizontal curves were found to be geometrically inconsistent.

Hasan et al. (2005) investigated the impact of several geometric parameters on drivers' perception of horizontal curves overlapped with vertical curves. The experiment was conducted on a randomly selected sample of 80 drivers using computer-generated images of roadway curves. The perceptual response was created by comparing two curves of equal radius but with and without a vertical curve. They found that the misperception was more in the case of horizontal curves overlapped with the sag curves. They also observed that the driver misperception of the horizontal curves increases as the radius of the horizontal curve increases. The presence of a spiral curve affects the drivers' perception of the horizontal curves in the case

of crest combination only. However, the length of the spiral curve does not affect the perception, whether on crest or sag combinations.

Xu et al. (2017) found that, any change in geometrical features such as radius, deflection angle, transition curve, road width, length of tangent, curve deflection direction, and obstacles on road surface will impact the trajectory shape, resulting in a change in driving speed. The radius of curvature is an indication of the sharpness of a horizontal curve, it can significantly affect the perception and judgment of drivers, and thus affects the track behavior on two-lane mountainous roads (Xu et al. 2018). Various studies have pointed out that there is a difference between the adopted and the actual radii of the horizontal curve, and many reasons contribute to this difference. Curve cutting appears to be an expected behavior on mountainous roads (Xu et al. 2017). The trajectory radius when the driver is cutting the curve is higher than the design radius. Additionally, Xu et al. (2018) observed that a higher speed at the entry point of the curve could result in the vehicle encroaching into the opposite lane. Inertia may cause the vehicle to move too close to the outer side of the curve after a cut. Also, they reported that in case of sharp horizontal curves, the trajectory of the vehicle enters the oncoming lane more frequently. The above review clearly indicates the effect of turning direction on the driver perception of horizontal curves.

2.5.3 Effect of turning direction of horizontal curves

Misaghi and Hassan (2005) have considered the direction of the curve as a model parameter and observed a significant speed reduction on the left-turning curves compared to the right-turning, for the highways located in Canada. Dhahir and Hassan (2019b) have compared the effect of left and right turning curves on driver comfort threshold (limit of lateral acceleration beyond which drivers feel discomfort) and speed on the curve for rolling and mountainous terrain. They mentioned that, turning direction and grade significantly affect the comfort threshold and speed on the curve. These findings are consistent with that of Misaghi and Hassan (2005). Liu et al. (2017) developed a method to evaluate the safety of combined horizontal and vertical alignments, using speed differential as the indicator of safety. Speed differential was calculated as the difference between the maximum and minimum speed on each combined alignment, of each driver.

They found that turning left makes the speed differential lower on horizontal curves combined with the crest curves. Morris and Donnell (2014) also developed OSMs for passenger cars and trucks on horizontal curves combined with steep vertical grades. They found that speed of passenger cars was higher on right-turning horizontal curves than the left-turning curves. Whereas, speed of trucks was lower on right-turning horizontal curves than the left-turning curves.

2.5.4 OSM with classification of curves

Several researchers have also modelled the operating speed on horizontal curves after classifying them based on the type of superimposed vertical alignment (Fitzpatrick et al. 2000b; Gibreel et al. 2001; Liu et al. 2017). All the studies that have classified the curves have modelled the operating speed for only the passenger cars.

Fitzpatrick et al. (2000b) studied the combination of horizontal and vertical curves (gradient ranging from -10% to +10%). They mentioned that the current design-speed-based or operating-speed-based methods for ensuring design consistency are oriented more towards horizontal alignment. They also have mentioned that here is no model to measure design consistency on combined horizontal and vertical alignment. Most studies have been directed toward either horizontal or vertical alignment, separately. They reported that horizontal alignments combined with vertical alignments increase the driver workload and lead to potential speed changes. They have studied the horizontal curves with upgrades, downgrades, with vertical sag curve, and with vertical hog curve. They found that the radius and the vertical curvature rate are the most important explanatory variables affecting the operating speed of passenger cars.

Abdul-Mawjoud and Sofia (2008) conducted a study in northern Iraq to evaluate the combined effect of curve and gradient on the operating speed. The grades were separated into four groups, i.e., <3% upgrade, ≥3% upgrade, <3% downgrade, and ≥3% downgrade, and the operating speed of passenger cars was predicted for each group of horizontal curves combined with these grades. The horizontal alignment characteristics such as the radius of curvature, deflection angle of the horizontal curve, and the speed at the approach tangent were found to have a significant effect on the operating speed of passenger cars, even

when the horizontal curves were combined with moderate and steep gradients. Whereas, the vertical alignment characteristics have no such impact.

Gibreel et al. (2001) conducted a study on the three-dimensional (3D) nature of the highways located in Ontario on level to rolling terrain with grades ranging between ±6%. Two types of combinations were considered: a horizontal curve combined with a vertical sag curve and a horizontal curve combined with a vertical hog curve. They mentioned that the existing operating speed models for design consistency in North America and Europe were mainly based on two-dimensional (2D) analysis of horizontal alignments. Authors found a significant difference between the predicted operating speed of passenger cars using the 2D and 3D models. They have also emphasized the need to develop reliable models for predicting operating speed based on combined horizontal and vertical alignments. They reported that the radius of the horizontal curve, the deflection angle of the horizontal curve, horizontal distance between the point of horizontal intersection and the point of vertical intersection, length of the vertical curve, gradients, the algebraic difference in grades, and superelevation rate were significant in predicting the 85th percentile operating speed of passenger cars on horizontal curves.

Liu et al. (2017) mentioned that the combined horizontal and vertical alignments are frequently used in mountainous freeways, but the effect of such alignments is not considered in the current design regulations and standards. The authors classified the combined horizontal and vertical alignments into four groups: upslope-curve, downslope-curve, crest vertical curve-curve and sag vertical curve-curve, with the longitudinal grade ranging from –6% to +4%. They considered that the combined horizontal and vertical alignments have distinct dependent variable profiles for design consistency indicators. They found that a particular geometric characteristic influences the speed differential of passenger cars differently in various combined alignments. The models developed showed that slope, curvature, length, and direction of the curve significantly influenced the speed differential of passenger cars. Wang and Wang (2018) examined speed changes on four types of combined curves (downslope, upslope, crest and sag) of mountainous freeway programmed into a driving simulator. The results showed that the speed change behaviors on the

four types of combined curve differ in frequency. Also, the significant effects of geometric design characteristics on speed change differed by type of combined curve. Table 2.5 summarizes some of the past attempts in modeling the operating speed on the 3D highway profile, after classifying the curves based on the vertical alignment.

Table 2.5 Summary of past studies of operating speeds on 3D alignments

Authors & Year	Vehicle type	Right/ Left Driving	No. of curves	No. of observations per site	Parameters	Curve Categories
Fitzpatrick et al. (2000b)	Passenger Car	Right	176	≥100	R	$-9<G<-4$
					R	$-4<G<0$
					R	$0<G<4$
					R	$4<G<9$
					R	Sag
					K	Hog
Gibreel et al. (2001)	Passenger Car	Right	38	1 hour	R, A, L_o, e, K	Sag
					R, L_v, G_1, A, L_o, e	Hog
Abdul-mawjoud and Sofia (2008)	Passenger Car	Right	48	≥150	V_{85AT}, R	$0<G<3$
					V_{85AT}, R	$3<G<9.3$
					$V_{85AT}, R, \Delta,$	$-3<G<0$
					$V_{85AT}, R,$	$-9.3<G<3$
Liu et al. (2017)	Passenger Car	Right	64	21 drivers	G, L_C	Upgrade
					G, L_C	Downgrade
					$L_D, \Delta G, Turn$	Hog
					L_{U-D}, G_U	Sag
Wang and Wang (2018)	Passenger Car	Right	70	21 drivers	$L_S, G_{mean}, \Delta C$	Upgrade
					$L_C, G_{max}, \Delta C$	Downgrade
					$L_C, K, \Delta C$	Hog
					$L_{at}, \Delta G', C_{max}$	Sag

After segregating the horizontal curves based on the type of combination with the vertical alignment, it was observed that most of the horizontal alignment characteristics such as L_{at}, e and DC, were not found to be influencing the operating speed of the passenger cars. The radius of curvature was the most common geometric parameter to influence the operating speed of passenger cars on mountainous roads. Gibreel et al. (2001) found that the models developed after segregating the horizontal curves were capable of predicting operating speed profiles along ‘‘isolated’’ combinations of horizontal and vertical curves. The predicted speed has shown excellent agreement with the observed values. Moreover, the operating speeds on sag and hog curves, estimated using the 3D models have closely matched with the observed speeds when compared to the values estimated using the 2D models (proposed by McFadden and Elefteriadou 1997).

These results suggest that the curve clustering and the 3D operating speed models should be used in the design and evaluation of geometric design consistency of combined highway alignments.

2.5.5 Scope for improved OSM for mountainous terrain

Literature review suggests that, in the case of mountainous terrains, the operating speeds of passenger cars are governed by the driver and his perception of the road alignment. Whereas, the operating speeds of trucks are governed by the mechanical characteristics of the vehicle. For mountainous terrain researchers have developed the models with and without classifying the horizontal curves based on the superimposed vertical alignment. A few studies found that the horizontal curve appears to be sharper when superimposed with a hog curve and flatter with a sag curve. They observed that the drivers consistently reduce the operating speed on the approach to horizontal curves combined with a crest curve and accelerate in case of the horizontal curves combined with sag curves. The misperception of the horizontal curve is directly proportional to the radius of the horizontal curve, and statistically significant difference between the actual and perceived radii was noticed. A few researchers have mentioned the importance of the direction of the curve on operating speed performance. The influence of the direction of the curve on the operating speed can be easily related to driver perception. The interaction of the horizontal and vertical alignments on driver perception is the least studied aspect of the geometric design because of the complexity of the geometry. Hence, it is essential to consider the driver perception based on the vehicle operations. Moreover, the literature suggests the importance of the 3D analysis of the curve geometry, considering both the horizontal and vertical alignments. Besides the above, the literature suggests separate operating speed models for different vehicle categories and at various points on the tangent and curves such as the start point, middle, and end of the curve.

2.6 Summary

Several measures of geometric design consistency have been identified in the literature. They can be classified into four main categories: speed consideration, safety consideration, alignment indices, and driver workload. Among the various techniques, operating speed-based method has been the most commonly used

measure to examine design consistency and its impact on safety. A higher variation in speeds is probably due to inconsistent designs, while uniform speeds are produced through consistent designs (Fitzpatrick et al. 2000c). A majority of the operating speed models were developed for the plain terrain and these models are not applicable for the roads located in mountainous terrain. The road alignment characteristics on mountainous terrain have significant influence on vehicle speeds, particularly on segments with overlapping horizontal and vertical alignment. Hence, drivers' behavior on mountainous terrains is very different compared to driving on plain terrain. The sight distance and perception are very much affected, which eventually affects the drivers' performance.

Numerous researchers have used spot speed data collected using radar guns to develop the operating speed models. These data collection methods assume a constant operating speed throughout the horizontal curve. The speeds were collected at specific locations or middle of the approach tangents, as well as PC, MC, and PT of the horizontal curve. Several researchers have also used the driver simulator and GPS devices to trace the continuous speed variation on tangent-to-curve transitions. They reported that the minimum speed at the curve does not coincide with the middle of the curve. Using such equipment enabled them to capture 85^{th} percentile speed differential ($\Delta_{85}V$) for individual vehicles from tangent-to-curve transition and to determine the actual speed reduction. Several studies have observed statistically significant differences between the speeds of passenger cars and trucks. Most researchers concluded that, while passenger car speeds are governed by the horizontal alignment, heavy vehicle speeds depend on both the horizontal and vertical alignment.

Studies that developed OSMs on horizontal curves without classifying the curves observed that radius of curvature is a common variable that affects the operating speed of passenger cars and trucks in mountainous terrain. However, the gradient of either the approach tangent or the curve controls the operating speed of trucks compared to the passenger cars. Also, OSMs were developed on horizontal curves after classifying the curves based on the type of superimposed vertical alignment (constant gradients, sag, hog curves), particularly for passenger cars. The radius of curvature was also the most common geometric parameter to influence the operating speed of passenger cars. However, most of the horizontal alignment

characteristics such as the tangent length, superelevation and degree of curvature were not found to be influencing the operating speed of the passenger cars.

Chapter 3

Data Collection and Analysis

3.1 Introduction

This chapter presents the study site description, data collection methodology, and a preliminary analysis of the speed data. The study highway, shown in Figure 3.1, is located in Meghalaya, a north-eastern state of India, and starts at Umiam in Ri-Bhoi District and ends at Mawryngkneng in East Khasi Hills District. This highway was designed as per IRC-SP-48-1998 (Hill Road Manual), and the design speed falls between 30-65km/h. The database required for this study comprised of four parts: roadway geometry details, vehicle speed along the selected sections, daily traffic volume, and the crash data.

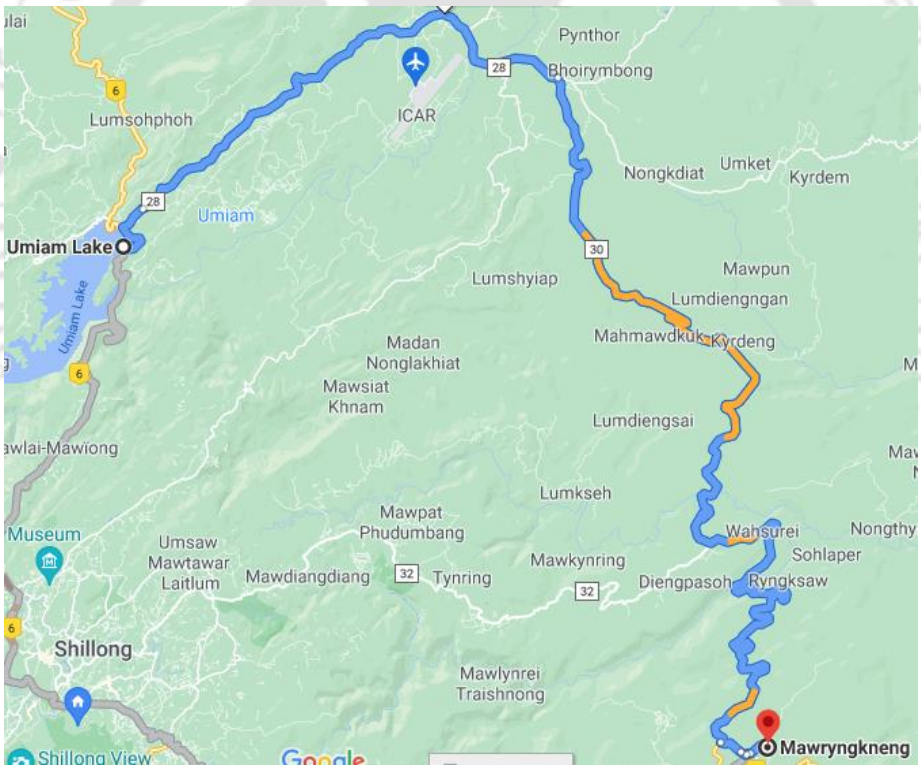

Fig. 3.1 Stretch of the highway selected for the study

3.1.1 Site Description

The road stretch is 48.765 km in length and starts at an elevation of 984.121m above the mean sea level, and goes as low as 871.577m along the stretch, and ends at 1333.507m. It comprises 253 horizontal curves

and 175 vertical curves, with grades ranging from -7 to +7%, and with the curve radius ranging between 35m to 1000m. About 151 horizontal curves are superimposed with either an upgrade or downgrade and 97 of them are superimposed with vertical curves (either sag or hog curves). Eighty-six horizontal curves were selected from the road stretch, and free-flow speed data were collected for both the travel directions, thereby accounting for 172 locations. It was ensured that the identified vehicles were moving freely without any restrictions other than the curve geometry. The horizontal curves were selected based on the following specific criteria.

i. They are situated away from any kind of roadside activity

ii. There should not be any intersection and speed breakers or any obstructions in the vicinity that may cause disturbance to the free-flow speed of a vehicle

iii. Superimposed with different types of vertical alignment (either sag, hog, upgrade, or downgrade)

Figure 3.2 shows a picture of one of the selected horizontal curves from the study area.

Fig. 3.2 A horizontal curve from the study road stretch

The curves were selected for the data collection so that the sample represents all types of horizontal curves constituting the alignment. Figure 3.3 shows the distribution of the curve radius and gradient

corresponding to the sampled and all the curves falling in the alignment. It is evident from the figures that the proportion of the sampled curves, in terms of their radii and gradient, is compatible with the curve radii and gradient adopted in the alignment design.

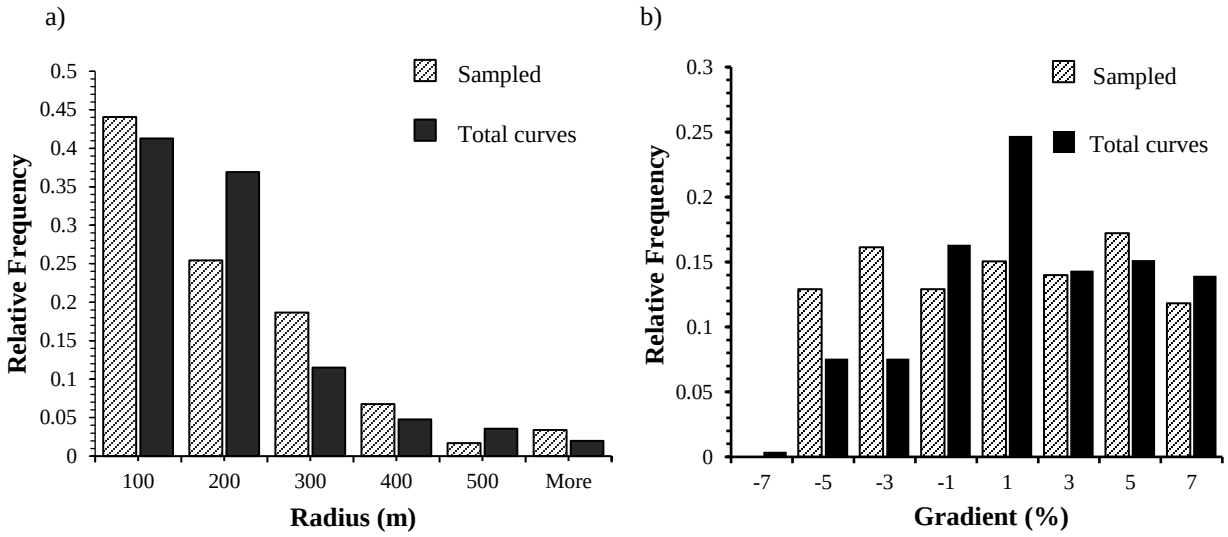

Fig. 3.3 Comparison of the sampled and the actual number of curves, constituting the alignment

Alignment details of the highway were obtained from the National Highway Authority of India (NHAI), Regional Office Guwahati. Table 3.1 shows the statistical summary of the geometric features of 86 horizontal curves considered in the present study. Features shown in the table correspond to both directions of traffic movement. It is evident from the table that the geometric variables are not uniform over the entire highway stretch. Range, mean, and standard deviation of various geometric characteristics exhibit skewed distributions, indicating the possibility of a few elements that are significantly different from the other elements. For e.g., length of the tangent varies between 1 to 322m, but the tangents longer than 150m are very few. Such a non-uniform distribution of geometric features could cause selection bias during operating speed modeling.

Table 3.1 Descriptive statistics of the characteristics of horizontal curves

Characteristic	Symbol	Mean	Range		Std. Dev.
Length of Approach tangent	L_{at}	76.74	1.00	322.28	78.75
Length of exit tangent	L_{et}	64.44	2.00	265.33	60.28
Grade at approach tangent	G_1	0.11	-6.00	6.00	3.86
Grade at start of curve	G_2	0.08	-6.00	7.78	3.95
Grade at middle of curve	G_3	0.00	-6.00	6.58	3.87
Grade at end of curve	G_4	-0.11	-6.00	6.92	3.97
Grade at exit tangent	G_5	-0.18	-6.00	7.00	3.97
Length of vertical curve	L_v	97.30	30.00	200.00	39.61
Rate of vertical curve	K	31.75	14.67	150.00	23.55
Transition length	L_t	36.14	15.00	55.00	11.75
Radius of curvature	R	161.98	57.00	600.00	114.19
Length of curve	L_C	64.32	22.50	213.41	41.46
Rate of Superelevation	e	0.07	0.03	0.10	0.02
Deflection angle	Δ	51.44	4.53	173.14	37.81
Degree of curvature	DC	14.40	2.87	30.17	6.45
Curvature change rate (proposed by Lamm et al. 2007)	CCR_S	379.70	91.47	869.28	168.77
Curvature change rate (Others)	CCR	958.05	123.70	2036.73	510.67
Single lane width	LW	3.77	3.50	5.00	0.57
Interaction between radius and lane width	$R \times LW$	606.35	210.00	2100.00	431.34

All the features corresponding to each direction were obtained from the alignment drawings. Figure 3.4 shows the plan view of the curve no. 189, falling at chainage 34+500 km.

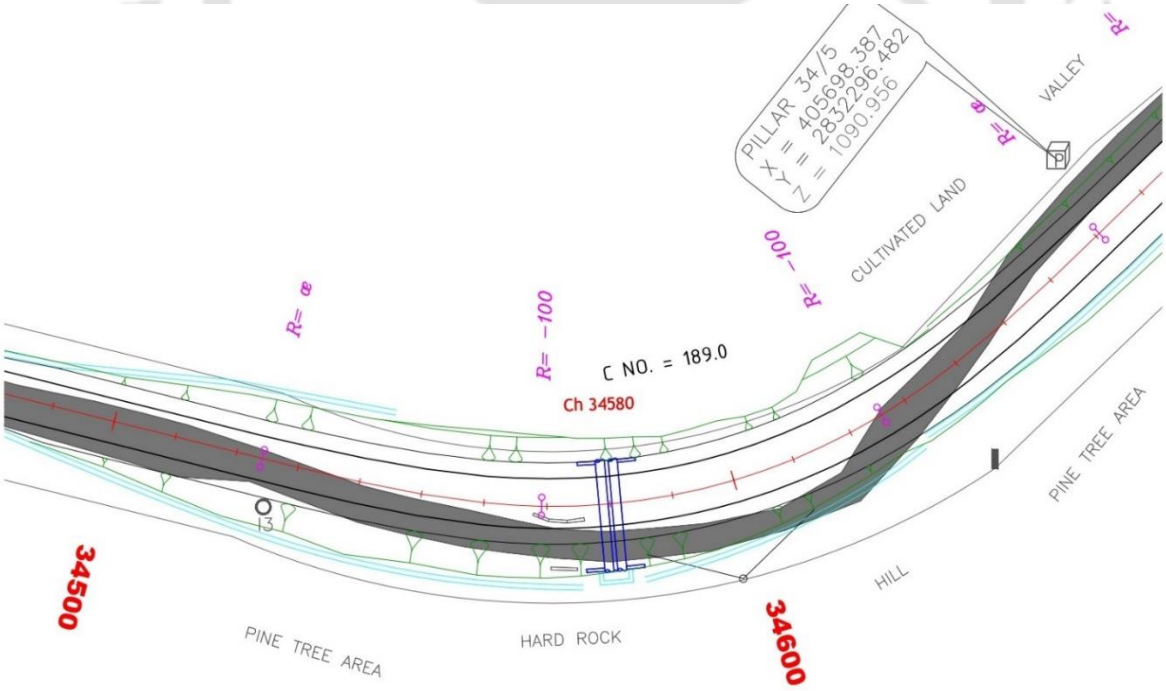

Fig. 3.4 Drawing plan of a horizontal curve

Curvature change rate (CCR_S) proposed by Lamm et al. (2007) and a few other researchers (Cafiso et al. 2010; Llopis-Castelló et al. 2018c; Zuriaga et al. 2010) were considered in this study. Vertical alignment characteristics considered include length, rate of the vertical curve, the gradient at the start, middle, and end of the horizontal curve, the gradient at the midpoint of the approach, and exit tangents (if the tangent length is less than 120m) or 60m ahead of the point of the curve if the tangent length is higher than 120m (Gibreel et al. 2001). Gibreel et al. (2001) mentioned that, at 60m upstream of the point of curvature, the driver might anticipate the effect of the combined alignment.

3.1.2 Speed data Collection

It is necessary to track the operating speed along the tangent and horizontal curve to evaluate the design consistency of the alignment. The free-flow speed data were collected on 93 horizontal curves (60 in the first phase, 33 in the second phase), including the respective entry and exit tangents. However, only 86 horizontal curves were selected from the road stretch since the remaining horizontal curves overlapped with more than one vertical alignment type. The average daily traffic was 2,866 vehicles with 2,347 heavy vehicles, indicating low traffic volumes carried by this highway. The traffic stream on this highway consists of passenger cars, motorized two-wheelers, LCV, buses, and trucks (two-axle, three-axle, and multi-axle trucks). Figure 3.5 shows the average daily composition of the traffic stream. The figure clearly shows that the traffic stream consists of 82% heavy vehicles (58% bus, 2 and 3 axle trucks, and 24% MAV). So, the speed of heavy vehicles and passenger cars were collected.

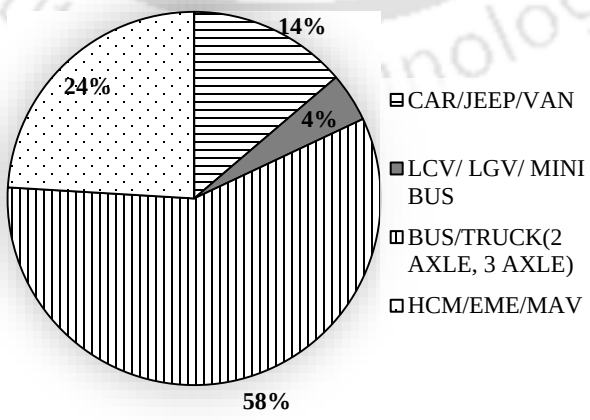

Fig. 3.5 Average daily traffic composition of the traffic stream, observed at chainage 45+000 km

3.1.2.1 Spot speed data collection (Both phases)

The speed data were collected between April and May 2017 and again in May 2018, during daylight and good weather conditions. The spot speed data were collected only for the vehicles moving in free-flow conditions, i.e., not affected by any other vehicle's presence. The observers were asked to collect the spot speed data only when there is no vehicle either following or preceding within a reasonable amount of time (more than 10 seconds). The speed data were collected using the radar guns situated at the five points mentioned below.

i. Middle of the approach tangent (AT) or at a distance of 60m ahead of the transition curve if AT length >120m
ii. Point of the start of the curve (PC)
iii. Middle of the horizontal curve (MC)
iv. Point of end of the curve (PT)
v. Middle of the exit tangent (ET) or at a distance of 60m after the transition curve ends if ET length >120m

Ten spots on each horizontal curve, considering both the directions of travel, were selected to collect the speed data. When the radar guns are used to record speeds, the cosine error occurs if there is a deflection angle between the target and the radar gun/beam. In theory, the radar gun should be aligned with the direction of vehicle movement. However, it is impossible to guarantee that there is no deflection angle in practice. In this study, the observers were asked to align themselves with the lane's centerline and collect the vehicle's speed when it reaches the designated point. Figure 3.6 depicts the points where the speed data were collected using radar guns, along the alignment.

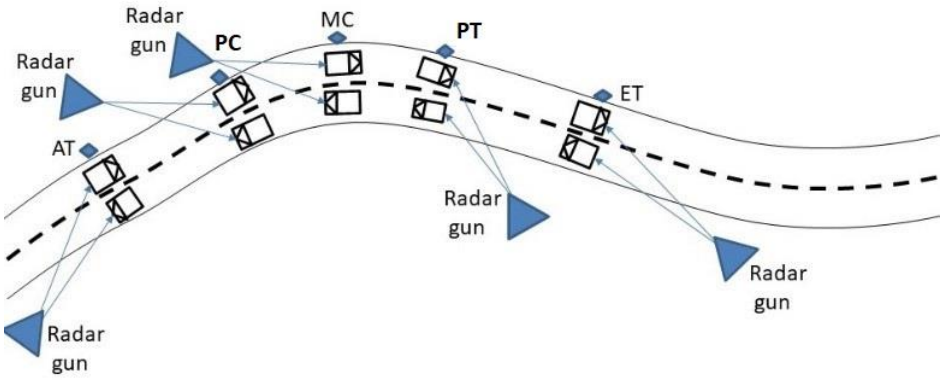

Fig. 3.6 Schematic representation of the data collection points and the observer locations, along the horizontal alignment

At least 30 observations on each vehicle type were collected at all five points of every curve to obtain an acceptable database for model development (Andueza 2000). The five points were obtained using the alignment report provided by NHAI and the chainage markings on the roadside furniture. Location identifiers were placed on both sides of the road, where the spot speed data were collected. Five persons were employed, and each individual was assigned to collect the speed data from one point, for both the travel directions (as shown in Figure 3.6). Moreover, the vehicle type was identified by the individual collecting the speed data.

A preliminary analysis of the trajectories and the operating speed data revealed that the drivers' perception of horizontal curves overlapping with vertical alignment affects the drivers' behavior. Besides, the turning direction of the horizontal curve was also found to influence the drivers' behavior. These observations indicate that it might not be appropriate to model the operating speed with all the curves together, particularly for mountainous roads. Chapter 4 explains the implications of these findings and the consequent clustering of the curves. The horizontal curves were classified based on the superimposed vertical alignment and the horizontal curves' turning direction. The curves were categorized as Left Upgrade, Right Upgrade, Left Downgrade, Right Downgrade, Left Hog, Right Hog, Left Sag, and the Right Sag. Out of the 60 sites covered in the first phase, only 53 sites (106 curves, considering both the travel

directions) fall under these categories. Therefore, the second phase of data collection was conducted based on the modeling requirement for each curve category. Data were collected from another 33 curves in the second phase, i.e., 66 curves when both the travel directions were considered. Table 3.2 summarizes the data collected in both phases for the considered curve categories. The number of curves falling in each category varies across the vehicle type. For example, for left-turning horizontal curves superimposed with vertical hog curve, the number of curves available for modeling the operating speed of passenger cars, empty trucks, and loaded trucks were 22, 17 and 23, respectively. This variation is because at some curves the minimum number of spot speed data of 30 vehicles could not be collected, hence avoided in further modeling.

Table 3.2 Number of curves used for OSM, corresponding to various curve categories

Type	No. of Sites, 1st phase	No. of Sites, 2nd phase	No. of sites used for OSM		
			Passenger Car	Empty Truck	Loaded truck
Left Hog	12	11	22	17	23
Left Sag	11	11	21	22	20
Left Downgrade	15	5	12	14	15
Left Upgrade	14	6	14	15	16
Right Hog	13	11	21	17	24
Right Sag	12	11	20	23	19
Right Downgrade	14	6	16	19	17
Right Upgrade	15	5	15	15	17

3.1.2.2 Speed profile using V- BOX

Besides the spot speed measurements, the trajectories of the instrumented vehicles were collected from the entire study road stretch. This study utilized the V-BOX data acquisition system of RACELOGIC for collecting the trajectory of the vehicle. The V-BOX data loggers provide highly accurate measurements of speed, distance, acceleration, position, and many other derived data. The V-BOX also has the facility to capture the videos of the surrounding traffic. A passenger car and a two-axle empty truck, equipped with the V-BOX data logger (Figure 3.7) were driven over the 48-km road stretch for two and three round trips, respectively. The drivers were asked to maintain their natural driving while traveling on the subject road stretch. The speed and path radius data were also extracted using the RACELOGIC software.

Fig. 3.7 Test vehicle (2-axle empty truck) equipped with V-Box

From the V-BOX, the parameters such as the speed, acceleration, deceleration, the radius of the path adopted by the vehicle, and the surrounding traffic information were obtained. The data was used to verify the variation in the path radius and the actual curve radius. This difference was compared for the left and right turning curves and investigated to explore the variation with the horizontal curve radius. Table 3.3 shows the mean, median, mode and standard deviation of the speed data.

Table 3.3 Speed statistics of instrumented vehicles

Parameters	Passenger car	Empty truck
Mean	63.28	55.11
Median	62.92	54.71
Modal	59.34	46.29
Standard deviation	10.05	7.54

3.1.3 Crash Data Collection

The crash data from December 2013 to September 2018 was collected from the NHAI, Regional Office Guwahati. Detailed information about the crash, including the nature of the injury, location, cause, and direction of vehicle movement were available in the acquired data. The crash report did not provide the timing of the crashes but only the date, hence the entire data was used for analysis. Three hundred forty-eight crashes have occurred during this period, with an average of 75 crashes occurring annually. There were 265 persons who sustained injuries (fatal/serious/minor) out of the total crashes. Many of these crashes

were attributed to the nearby curve, depending on the location of the crash. Crashes that occur on the transition curves or on the tangents within a distance of 10-20m from the transition curves were also attributed to the nearest horizontal curve. Out of the 253 horizontal curves constituting the alignment, crashes have occurred on or near 139 curves, with the number of crashes per curve ranging from 1 to 23. Figure 3.8 represents the nature, classification, vehicles involved, and persons involved in the crashes. The figure shows that run-off-road and overturning are the leading types of crashes observed on the study stretch. The figure also shows that in most crashes, trucks were involved as a primary vehicle causing the crash. Run-off-road and overturning crashes (i.e. crashes involving single vehicles) are linked to the free-flowing vehicles and these two types of crashes observed in the study. This signifies the relevance of operating speed and design consistency on the crash occurrence. Crash data clearly indicates that close to 65% of crashes involve single vehicle. Similar figures were reported for the two-lane low-volume rural highways located in Texas (Fitzpatrick et al. 2002; Rosey and Auberlet 2012).

a)

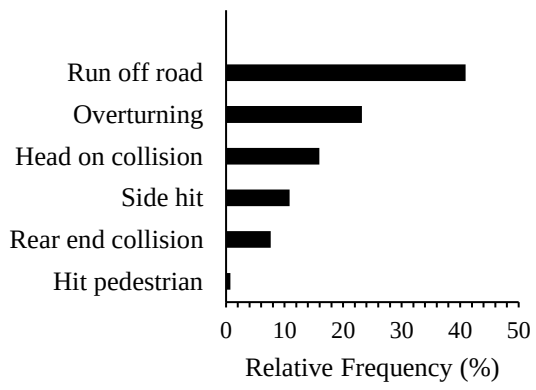

b)

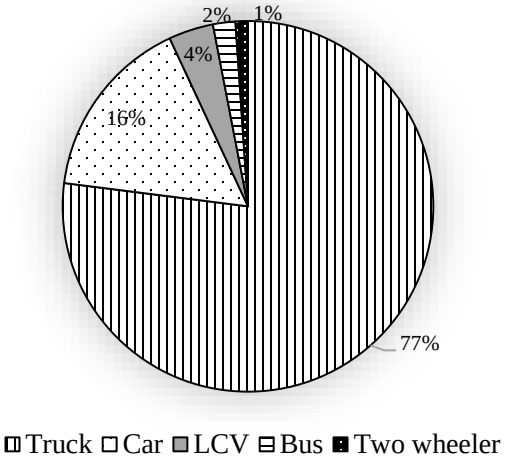

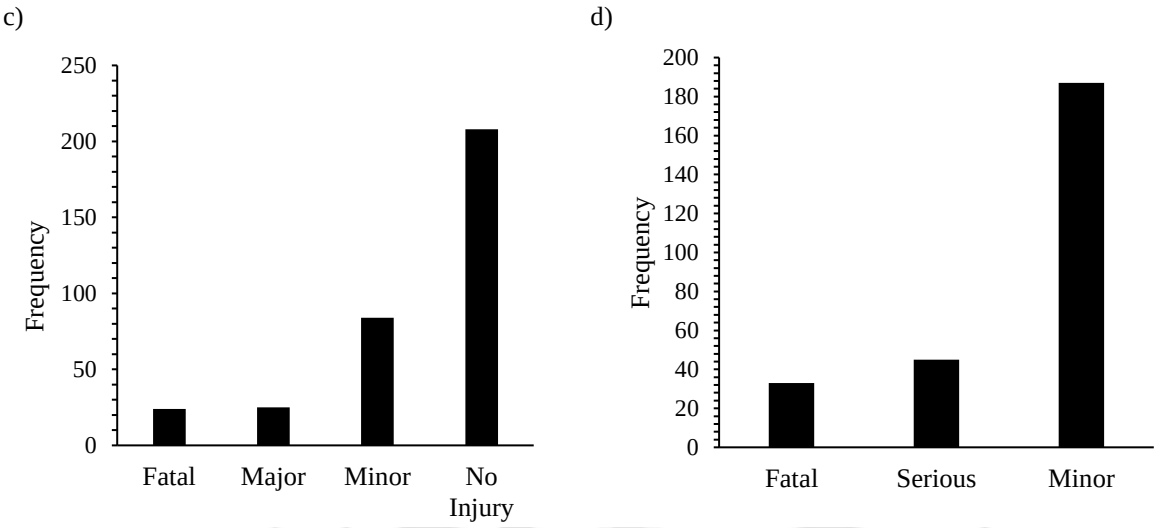

Fig. 3.8 Analysis of the crash data a) Type of crash; b) Percentage of various types of vehicles involved in crashes; c) No of crashes classified as per the severity; d) No. of injured persons classified as per the injury severity

The crash data were segregated according to the type of horizontal curve superimposed with the vertical alignment, along with its turning direction. Table 3.4 shows the number of crashes corresponding to eight types the horizontal curves along with the relevant geometric characteristics.

Table 3.4 Details of the crash data segregated into different curve categories

Curve category	No. of Crashes	No. of curves	Gradient	Length of curve	Radius
Left Downgrade	67	32	-0.3 to -6	24 to 210	35 to 1000
Right Downgrade	57	31	-0.5 to -6	23 to 162	35 to 400
Left hog	23	16	-4.9 to 5.6	28 to 110	55 to 250
Right hog	14	13	-5.6 to 4.5	26 to 143	60 to 600
Left sag	30	21	-6.58 to 5	25 to 213	60 to 500
Right sag	32	20	-4.69 to 6.58	27 to 186	60 to 300
Left Upgrade	36	20	0.5 to 6	12 to 162	37 to 400
Right upgrade	43	22	0.3 to 6	24 to 108	35 to 600

3.2 Database Preparation

This section explains the steps followed in preparing the data for model development. These steps include screening the spot speed data, comparing the mean speed of vehicles belonging to different classes, and the mean speed observed at different points along the curve.

3.2.1 Screening of the spot Speed Data

The outliers in the speed data have been identified and removed using the Quartile analysis. The outliers in the speed data were defined as the speed values that fall outside Speed$^+$ or Speed$^-$, defined as follows.

$$Speed^+ = \max_{v_i}\{v_i \mid v_i < Q_3 + 1.5 \times IQR\} \quad (3.1)$$

$$Speed^- = \min_{v_i}\{v_i \mid v_i > Q_1 - 1.5 \times IQR\} \quad (3.2)$$

Where Q_1, Q_3, and IQR are the 25th percentile speed, 75th percentile speed, and the interquartile range ($IQR=Q_3-Q_1$) at each level, respectively.

Figure 3.9 shows the box plot for passenger cars' speed data corresponding to the mid-point of the curve, for one direction of travel. A similar procedure was adopted for all the remaining speed data collected from all the horizontal curves, and for different vehicle categories.

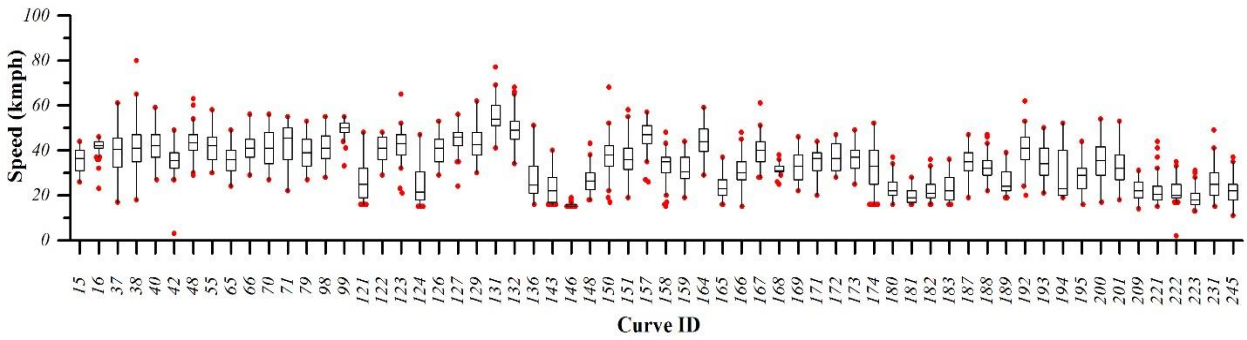

Fig. 3.9 Box plot of speed of passenger car, collected at mid-point of the curve

3.2.2 Normality test

A fundamental property of the free flow speed data of a particular vehicle type is that the observations follow a normal distribution. A normality test was conducted on the data corresponding to the curves where the sample size was less than 100. However, those sites with more than 100 spot speeds meet the minimum sample size requirement for speed study (HCM, 2000). On a few curves, sufficient data could not be obtained during the data collection period due to low traffic volume. Such curves, where the speed observations were less than thirty were avoided from the further analysis. There were some curves where the speed observations were close to thirty. For all those cases, the Kolmogorov-Smirnov test was performed to check the sample size's adequacy (Gong and Stamatiadis 2008). Figure 3.10 shows the

frequency histogram and the normal Q-Q plot corresponding to one such curve where the data were less than 100. The data are normally distributed as indicated by the proximity of the data to the diagonal line. Also, Table 3.5 presents the result of the normality test, with the significance value of the Shapiro-Wilk Test greater than 0.05, proving that there is no evidence showing that the data is not normal.

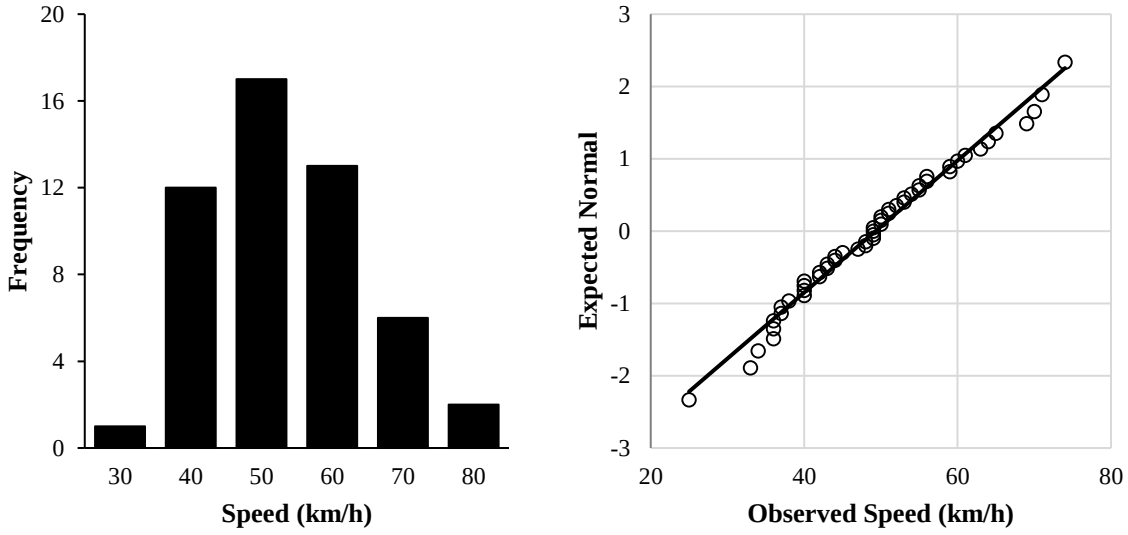

Fig. 3.10 Frequency histogram and Normal Q-Q plot corresponding to spot speeds of passenger car observed at Curve no. 98

Table 3.5 Tests of Normality

Curve no.	Kolmogorov-Smirnov			Shapiro-Wilk		
	Statistic	df	Sig.	Statistic	df	Sig.
98	0.066	51	.200	.982	51	0.642

3.2.3 Calculation of the operating speed

The vehicle's operating speed is represented by the 85th percentile value of the free-flowing speed's cumulative frequency. The cumulative percentages were tabulated, and the 85th percentile speed was determined using a cumulative distribution plot (Figure 3.11).

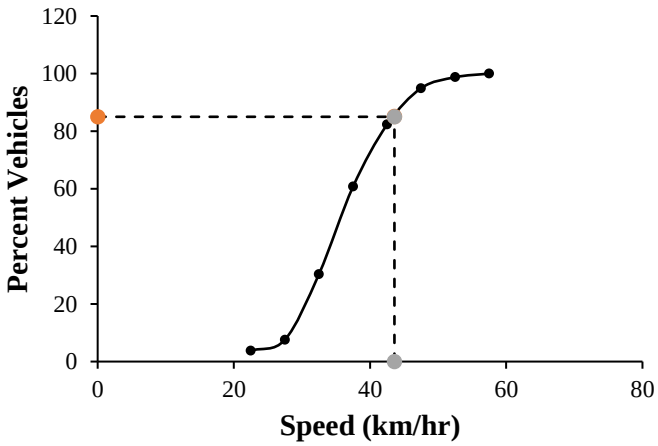

Fig. 3.11 Cumulative distribution of the spot speed data and the 85th percentile speed (Curve no. 243, Loaded truck)

Besides the 85th percentile speed, a few other statistics of the speed distribution, such as the mean speed, minimum and maximum speed, and standard deviation, were also calculated. Table 3.6 shows the statistics of the operating speed corresponding to various vehicle categories. Variability in the operating speed indicates the suitability of the data for further modeling.

Table 3.6 Speed statistics by vehicle category

Parameter	Symbol	Mean	Min (km/h)	Max (km/h)	Std Dev (km/h)
Operating speed of loaded truck	V_{85LT}	38.20	20.75	62.00	9.20
Operating speed of empty truck	V_{85T}	50.33	39	70.65	7.09
Operating speed of passenger car	V_{85C}	58.17	42.00	81.60	8.23

The operating speeds of the three vehicle types, were compared with each other. The operating speed of passenger cars (V_{85C}) was found to be 15km/h higher than operating speed of empty trucks (V_{85T}) for 11.6% of the horizontal curves, but higher than operating speed of loaded trucks (V_{85LT}) for 58.8% of the horizontal curves. This shows the significant difference in operating speed of passenger cars and loaded trucks. Fitzpatrick et al. (1997) studied the relationships between design speed, operating speed, and the posted speed on two-lane rural highways. They found that V_{85} on horizontal curves was less than V_D for all curves with V_D>70 km/h and greater than V_D for most of the curves with V_D<70 km/h. In the present study, the operating speed of the vehicles was compared with the design speed of the road sections (40, 50km/h). Figure 3.12 presents the comparison of the design speed and operating speed corresponding to various

vehicle categories, along with their crash data. The operating speed of passenger cars is higher than the design speed on all the curves whose design speed is 40km/h. When the design speed is 50km/h, operating speeds of passenger cars are lower than the design speed at a few curves (11.6%). For empty trucks the operating speeds are higher than the design speed of 40km/h (88.5%), for curves with a 50km/h, the operating speeds of empty trucks are lower at most of the curves (57.1%). The operating speeds of the loaded trucks was lower at almost all the curves, with a few exceptions (90.3% for 50km/h design speed).

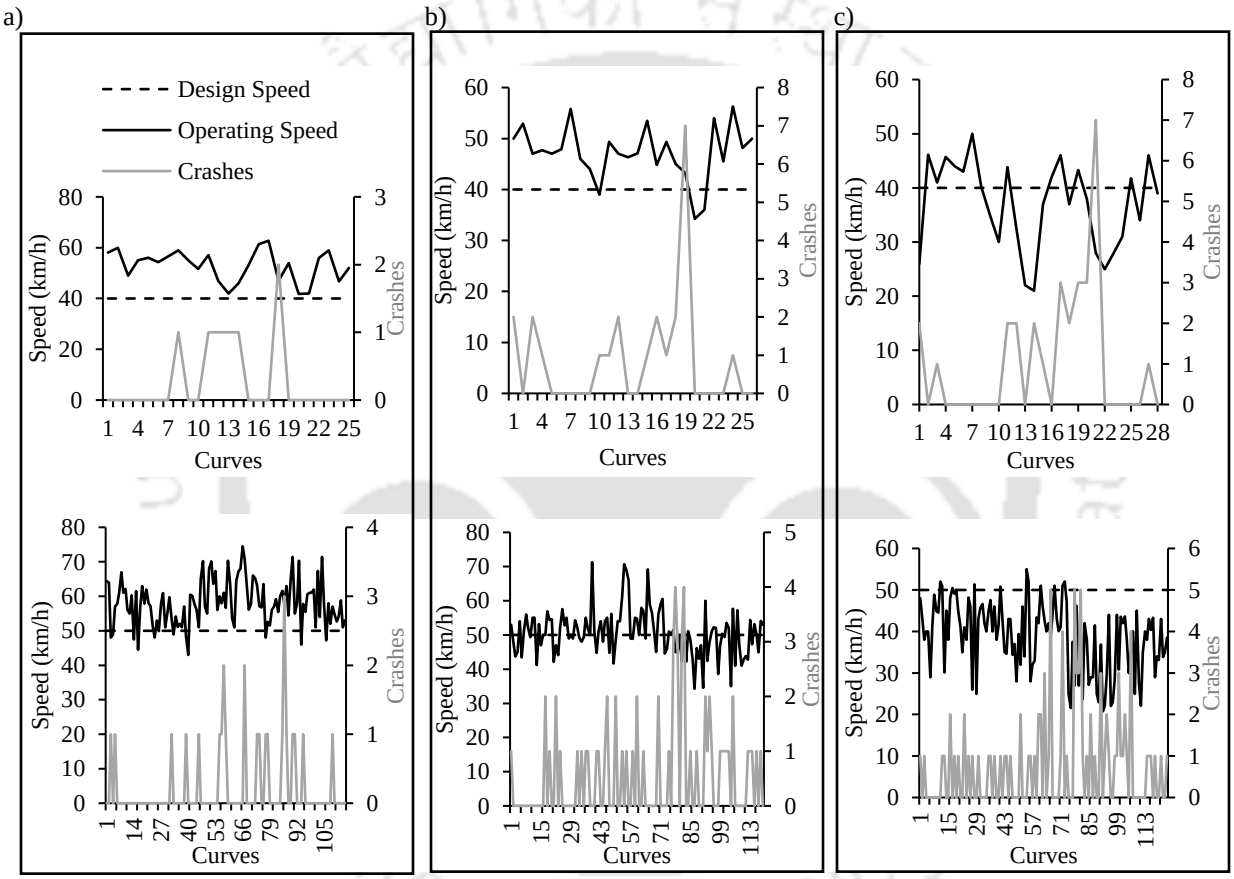

Fig. 3.12 Comparison of the Operating and Design speeds at the sampled curves along with the crash data for a) passenger car b) empty truck, and c) loaded truck

3.2.4 Comparison of the vehicle speeds of different vehicle classes

Passenger cars are the most common type of vehicle classes considered for modeling the operating speed. However, considering the differential effect of road geometry corresponding to mountainous terrain, this study considered empty trucks and loaded trucks also for the operating speed analysis. ANOVA testing

was performed to verify the difference in the mean speeds of passenger cars, empty trucks, and loaded trucks. The following hypotheses were tested.

H_0: The mean speeds of passenger cars, empty trucks, and loaded trucks are the same

The test results rejected the null hypothesis at a 5% significance level. Table 3.7 shows the operating speed of these vehicle types on seven different horizontal curves in the middle of the curve, along with the ANOVA test results with the $F>F_{critical}$ and p-value<0.05. The operating speed for passenger cars, empty trucks, and loaded trucks were modeled separately. The results corresponding to the remaining curves are presented in Appendix, Table A-1.

Table 3.7 Comparison of the operating speeds of passenger car, empty truck and loaded truck at selected curves

Curve No.	V_{85C} (km/h)	V_{85T} (km/h)	V_{85LT} (km/h)	V_{avgC} (km/h)	V_{avgT} (km/h)	V_{avgLT} (km/h)	F	P-value	$F_{critical}$
40	57.2	46	30	46.28	39.4	25.36	25.09	<0.001	3.04
55	62	55.45	50.1	51.60	50.13	45.47	15.90	<0.001	3.04
65	50	44.1	38	42.85	38.79	28.94	34.55	<0.001	3.04
121	56.25	51	35	47.41	37.98	25.97	87.04	<0.001	3.05
123	63.3	54	43	51.84	49.02	34.69	9.37	<0.001	3.08
126	58	48.7	32.75	50.17	41.91	26.22	10.87	<0.001	3.08
129	70.3	65.5	55	58.38	56.75	48.21	19.85	<0.001	3.07

3.2.4 Comparison of the vehicle Speed observed at different points along the curve

The analysis of variance (ANOVA) was carried out to examine the effect of the position along the horizontal curve on the operating speeds. The mean speed values on the three locations along the horizontal curve, which are the start, middle, and end of the curve were compared. Only those curves with a minimum of 30 vehicle was used for this test for accurate results. The ANOVA test results (Table 3.8) failed to reject the null hypothesis, which states that the means of the speed at PC, MC, and PT are same, indicating that there is statistically significant difference between the operating speeds at the three locations of the horizontal curve for majority of the sites ($F>F_{critical}$, $p<0.05$).

Table 3.8 Comparison of the operating speeds of passenger car at PC, MC, PT for right turning horizontal curve superimposed with hog curve

Curve no.	V_{85PC} (km/h)	V_{85MC} (km/h)	V_{85PT} (km/h)	V_{avgPC} (km/h)	V_{avgMC} (km/h)	V_{avgPT} (km/h)	F	P-value	$F_{critical}$
37	55	60	59	44.64	49.13	49.51	**8.30**	**0.0003**	**3.02**
75	50	52	50	42.81	45.45	44.11	**4.26**	**0.0149**	**3.02**
90	44	43	40	37.31	35.77	32.91	**7.51**	**0.0007**	**3.02**
105	51.55	51	64	40.91	44	53.29	**28.607**	**<0.0001**	**3.04**
118	60	51.65	54	46.62	39.94	41.77	**5.25**	**0.006**	**3.04**
15	54	57.8	47	44.10	46.59	37.13	**23.174**	**<0.0001**	**3.02**
47	64.1	44.55	61	54.87	38.5	48.48	**78.69**	**<0.0001**	**3.02**
56	55	57.15	55.45	48.24	49.39	47.28	2.34	0.09	3.02
61	46	48	47	40.53	42.01	41.22	1.28	0.28	3.02
65	54	49.9	48	44.6	42.63	40.71	**7.003**	**0.0011**	**3.02**
79	58	57	54	48.94	47.99	44.74	**7.5**	**0.0007**	**3.02**
98	60.25	60.1	55.6	49.49	47.24	44.61	2.87	0.059	3.05
100	53.1	54.25	57	42.40	43.09	47.40	**6.26**	**0.0023**	**3.04**
121	56.35	55	57.5	45.15	45.8	45.19	0.05	0.95	3.05
122	72.6	70.1	73.1	60.82	56.77	56.64	1.35	0.26	3.07
162	68	57.8	66.1	55.22	44.14	53.62	**7.51**	**0.0009**	**3.07**
165	44	42	47	38.91	36.08	41.86	**17.256**	**<0.0001**	**3.05**
250	51.6	52.7	54	41.03	42.23	43.39	0.71	0.49	3.06
253	58	53.05	60.55	46.28	70.95	67.65	**8.21**	**0.0004**	**3.05**

Table 3.9 shows that 68.4% of the curves belonging to right turning curves superimposed with hog curve have the speed of passenger cars statistically different at PC, MC, and PT. The same test was conducted for the speed of the vehicles on all the curve categories. Table 3.9 shows the percentage of curves that have the speed of the vehicles statistically different at PC, MC, and PT. The speed of passenger cars is statistically different for all the categories, except for Left Upgrade, Right Downgrade, and Right Upgrade. The number of curves for testing the speeds of empty truck is too low, hence the results do not interpret a concrete conclusion. Whereas, the speeds of loaded truck are statistically different for all the categories, except for Right Downgrade and Right Sag. Table 3.9 shows that 50-60% of the curves for each category are having statistically different speed. This indicates that, the modeling based on the location corresponding to the lowest operating speed cannot be applied to the remaining 40 to 50% of the curves where the differences are not statistically significant. Also, the speed estimation for the remaining curves that were not considered in modeling might get complicated. Hence, the present study carried out the modeling of operating speed corresponding to the middle of the curve, with the assumption that speed is constant throughout the horizontal curve.

Table 3.9 Percentage of Curves having statistically different and same mean speeds at PC, MC, PT for different curve categories and vehicle types

Curve Type	Vehicle								
	Passenger Car			Empty Truck			Loaded Truck		
	Total curves	Diff speed (%)	Same speed (%)	Total curves	Diff speed (%)	Same speed (%)	Total curves	Diff speed (%)	Same speed (%)
Left Downgrade	11	54.5	45.5	5	60	40	11	54.5	45.5
Left Hog	16	62.5	37.5	5	60	40	17	52.9	47.1
Left Sag	17	58.8	41.2	5	28.6	71.4	16	62.5	37.5
Left Upgrade	10	40	60	3	66.7	33.3	13	61.5	38.5
Right Downgrade	12	33.3	66.7	8	75	25	13	46.2	53.8
Right Hog	19	68.4	31.6	2	0	100	22	77.3	22.7
Right Sag	18	61.1	38.9	7	100	0	17	41.2	58.8
Right Upgrade	10	40	60	3	33.3	66.7	15	60	40

3.3 Applicability of the existing models

The applicability of the existing operating speed models developed for passenger cars as well as trucks on the highways passing through mountainous terrains was studied. Operating speed data corresponding to the mid-point of the horizontal curve and approach tangent was considered for this purpose. Geometric parameters such as radius, curve length, superelevation, deflection angle, the degree of curvature, and gradient were used to evaluate the existing operating speed models. The model parameters were estimated with 80% of the data and validated using the remaining 20%.

The geometric features and speed data were used to estimate a few existing models (presented in Table 3.10). The models proposed by Donnell et al. (2001), Gibreel et al. (2001), Lamm et al. (2007), Llopis-Castelló et al. (2018c) and others were used for this purpose. These models are meant for predicting the operating speed of passenger cars and trucks on mountainous terrains.

Table 3.10 Operating speed models meant for mountainous terrain

Author	Vehicle	Section	Model
Al-Maseid et al. (1995)	Passenger Car	Tangent	$115-\frac{3722}{L_{at}}-0.70\left(\frac{\Delta_1\times\Delta_2}{\Delta_1+\Delta_2}\right)$
	Light Truck	Tangent	$106-\frac{3391}{L_{at}}-0.73\left(\frac{\Delta_1\times\Delta_2}{\Delta_1+\Delta_2}\right)$
	Truck	Tangent	$99.3-\frac{3099}{L_{at}}-0.75\left(\frac{\Delta_1*\Delta_2}{\Delta_1+\Delta_2}\right)$
Andueza	Passenger Car	Tangent	$100.69-\frac{3032}{R}+27.819L_{at}$
Donnell et al. (2001)	Truck	Curve	$75.1+0.0176R-1.48G_5-0.00836L_{et}$
		Tangent	$56.1+0.117R-1.15G_1-0.0060L_{at}-0.000097(L_{at}\times R)$
Lamm et al. (2007)	Passenger Car	Curve	$105.31+0.071CCR_S+2\times10^{-5}CCR_S^2$
Gibreel et al. (2001)	Passenger Car	Curve with sag	$76.42+0.023R+2\times10^{-4}K^2-0.008\exp(A)-1.23\times10^{-4}L_O^2+0.062\exp(e)$
		Curve with hog	$26.44+0.251\sqrt{R}+10.318\ln(L_V)-0.423G_1+\frac{6.462}{\ln(A+1)}+0.051\exp(e)-0.028L_O$
		Tangent for sag	$91.81+0.010R+0.468\sqrt{L_V}-0.006G_1^3-0.878\ln(A)-0.826\ln L_O$
		Tangent for hog	$82.29+0.003R-0.05\Delta+3.441\ln(L_V)-0.533G_1+0.017\exp(e)-0.000097L_O^2$
Llopis-Castelló et al. (2018c)	Loaded Truck	Curve	($G\leq4.23\%$): $75.96-\frac{44.56}{e^{0.00685R}}$
		Curve	($G>4.23\%$): $75.96-\frac{44.56}{e^{0.00685R}}-5.06(G-4.23)$
	Empty Truck	Curve	($G\leq3.19\%$): $85.02-\frac{60.62}{e^{0.0124R}}$
		Curve	($G>3.19\%$): $85.02-\frac{60.62}{e^{0.0124R}}$ -1.95(G-3.19)

Table 3.11 shows the estimated models, along with the R^2 value and the root mean square error (RMSE). Besides this, the table indicated the geometric variables that are not statistically significant.

Table 3.11 Parameter Estimates corresponding to the existing operating speed models

Author	Vehicle	Section	Model	R^2	RMSE
Al-Maseid et al. (1995)	Passenger Car	Tangent	$60.07-\frac{21.02}{L_{at}}+42.94\left(\frac{\Delta_1\times\Delta_2}{\Delta_1+\Delta_2}\right)$	0.24	8.51
	Light Truck	Tangent	$48.005-\frac{3.10}{L_{at}*}+45.43\left(\frac{\Delta_1\times\Delta_2}{\Delta_1+\Delta_2}\right)$	0.26	6.39
	Truck	Tangent	$37.87-\frac{6.31}{L_{at}*}+34.5\left(\frac{\Delta_1\times\Delta_2}{\Delta_1+\Delta_2}\right)$	0.07	9.43
Andueza (2000)	Passenger Car	Tangent	$60.39-\frac{238.73}{R*}+53.43L_{at}$	0.28	6.98
Donnell et al. (2001)	Truck	Curve	$45.151+0.0283R-0.0283G_5*-0.0042L_{et}*$	0.24	12.32
		Tangent	$49.15+0.0028R*-0.608G_1+0.0093L_{at}*+0.000101(L_{at}\times R)*$	0.43	6.41
Lamm et al. (2007)	Passenger Car	Curve	$74.527+0.0747CCR_S+7.22\times10^{-5}CCR_S^2$	0.3	5.55
Gibreel et al. (2001)	Passenger Car	Curve with sag	$82.14*+0.043R+8.9\times10^{-5}K^2*-0.084\exp(A)*+4.71\times10^{-4}L_O^2*+27.7\exp(e)*$	0.48	3.42
		Curve with hog	$43.77*+1.344\sqrt{R}-4.46\ln(L_V)*-0.216G_1*+\frac{0.022}{\ln(A+1)}*+14.5\exp(e)*-7.7\times10^{-5}L_O*$	0.49	5.48
		Tangent for sag	$53.47+0.041R+0.427\sqrt{L_V}*-0.025G_1^3+3.14\ln(A)*-0.528\ln L_O*$	0.57	6.96
		Tangent for hog	$-25.21*+0.059R*-0.04\Delta*-0.29\ln(L_V)*-0.117G_1*+71.26\exp(e)*-0.00052L_O^2*$	0.19	5.77
Llopis-Castelló et al. (2018c)	Loaded Truck	Curve	($G\leq4.23\%$): $49.551-\frac{19.2}{e^{0.00685R}}$	0.15	7.02
		Curve	($G>4.23\%$): $35.856-\frac{8.817}{e^{0.00685R}*}-1.012(G-4.23)$	0.33	5.06
	Empty Truck	Curve	($G\leq3.19\%$): $55.188-\frac{19.22}{e^{0.0124R}*}$	0.13	3.04
		Curve	($G>3.19\%$): $51.994-\frac{18.8}{e^{0.0124R}}-0.451(G-3.19)$	0.29	3.58

* Indicates variables that are not statistically significant

Although these RMSE values are acceptable, most of the important geometric variables are not statistically significant at a 95% confidence level. The tangent length, the gradient of the approach tangent, length of the vertical curve, and horizontal curve are some of the variables found to be statistically not

significant. These variables are commonly observed to be significant in the operating speed models for mountainous terrain. Hence, this study has further analyzed the reasons behind the insignificance of such variables in modeling the operating speed. As explained earlier, the applicability of field data and the complexity of driver perception towards the combined alignment need to be further analyzed. The following chapters addressed these issues.

Chapter 4

Clustering of Curves

4.1 Introduction

Operating speed is widely considered the most significant geometric design consistency measure (Fitzpatrick 2000; Poe and Mason 2000). Identifying the critical factors that affect the operating speed is essential in geometric design consistency analysis (Camacho-Torregrosa et al. 2013; Krammes et al. 1995) and safety assessment (Fink L et al. 1995). The geometric details of a highway are the primary factors that control a driver's operating speed decisions (Wang et al. 2014). Also, driver and vehicle characteristics, weather conditions, and geographic location affect the operating speed. Most of the previous studies focused on modeling the operating speed as a function of geometric parameters. A majority of those studies proposed terrain-specific operating speed models (Castro et al. 2011; Llopis-Castelló et al. 2018c; Misaghi and Hassan 2005). However, a single operating speed model is appropriate only if the driver's perception of the geometry is consistent throughout the road alignment, passing through a particular terrain. More specifically, errors in the driver's perception caused by complex highway geometry should be minimal. Indeed, the perception variability increases as the complexity of the geometry increases. Thus, for mountainous terrain, the operating speed models need to consider the differences in the driver's perception of the road geometry.

Researchers believe that about 80-90% of the driving tasks are performed based on visual information and subsequent perceptions (AASHTO 2010; Kowler 2011). Drivers may obtain varied visual information while traveling on roads with complex geometries. Several researchers found that the superimposed horizontal and vertical alignments result in varying driver perception (Bidulka et al. 2002; Hassan et al. 2002; Hassan and Easa 2003). Thus, it is essential to study the effect of superimposed curves on drivers' perception and, consequently, their preferred operating speed. However, the driver's perception is a latent variable and is challenging to measure. One of the most common practices for studying human

perception is to analyze the response patterns that reflect this perception. Thus, the identification of appropriate response patterns is essential for analyzing the driver's perception.

Previous studies have carried out driving performance measurements with the help of instrumented vehicles. The results were measured in terms of such as speed distribution and related statistics (Fitzpatrick et al. 2000c), speed profile, longitudinal and transversal acceleration profile, and curvature of driving path (Cafiso et al. 2003, 2004, 2005). Using a test vehicle, two studies (Said et al. 2006, 2007) also investigated at how highway geometric features, particularly horizontal curves, effected driving behavior in terms of trajectory, steering angle, rate of change of steering angle, and lateral shift. They aimed to improve highway design by comparing the investigated parameters to the actual geometric alignment and identifying differences in order to identify discrepancies in the design procedure in terms of driving behavior.

The present study analyzed the significance of the driver's perception of the road geometry on operating speed. As shown in the following sections, field data collected in this study indicated that the drivers' speed and path radius reflect the driver's perception of the geometry. Further analysis showed that the curve direction and the superimposed vertical curve significantly influence the driver's perception. Therefore, this chapter proposes an approach to cluster the curves on the basis of driver perception for highways passing through mountainous terrain. The highway alignment was clustered into eight groups considering the curve direction and the horizontal and vertical alignment combination. Before-and-after studies revealed that the clustering of curves was useful in developing a better operating speed model.

4.2 Driver's Perception Analysis

Clustering the curves is a challenging task, and numerous approaches are available for this purpose. Machine learning algorithms are useful for such clustering, but these algorithms require large quantities of data. However, most of the previous studies related to OSM clustered the curves based on geometric parameters (e.g., Donnell et al. 2001; Fitzpatrick et al. 2000b; Gibreel et al. 2001). Since driver perception plays a significant role in speed choice, it is essential to consider this aspect when clustering the curves. As discussed in the previous section, driver perception is not quantifiable, but it can be captured through the

driver's response pattern. The present study analyzed the driver response in terms of speed variation and the path radius. The differences in the operating speed, difference between the adopted and actual radius of curvature, and geometric parameters affecting the operating on left-and right-turning direction of horizontal curve were investigated to measure the driver behavior. The combined effect of the horizontal curve direction and the superimposed vertical alignment was also investigated by analyzing the difference in the adopted and actual radius of curvature. A logical clustering of the curves was performed based on the factors influencing the driver perception.

4.3 Impact of Curve Direction on Driver Perception

This section analyzes the impact of curve direction on the driver's perception. First, the perception difference was quantified by analyzing the differences between operating speeds on the left- and right-turning curves with similar geometric features. Besides, the path radii were also analyzed to study the impact of curve direction on driver perception. The latter part of this section presents the correlation analysis of the operating speed and various geometric parameters.

4.3.1 Analysis of Speed Variability

The perception of a driver towards the left- and right-turning curves reflects in her/his speed decisions, consequently operating speed. A driver's speed decision on a curve profoundly depends on several psychological factors, such as perceived safety and mental workload. The speed data collected on a flat horizontal curve (Curve no. 159) was used to understand the perception differences. The selected curve was flat (<3%), 162 m long, and had a radius of 70 m. Figure 4.1 shows the variation in operating speeds of different vehicle types at various points on the entry tangent, curve, and exit tangent. There was a significant difference in the operating speeds of the vehicles while turning left and right.

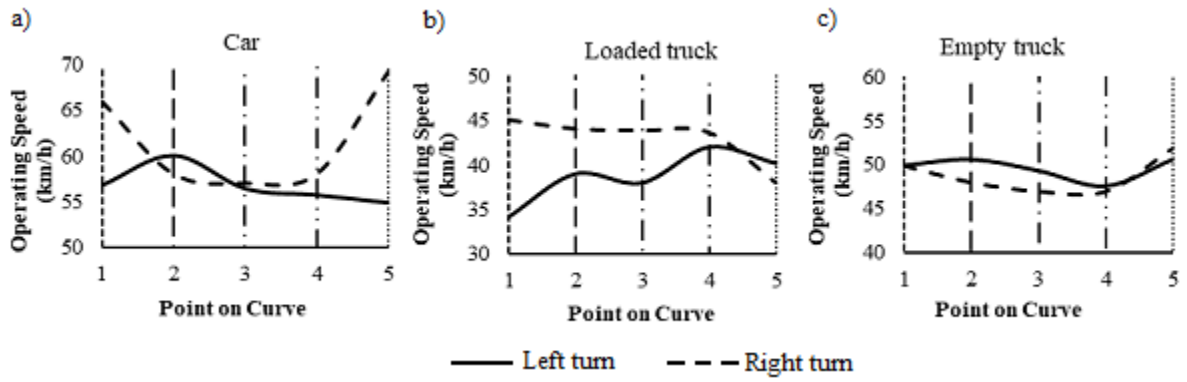

Fig. 4.1 Operating speed for a) passenger car b) empty truck c) loaded truck at various points on entry tangent, PC, MC, PT and exit tangent

To verify the above findings, the free flow data from an instrumented vehicle was also studied. A passenger car and an empty truck were equipped with the V-BOX and driven along the study stretch during the free-flowing conditions. Figures 4.2 shows the speed profiles of the free-flowing passenger car and empty truck extracted from the V-Box. The figures clearly show a substantial difference in the operating speed performance of the vehicles while turning left and right for the same curve geometry.

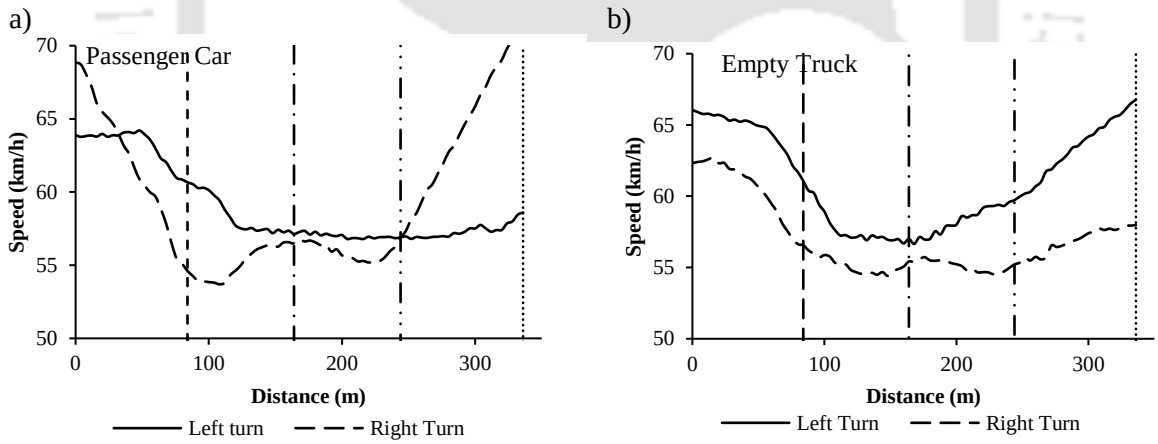

Fig. 4.2 Speed profile along the tangent and the subsequent curve of a) passenger car b) empty truck

A statistical test for the operating speed based on Crammer's theory of the sample quantiles' asymptotic distribution was used to check the significance of operating speed differences for left- and right-turning curves (Hou et al. 2012).

$$Z = \left(\frac{V_{85}^{L} - V_{85}^{R} - 0}{1.530\sqrt{\frac{S_L^2}{n_L} + \frac{S_R^2}{n_R}}} \right) \tag{4.1}$$

The V_{85}^{L}, V_{85}^{R} are the operating speeds on the left and right turning curves, s_L^2, s_R^2 are the sample variances, and n_L, n_R are the sample sizes. The obtained p-values were checked at 95% confidence level for operating speed of the Left and Right population quantiles of all the vehicles.

Table 4.1 lists the statistical test results of the null hypothesis stating that the operating speeds are the same on the left- and right-turning of the same flat horizontal curve (Curve no. 159). For passenger cars, the operating speeds on left- and right-turning curves were statistically different at entry and exit tangent. Speeds adopted by empty trucks were statistically different at PC and MC, whereas loaded trucks had a significant difference at the entry tangent, PC, and MC.

Table 4.1 Statistical comparison of the operating speeds on the left and right turning curves

Vehicle Type	Point on Curve		V_{85}	S^2	n	Z	P
Passenger Car	Entry tangent	*L*	56.75	58.55	26	-2.377	0.0008
		R	66	126.49	30		
	PC	*L*	60	71.78	20	0.538	0.295
		R	58.05	68.78	34		
	MC	*L*	56.4	54.49	23	-0.197	0.421
		R	57	57.78	36		
	PT	*L*	55.7	27.32	23	-0.773	0.219
		R	58	82.96	32		
	Exit tangent	*L*	54.85	22.90	22	-4.47	<0.0001
		R	69.35	110.51	32		
Empty Truck	Entry tangent	*L*	49.95	81.44	28	0.013	0.49
		R	49.9	40.40	15		
	PC	*L*	50.65	32.19	50	2.138	0.016
		R	47	13.21	22		
	MC	*L*	49.35	28.52	52	1.445	0.074
		R	47	17.99	31		
	PT	*L*	47.6	15.06	37	-0.159	0.43
		R	48	29.75	13		
	Exit tangent	*L*	50.7	23.74	43	-0.476	0.31
		R	51.9	75.32	35		
Loaded Truck	Entry tangent	*L*	34.15	42.45	40	-6.122	<0.0001
		R	45	28.85	103		
	PC	*L*	39	62.47	26	-1.875	0.03
		R	43.6	16.06	97		
	MC	*L*	38	45.81	28	-2.736	0.003
		R	43.8	25.14	89		
	PT	*L*	42	67.81	31	-0.839	0.2
		R	44	27.14	107		
	Exit tangent	*L*	40.2	47.09	29	0.946	0.17
		R	38	56.06	82		

Note: *L*=Left, *R*=Right

4.3.2 Analysis of Difference between Adopted Path Radius and the actual Curve Radius

The impact of the curve direction was analyzed through the path radius adapted by the drivers. Usually, the actual curve radius and the vehicle path radius on the curve are not equal. Several studies have reported that the radius of the vehicle path deviates from the design radius of the horizontal curve (Xu et al. 2018; Ben-Bassat and Shinar 2011). A few trajectories of a passenger car and an empty truck were collected using the VBOX data acquisition system to verify the variation in the path radius. VBOX was used to obtain the speed and the radius adopted by the driver. 'Speed' is the speed of the instrumented vehicle at a particular point of the highway which is calculated directly at the reference antenna. 'Radius of turn' is a term used when extracting the data from the VBOX, representing the path radius of the instrumented vehicle. It

indicates the average turning radius that the vehicle takes to cover a horizontal curve. 'Distance' is the accumulated total distance in meters with reference to the starting point. Figure 4.3 (a) shows the variation in speed and radius over a section of the road stretch and Figure 4.3 (b) shows the speed and path radius corresponding to curve number 4. The curve was identified through the trajectory obtained from the VBOX software and shown in. The length of the transition curve, horizontal curve, approach, and exit tangents of the curve of each site were obtained from the design drawings. The start of the horizontal curve was defined on the Racelogic VBOX program's trajectory plot using the dimensions of tangents, transition and the horizontal curve. The beginning up to the end of each horizontal curve was carefully chosen. There were significant differences in the length of curve and the distance covered by the vehicle for that curve. Also, there were noticeable difference in the path radius of the vehicle from the actual radius. This arose since the vehicles were not following the road's exact route, which is usually the lane's centerline.

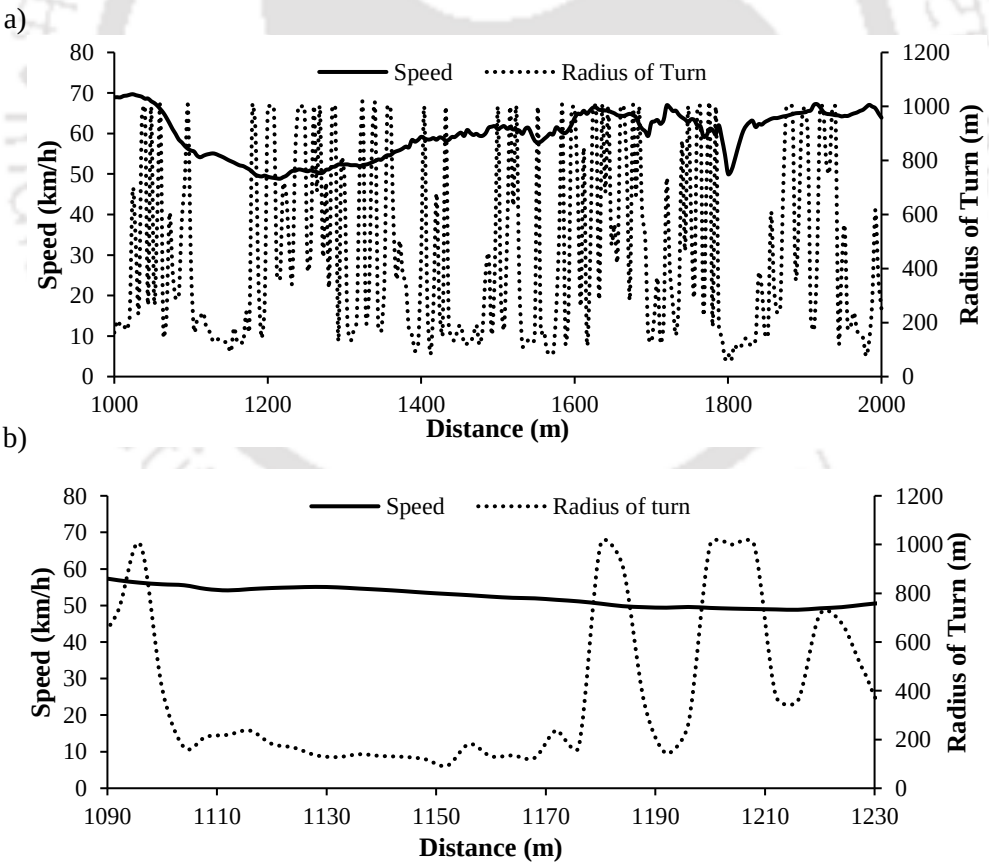

Fig. 4.3 Speed and Path radius extracted from VBOX for a) a section of the road stretch b) Curve no. 4

Table 4.2 shows the vehicle characteristics obtained from Curve no. 4. Data such as speed, acceleration, and the radius of the test vehicle's turn (passenger car) are shown in this table. These data were collected for all the test vehicles, and for all the curves, falling in the alignment. Traffic conditions ahead of the test vehicle were captured through a video camera mounted on the test vehicle. Only the data corresponding to free-flowing conditions were used for further analysis.

Table 4.2 Speed, acceleration and path radius adopted by Passenger car, on Curve no. 4 (Radius 170m)

Parameters	Start	End Value	Difference	(Max)	(Min)	Average
Speed (km/h)	55.55	51.24	-4.31	55.622	51.24	53.83
LatAcc (m/s^2)	-0.082	-0.118	-0.036	-0.078	-0.206	-0.15
LongAcc (m/s^2)	-0.06	-0.041	0.019	0.025	-0.061	-0.025
Radius of Turn (m)	441.51	373.83	-67.68	446.272	128.903	209.451

The difference in the radius of the actual path followed by the vehicle and radius of the curve was analyzed for both the left turning and right turning curves. Data collected from the flat horizontal curves (grade < 3%) were considered in the initial analysis. The difference in the actual curve radius and the path radius (Figure 4.4) were compared for the left and right turning curves. Figure 4.4 shows the variation of the difference in radius with respect to the curve radius. The average difference in the radii show a distinctive trend for left and right-turning curves (Figure 4.4). It can be observed that for a smaller radius range, the mean of differences in the radii was less (say R<100m, the difference is 10m for passenger car), and it increases with the curve radius (say R>300m, the difference is 150m for passenger car). The vehicles were observed to operate at a higher speed on the horizontal curves of higher path radius and follow a comfortable higher radius relative to the actual curve radius. However, vehicles were found to be travelling at lesser speed on horizontal curves with a smaller radius to safely negotiate the curve, resulting in a relatively smaller difference between the adopted and the actual radius. An interesting finding is that, the difference between the adopted and the actual radius is higher for the passenger car (152m) than the empty truck (107m), for a curve with 300m radius. This could be attributed to the difference in the mechanical characteristics of passenger car and empty truck. Besides, the difference between the two radii is higher for left turning curves (152m) than the right turning (142m) for passenger cars, whereas the opposite is

observed for empty trucks (left turn with 86m and right turn 107m). This may be due to difference in the sight distances available for the drivers of passenger car and empty truck.

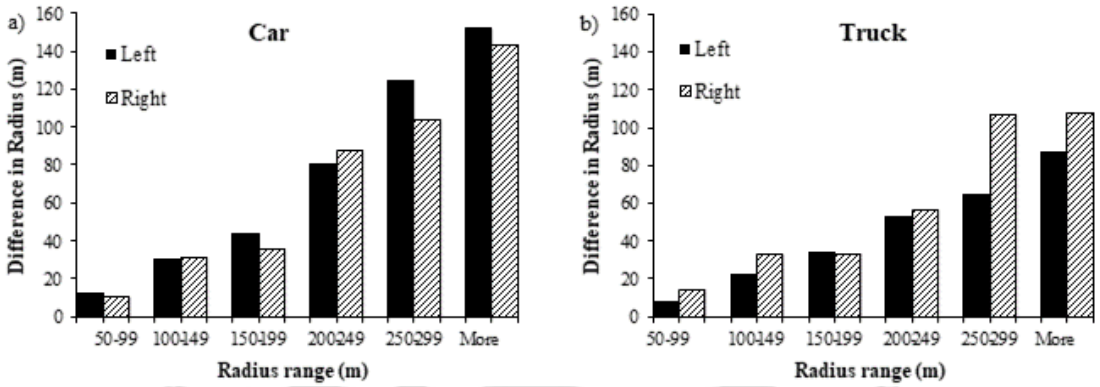

Fig. 4.4 Variation of radii difference for left and right turning curves, for a) passenger car b) empty truck

A two-sample t-test was performed to confirm whether the difference between the radius of the chosen path and the actual radius differ statistically for the left- and right-turning curves. Table 4.3 summarizes the results of the t-test. The results clearly indicate that the curve direction has a significant influence on the chosen path. Table 4.3 confirms the difference in radii, at a 95% confidence level, for almost all the ranges of curve radius. This further indicates that the turning direction of the curve has an impact on the vehicle operations. Moreover, for passenger cars, the difference between curve and path radius was relatively more for left-turning curves, whereas the trend was opposite for empty trucks. These analyses indicate that the driver perception differs with curve direction as well as vehicle class.

Table 4.3 Statistical comparison of the path radius for left and right turning of empty trucks and passenger cars

Radius Range (m)	Empty Truck			Passenger Car		
	t stat	t-Critical	P-value	t stat	t-Critical	P-value
50-99	4.72	2.06	<0.001	-2.99	2.09	0.01
100-149	4.51	2.01	<0.001	-1.35	2.03	0.17
150-199	-1.76	2.06	0.09	-2.45	2.18	0.03
200-249	3.27	2.10	0.004	-2.67	2.26	0.03
250-299	2.86	2.10	0.01	-2.41	2.20	0.03
More>300	2.88	2.45	0.028	-3.88	2.45	0.01

The influence of gradient along with the hog and sag curves was considered and the variation in the path radius is shown in the Appendix, Figure A-1. For both left and right turning directions, the path radius changes with the actual radius as well as with the gradient corresponding to sag and hog curves, both for passenger car and truck. This signifies the influence of gradient along the hog and sag curves on the path radius of the vehicles.

4.3.3 Correlation Analysis of the Geometric Parameters and Operating Speed, based on the turning direction of the curve

This section presents the correlation between various geometric parameters and the operating speed. Strength of the linear association among the dependent and explanatory variables was captured through Pearson's correlation matrices. The correlation analysis provides information about the magnitude of the association, or correlation, as well as the direction of the relationship between the geometric variables with the operating speed. Akoglu (2018) have interpreted the strength of the correlation based on the correlation coefficient and classified as moderate (0.30–0.39), strong (0.40–0.69), and very strong (above 0.70).

Table 4.4 Correlation matrix of the Operating speed and the geometric variables, without classifying the curves

	L_t	L_c	e	Δ	R	L_{at}	L_{et}	DC	G	V_{85C}	V_{85T}	V_{85LT}
L_t	1											
L_c	0.20	1										
e	0.89	0.13	1									
Δ	0.75	0.65	0.62	1								
R	-0.82	-0.07	-0.80	-0.60	1							
L_{at}	-0.22	0.23	-0.23	-0.03	0.29	1						
L_{et}	-0.02	0.17	-0.07	-0.03	0.08	-0.23	1					
DC	0.85	0.17	0.75	0.80	-0.84	-0.22	-0.17	1				
G	0.00	0.00	0.00	0.00	0.00	-0.01	0.01	0.00	1			
V_{85C}	**-0.51***	-0.03	**-0.42***	**-0.50***	**0.61***	0.24	0.11	**-0.66***	-0.17	1		
V_{85T}	**-0.34**	-0.09	-0.29	**-0.38**	**0.43***	0.13	0.15	**-0.48***	**-0.34**	0.79	1	
V_{85LT}	-0.20	-0.03	-0.23	-0.23	0.29	0.18	0.00	-0.28	**-0.41***	0.63	0.78	1

Note: Bold*=Strongly correlated; Bold=Moderately Correlated

Table 4.4 provides the correlation matrix before clustering and the values clearly indicate that the correlation between geometric parameters and operating speed was not strong.

Many researchers have investigated the influence of curve direction on the operating speed (e.g., Liu et al. 2017; Misaghi and Hassan 2005). Misaghi and Hassan (2005) have considered the curve direction as a binary variable for modeling the operating speed. It is evident from Tables 4.5 and 4.6 that the

geometric parameters have a differential impact on the operating speed on the left- and right turning curves. This indicates that, a single model for all horizontal curves cannot capture the operating speed variability. The operating speeds of all the three vehicle types, that are turning left on the horizontal curves are influenced by geometric variables such as transition length (L_t), superelevation *(e)*, deflection angle (Δ), radius of curvature (R), and degree of curvature (DC). The operating speeds of empty and loaded trucks are also affected by the gradient (G) besides the above variables. However, on the right turning curves, the variables DC and G are the only parameters influencing the operating speed of the empty trucks, while G is the only variable affecting the loaded trucks. This implies that, separating the horizontal curves based on turning direction is necessary as the variables affecting the operating speed of the different types of horizontal curves are different. Hence, it was decided to consider the direction of the curve as a clustering criterion.

Table 4.5 Correlation matrix of the Operating speed and the geometric variables for the left-turning horizontal curves

	L_t	L_c	e	Δ	R	L_{at}	L_{et}	DC	G	V_{85C}	V_{85T}	V_{85LT}
L_t	1											
L_c	0.20	1										
e	0.89	0.13	1									
Δ	0.75	0.65	0.62	1								
R	-0.82	-0.07	-0.80	-0.60	1							
L_{at}	-0.25	0.22	-0.25	-0.05	0.30	1						
L_{et}	0.01	0.19	-0.05	-0.02	0.06	-0.23	1					
DC	0.85	0.17	0.75	0.80	-0.84	-0.24	-0.15	1				
G	0.21	0.05	0.21	0.15	-0.18	-0.04	-0.13	0.22	1			
V_{85C}	**-0.62***	-0.17	**-0.48***	**-0.62***	**0.70****	0.29	0.07	**-0.76****	-0.17	1		
V_{85T}	**-0.50***	-0.16	**-0.41***	**-0.52***	**0.56***	0.16	0.19	**-0.65***	**-0.31**	0.80	1	
V_{85LT}	**-0.40***	-0.19	**-0.38**	**-0.45***	**0.47***	0.19	0.01	**-0.49***	**-0.37**	0.61	0.71	1

Note: Bold**=Very strongly correlated; Bold*=Strongly correlated; Bold=Moderately Correlated
DC=Degree of Curvature; e=Super elevation; G=Grade; L_{at}=Length of entering tangent; L_{et}=Length of exit tangent; L_c=Length of Curve; L_t=Transition length; R=Curve radius; V_{85C}=Operating speed of the car; V_{85LT}=Operating speed of loaded truck; V_{85T}=Operating speed of empty truck; Δ=Deflection angle

Table 4.6 Correlation matrix of the Operating speed and the geometric variables for the right-turning horizontal curves

	L_t	L_c	e	Δ	R	L_{at}	L_{et}	DC	G	V_{85C}	V_{85T}	V_{85LT}
L_t	1											
L_c	0.20	1										
e	0.89	0.13	1									
Δ	0.75	0.65	0.62	1								
R	-0.82	-0.07	-0.80	-0.60	1							
L_{at}	-0.20	0.25	-0.21	-0.01	0.27	1						
L_{et}	-0.04	0.16	-0.09	-0.05	0.09	-0.23	1					
DC	0.85	0.17	0.75	0.80	-0.84	-0.20	-0.19	1				
G	-0.21	-0.05	-0.21	-0.15	0.18	0.01	0.15	-0.22	1			
V_{85C}	**-0.40***	0.12	**-0.35**	**-0.36**	**0.50***	0.18	0.16	**-0.55***	-0.15	1		
V_{85T}	-0.16	-0.02	-0.17	-0.23	0.29	0.11	0.11	**-0.31**	**-0.37**	0.77	1	
V_{85LT}	-0.02	0.12	-0.08	-0.01	0.13	0.16	0.00	-0.08	**-0.45***	0.64	0.85	1

Note: Bold*=Strongly correlated; Bold=Moderately Correlated

4.4 Impact of Superimposed Vertical alignment on the Driver Perception

Several researchers have observed that the drivers cannot perceive the actual curve geometry, specifically when the horizontal curve is superimposed with a vertical curve. A few studies have considered the type of superimposed vertical alignment as a criterion for clustering the curves (Donnell et al. 2001; Gibreel et al. 2001; Abdul-Mawjoud and Sofia 2008; Morris and Donnell 2014; Llopis-Castelló et al. 2018c). The road alignment considered for the present study has about 61% of horizontal curves superimposed with upward/ downward gradients and about 39% of horizontal curves superimposed with sag/hog curves.

The present study analyzed the effect of a superimposed vertical alignment on the operating speed. Straight upgrade, straight downgrade, hog, and sag curves were the vertical alignment characteristics considered for this purpose. The combined effect of curve direction and the superimposed vertical alignment was studied by analyzing the difference in the adopted and actual curve radius. A separate analysis was performed for each curve combination and direction. Figures 4.5 and 4.6 show the differences in curve and path radius for passenger cars and empty trucks, respectively. Analysis of the difference in radii could not be made for the loaded trucks since the V-BOX data was not collected for this vehicle type.

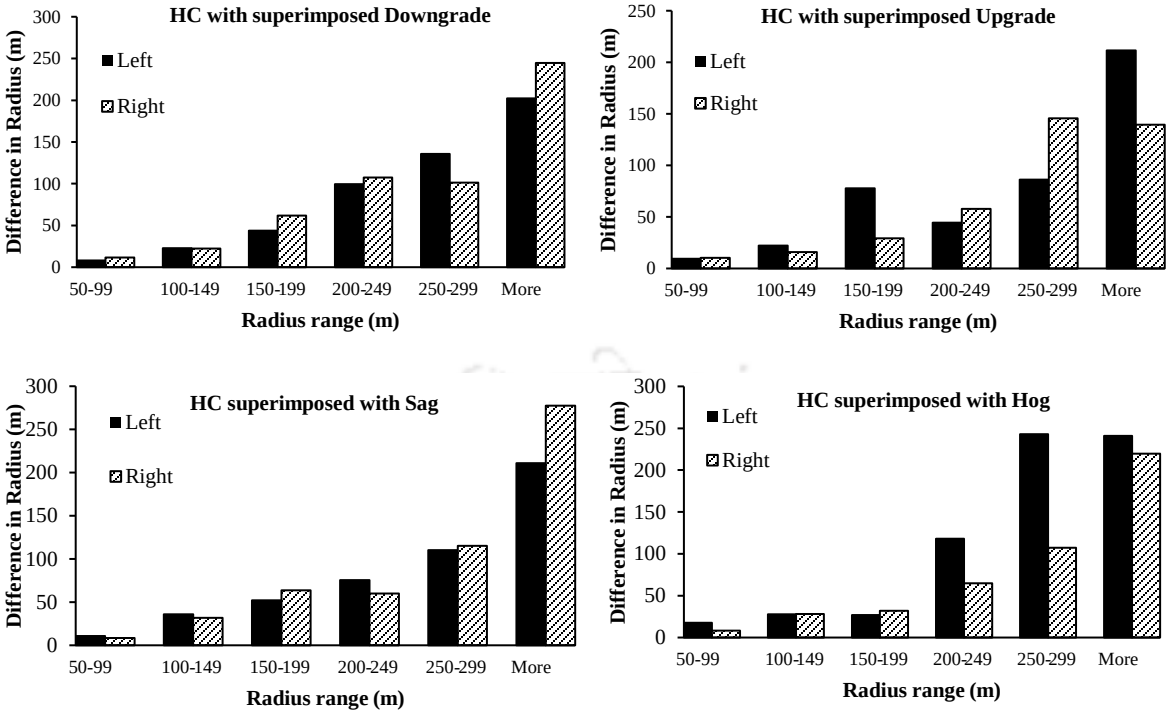

Fig. 4.5 Variation in the average difference in the curve and path radius for the left and right turning curves for different types of horizontal and vertical alignment, for Passenger car

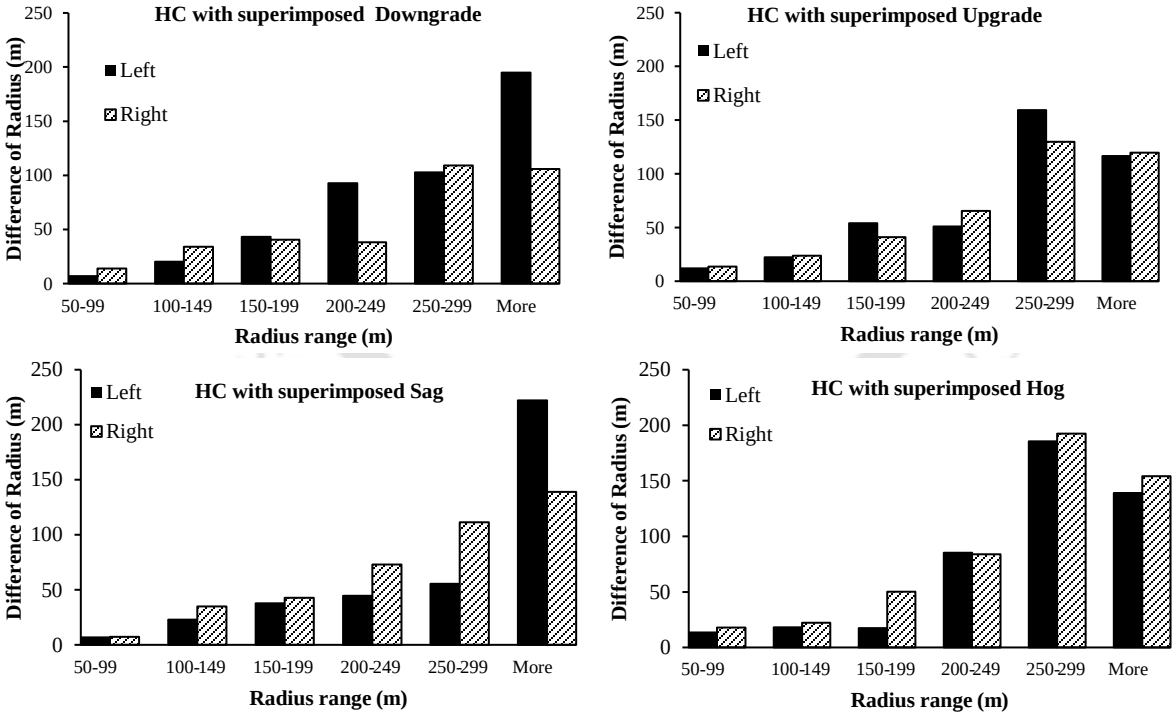

Fig. 4.6 Variation in the average difference in the curve and path radius for the left and right turning curves, for different types of Horizontal and Vertical alignment, for Empty Truck

In general, the path radius adopted by drivers increase with the increasing curve radius. Furthermore, the trends in Figures 4.5 and 4.6 indicate that the drivers were more cautious on the sharp curves. In case of the horizontal curve with a radius less than 100m and superimposed with a downgrade, the difference in the adopted radius and the actual radius is relatively less (8 and 11m) for the left and right turning curves, respectively. Drivers tend to follow the design radius of the curve, thereby controlling their operating speed to negotiate the sharp curves safely. In comparison, a higher difference (202 and 244m) was observed in case of horizontal curves with a radius of more than 300m. These differences for horizontal curves superimposed with a vertical alignment were greater when compared with the horizontal curves of flat gradient. This implies that the difference in driver perception of the horizontal curves varies based on the gradient. The difference between the path radius and curve radius was statistically tested for all the curve combinations. Tables 4.7 and 4.8 show the test results for passenger cars and empty trucks. The results indicate that the chosen vehicle path significantly depends on the vertical alignment.

Table 4.7 Statistical comparison of the path radius adopted by Passenger car, on left and right turning curves of different types of horizontal and vertical alignment

Radius Range (m)	Downgrade			Upgrade			Sag			Hog		
	$t_{stat.}$	$t_{Crit.}$	P-value	$t_{stat.}$	$t_{Crit.}$	P-value	$t_{stat.}$	$t_{Crit.}$	P-value	$t_{stat.}$	$t_{Crit.}$	P-value
50-99	-6.40	2.06	0.00	-0.32	2.06	0.75	1.72	2.13	0.10	1.67	2.14	0.11
100-149	1.61	2.03	0.11	1.49	2.04	0.14	1.02	2.14	0.32	-0.25	2.08	0.79
150-199	-2.20	2.22	0.05	2.23	2.22	0.05	-1.82	2.17	0.09	1.66	2.30	0.13
200-249	-1.93	2.44	0.10	-0.65	2.26	0.53	3.92	3.18	0.03	3.20	2.30	0.01
250-299	6.43	2.77	0.00	-3.41	3.18	0.04	-0.38	2.77	0.71	1.95	4.30	0.18
More	-6.60	2.20	0.00	2.25	2.26	0.05	-4.32	2.22	0.00	2.19	2.57	0.08

Table 4.8 Statistical comparison of the path radius adopted by Empty trucks, on left and right turning curves of different types of horizontal and vertical alignment

Radius Range (m)	Downgrade			Upgrade			Sag			Hog		
	$t_{stat.}$	$t_{Crit.}$	P-value	$t_{stat.}$	$t_{Crit.}$	P-value	$t_{stat.}$	$t_{Crit.}$	P-value	$t_{stat.}$	$t_{Crit.}$	P-value
50-99	1.01	2.03	0.31	0.34	2.03	0.73	-0.81	2.11	0.42	-2.01	2.06	0.05
100-149	-4.73	2.00	0.00	-1.57	2.01	0.12	-4.75	2.09	0.00	0.53	2.05	0.59
150-199	-2.01	2.13	0.06	2.37	2.10	0.03	-1.29	2.13	0.21	-2.36	2.10	0.03
200-249	22.16	2.20	0.00	-6.98	2.22	0.00	-3.04	4.30	0.09	-0.54	2.11	0.59
250-299	0.81	2.30	0.43	-4.20	2.57	0.01	-5.73	2.57	0.00	0.59	2.77	0.58
More	10.02	2.07	0.00	5.27	2.14	0.00	3.41	2.14	0.00	2.52	2.36	0.03

4.5 Clustering of Curves

The criteria mentioned in the above sections, i.e., the curve direction and the type of superimposed vertical alignment, could be adequate to capture the driver perception's while driving on a highway passing through mountainous terrain. Based on these criteria, the curves were clustered into eight groups (Figure 4.7). Certain past studies considered some of these combinations. For example, Liu et al. (2017) reported that the turning direction is significant for horizontal curves superimposed with the hog curves. Wang et al. (2014) studied the combination of a horizontal curve and a straight downgrade and identified the significant factors influencing the operating speed. Figure 4.7 shows the representative sketches for all the eight categories of curves considered in the present study.

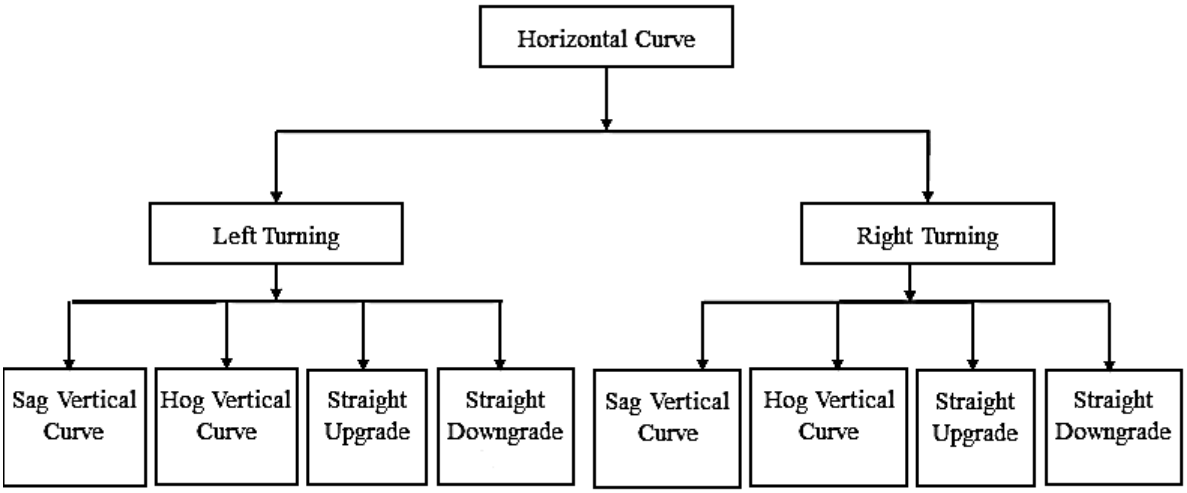

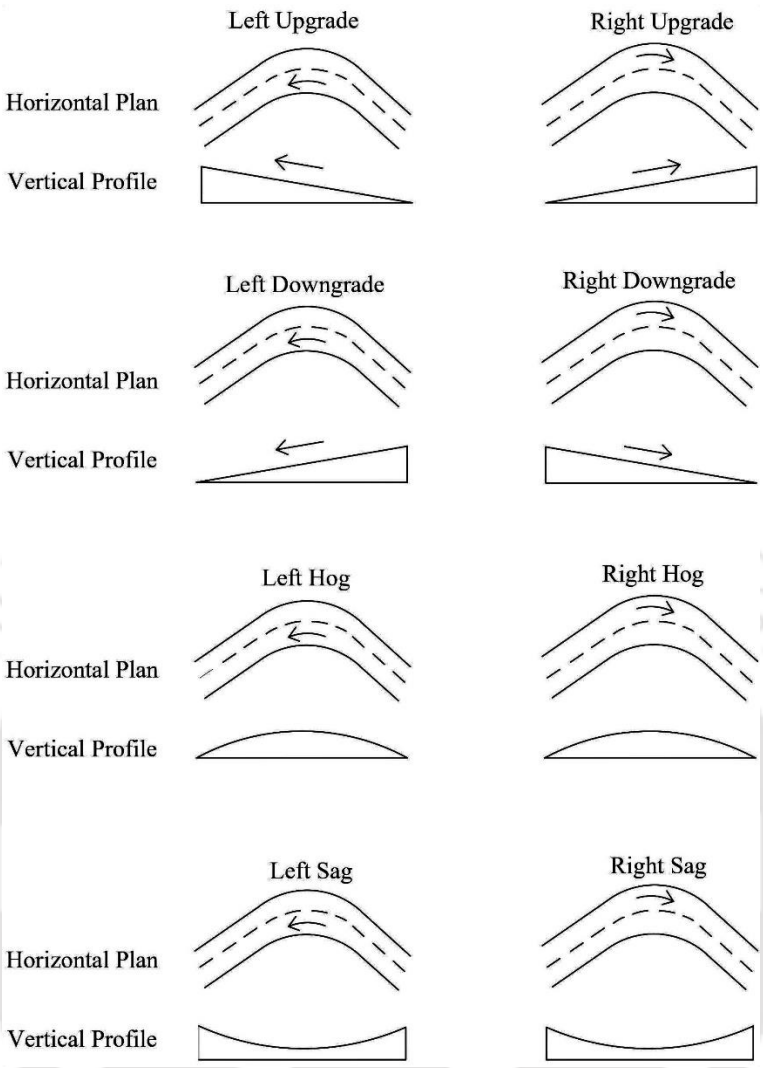

Fig. 4.7 The typical plan and profile of the curves considered for operating speed analysis

Table 4.9 shows the details of the radius and gradient corresponding to the 86 curves (for Umiam to Jowai travel direction).

Table 4.9 Ranges of Radius and Gradient of the 86 curves group under the 8 curve categories

Category	Left downgrade	Right downgrade	Left hog	Right hog	Left sag	Right sag	Left upgrade	Right upgrade
Gradient (%)	-4.75 to -0.3	-5.7 to -3	-3.52 to 5.6	-2.04 to 4.03	-6.58 to 3.68	-4.69 to 5.33	0.5 to 6	3.5 to 6
Radius (m)	100 to 600	60 to 350	60 to 250	90 to 150	80 to 170	65 to 500	70 to 500	80 to 300

4.6 Geometric Parameters Affecting the Operating Speed

This study conjectured that the weak correlation of the geometric parameters with the operating speed could be due to the difference in driver perception. To validate this conjecture, correlation analysis was performed after clustering the horizontal curves superimposed with the straight grades. Table 4.10 presents the correlation coefficients for the operating speed and various geometric parameters. Similarly, Table 4.11 provides the correlation coefficients corresponding to the horizontal curves superimposed with the vertical curves (hog/sag curves). Both the tables indicate that the correlation between the operating speed and geometric parameters has substantially improved after clustering the curves. In addition, after clustering, many relevant geometric parameters were found to be strongly correlated with the operating speed. Variables such as L_{at}, $L_{et,}$ and L_V were found to be significant variables for developing operating speed models of Passenger cars. Similarly, L_{at}, L_{et}, L_V, $L_{C,}$ and e were found to influence V_{85T}, while L_{at}, L_{et}, e, R, and Δ were found to influence V_{85LT}. Hence, it is evident that, clustering the curves based on the driver perception can significantly improve the operating speed models.

Table 4.10 Correlation matrix for the horizontal curves with straight grades

Cluster	V_{85}	L_t	L_c	e	R	Δ	DC	G	L_{at}	L_{et}
Left-Upgrade	V_{85C}	**-0.70****	-0.11	**-0.62***	**0.85****	**-0.45***	**-0.78****	-0.03	**0.52***	-0.04
	V_{85T}	**-0.58***	0.09	**-0.46***	**0.62***	-0.24	**-0.62***	**-0.32**	0.27	-0.12
	V_{85LT}	**-0.45***	-0.11	**-0.57***	**0.48***	-0.26	**-0.45***	-0.13	0.08	-0.07
Left-Downgrade	V_{85C}	**-0.54***	**-0.42***	**-0.47***	**0.56***	**-0.66***	**-0.66***	**-0.42***	-0.07	0.31
	V_{85T}	-0.28	-0.21	**-0.30**	**0.36**	**-0.37**	**-0.40***	-0.26	-0.28	0.28
	V_{85LT}	**-0.33**	**-0.70****	**-0.30**	**0.40***	**-0.49***	**-0.37**	0.24	**-0.58***	-0.21
Right-Upgrade	V_{85C}	0.08	-0.06	0.13	-0.07	-0.06	-0.01	-0.09	0.14	**-0.51***
	V_{85T}	0.20	**-0.48***	0.25	-0.17	-0.03	0.15	**-0.33**	0.03	**-0.60***
	V_{85LT}	0.29	**-0.33**	**0.33**	-0.29	0.10	0.25	**-0.38**	0.04	**-0.54***
Right-Downgrade	V_{85C}	**-0.63***	-0.20	**-0.69***	**0.71****	**-0.49***	**-0.71****	0.26	0.00	**0.49***
	V_{85T}	**-0.44***	-0.09	**-0.54***	**0.61***	**-0.37**	**-0.62***	0.07	0.02	**0.35**
	V_{85LT}	**-0.49***	0.01	**-0.63***	**0.57***	-0.28	**-0.59***	**0.30**	-0.11	**0.35**

Note: Bold**=Very strongly correlated; Bold*=Strongly correlated; Bold=Moderately Correlated

Table 4.11 Correlation matrix for the horizontal curve superimposed with vertical curves

Cluster	V_{85}	L_t	L_c	e	R	Δ	DC	L_v	G	L_{at}	L_{et}
Left-Sag	V_{85C}	**-0.50***	**-0.68***	**-0.30**	**0.61***	**-0.72****	**-0.64***	**-0.42***	-0.28	0.22	0.06
	V_{85T}	**-0.47***	**-0.72****	**-0.33**	**0.71****	**-0.72****	**-0.69***	**-0.59***	-0.15	0.09	0.02
	V_{85LT}	-0.25	**-0.48***	-0.19	**0.68***	**-0.46***	**-0.52***	-0.22	-0.15	0.18	-0.02
Left-Hog	V_{85C}	**-0.72****	-0.17	**-0.58***	**0.68***	**-0.78****	**-0.83****	**-0.67***	**-0.40***	-0.18	-0.14
	V_{85T}	**-0.60***	**-0.46***	**-0.83****	**0.66***	**-0.80****	**-0.77****	**-0.85****	**-0.52***	0.00	0.26
	V_{85LT}	0.15	**0.30**	-0.05	0.10	-0.01	-0.14	-0.19	**-0.83****	**-0.65***	**0.41***
Right-Sag	V_{85C}	**-0.83****	**-0.56***	**-0.77****	**0.75****	**-0.77****	**-0.82****	**-0.52***	-0.16	0.13	**0.37**
	V_{85T}	**-0.33**	**-0.35**	**-0.38**	**0.63***	**-0.37**	**-0.41***	-0.20	**-0.53***	**-0.30**	**0.49***
	V_{85LT}	-0.19	-0.09	**-0.30**	**0.48***	-0.13	-0.24	0.12	**-0.50***	-0.13	**0.40***
Right-Hog	V_{85C}	**-0.54***	-0.22	**-0.62***	**0.56***	**-0.70****	**-0.73****	**-0.91****	0.19	0.13	0.00
	V_{85T}	-0.19	-0.23	**-0.43***	0.20	**-0.45***	**-0.43***	**-0.78****	-0.09	**0.38**	-0.08
	V_{85LT}	-0.06	-0.13	-0.27	-0.02	**-0.30**	-0.25	**-0.61***	-0.23	**0.50***	0.01

Note: Bold**=Very strongly correlated; Bold*=Strongly correlated; Bold=Moderately Correlated
L_v=Length of the vertical curve

4.7 Summary and Conclusions

This section analyzed the importance of driver perception of highway geometry in modeling the operating speed. It was assumed that the curve direction and the superimposed vertical alignment influence the driver perception and the operating speed. The assumption was statistically tested using the differences in driver response patterns such as operating speed variations and the chosen path radius. Results confirmed the influence of curve direction and the type of superimposed vertical alignment on driver perception. It was found that the drivers of both passenger car and empty truck were adopting the actual radius in case of sharp curve radius, but their paths tend to have a larger radius than the actual (difference of 26 to 77m), as the radius of the curve increases beyond 150m. Based on these findings, the curves were clustered into eight categories. The correlation between the geometric parameters and operating speed has significantly improved after clustering.

Moreover, the number of geometric variables influencing the operating speed also increased, indicating that operating speed decisions are more influenced by driver perception of curve geometry. The highly correlated variables after clustering for V_{85C} were L_{at}, $L_{et,}$ and L_V; for V_{85T} were L_{at}, L_{et}, L_V, $L_{C,}$ and $e_{;}$ and finally for V_{85LT} were L_{at}, L_{et}, e, R, and Δ.

For the curves superimposed with straight grades, the rate of super-elevation, the degree of curvature, and the curve radius have a shown a strong linear association with the operating speed. Several studies have used the degree of curvature (*DC*) in place of radius (*R*) as the former has shown a relatively stronger linear association with the operating speed. However, this study revealed that selecting either the degree of curvature or radius as a model parameter depends on the vehicle type and the curve geometry. For example, in the case of a left-turning curve superimposed with a straight upgrade, *R* had a higher correlation with passenger cars' operating speed. It was also found that the length of the vertical curve was highly correlated with the operating speed for the majority curve clusters (sag/hog) and all the vehicle types. Therefore, it is evident that the clustering of curves could elicit the effect of several relevant geometric variables. The proposed approach can improve the operating speed models, leading to better consistency studies. The impact of curve direction on the operating speed is directly related to the driving style followed in a country. Hence, the proposed approach can be extended to study driver perception for right-side-driving conditions as well.

Chapter 5

Development of the Operating Speed Models

5.1 General

This chapter presents the development of the operating speed models considering the interaction between the driver, vehicle, and complex highway geometry. The hypothesis was that this complex interaction could be captured through proper clustering of the horizontal curves based on the superimposed vertical alignment geometry. In this process, it was realized that the curve clustering could result in sampling bias. The present study proposes a weight estimation procedure to capture the effect of selection bias. The results indicate that the curve-clustering and the consideration of selection bias resulted in an improved operating speed model.

5.2 Identification of geometric variables for modeling the operating speed

The important geometric variables were identified through Pearson correlation analysis. A total of 172 data sets, collected from eighty-six horizontal curves, were used for this purpose. As discussed in Chapter 4, the curves were clustered into eight categories. Straight upgrade, straight downgrade, hog, and sag curves were the vertical alignment characteristics considered for clustering. Chapter 4 presented a clustering-based approach dealing with the drivers' perception to capture the effect of combined alignment. The curve direction and superimposed vertical alignment geometry were the criteria used for clustering the horizontal curves into eight groups. The clustering criteria have helped in improving the correlation between the operating speed and various geometric variables.

This study considers developing separate models for different types of vehicle classes corresponding to the eight curve types. Figure 5.1 shows the dissimilarities in the speed distribution for different curve categories and vehicle types. The normality test was also carried out using Kolmogorov-Smirnov and Shapiro-Wilk and it was found that the data follow normal distribution. Therefore, separate OSM needs to be developed for different curve types and vehicle classes. Eighty percent of the curves available for each

category were considered for estimating the OSM, and the remaining 20% were used for validation (Table 5.1).

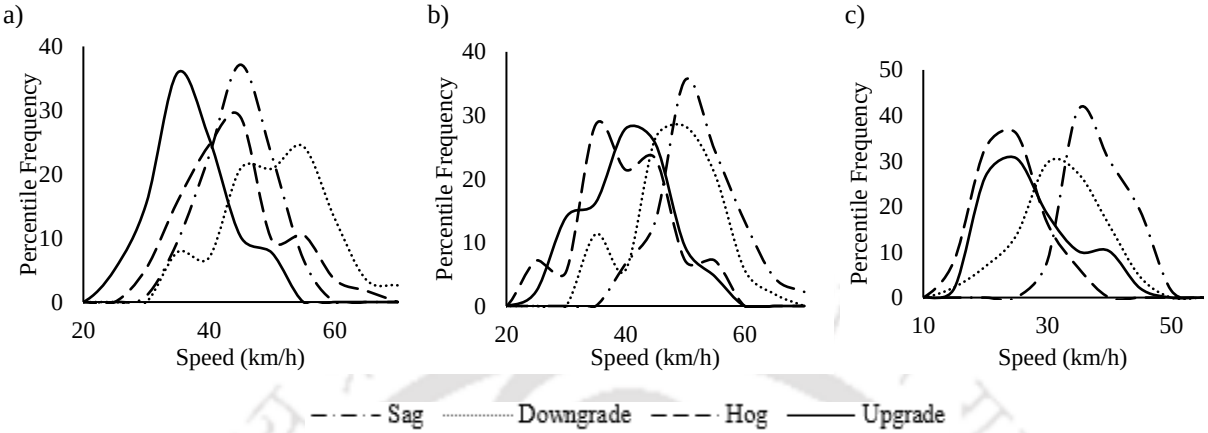

Fig. 5.1 Free flow speed distributions observed at different combinations of horizontal curve and the superimposed vertical alignment for a) Passenger Car b) Empty truck c) Loaded truck

Table 5.1 List of number of curves used for modeling and validating data

Type	Passenger car		Empty truck		Loaded truck	
	For modeling	For validation	For modeling	For validation	For modeling	For validation
Left Downgrade	10	2	12	2	12	3
Left Hog	17	5	13	4	18	5
Left Sag	16	5	17	5	15	5
Left Upgrade	11	3	11	4	12	4
Right Downgrade	13	3	15	4	13	4
Right Hog	16	5	13	4	19	5
Right Sag	16	4	17	6	14	5
Right Upgrade	11	3	12	3	13	4

The variables to be used in developing the operating speed models of passenger cars, empty and loaded trucks were selected based on the correlation analysis. For each category of curves, the independent variables showing a linear association with the operating speed and a correlation coefficient greater than 0.3 (Table 5.2(a) to 2(h)) were used for the OSM development. Independent variables with a strong linear association (with a correlation coefficient greater than 0.5) were considered correlated, and only one of the variables was considered for further modeling. As mentioned earlier, for interpreting the strength of the correlation, the ranges of correlation coefficients adopted were 0.30–0.39 (moderate), 0.40–0.69 (strong), and above 0.70 (very strong) (Akoglu 2018). Table 5.2(a) shows the obtained results for a particular category, i.e., left-turning horizontal curve superimposed with an upgrade, for modeling V_{85C}. For this

specific category, L_{at}, L_{et}, G_2, G_5, L_C, and LW were considered as the independent variables. After considering the multi-collinearity, only L_{at}, G_2, and LW were considered for further stepwise multiple linear regression. L_{at}, and G_2 are negatively correlated with operating speed of passenger car. This indicates that the operating speed at the curve reduces with the increasing L_{at} and the gradient at start of the curve. LW is positively correlated with operating speed, meaning that as LW increases, the operating speed increases.

The operating speed models were developed using the backward stepwise regression, and insignificant variables were removed iteratively. A similar procedure was carried out to model the operating speed of passenger cars, empty and loaded trucks for the other seven categories of horizontal curves superimposed with different vertical alignments. Figure 5.2 presents an overall procedure of the operating speed modeling.

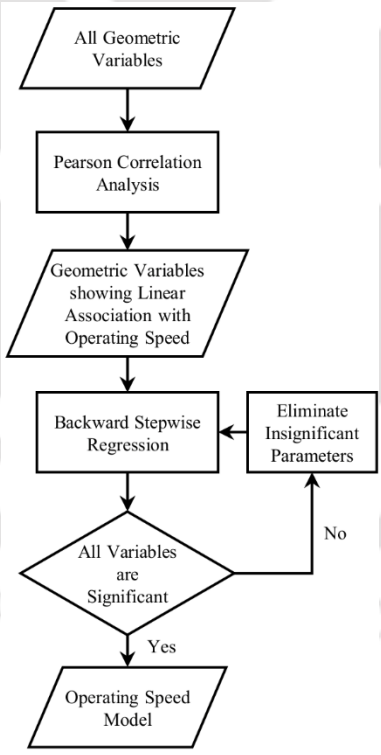

Fig. 5.2 The overall methodology adopted for modeling operating speed

The operating speed modeling was performed using the conventional OLS approach considering the highly correlated geometric variables. Table 5.3 shows that a few geometric variables are not significant

at 5% significance level, and the goodness of fit, in terms of R^2, is low in most of the cases. Weak association of important geometric variables in the OLS approach point towards the selection bias in the modeling process, and the following section describes the same in detail.

Table 5.2(a) Correlation matrix of the Operating speed and the geometric variables, of passenger car for Left-turning horizontal curve superimposed with an upgrade

	L_{at}	L_{et}	G_1	G_2	G_3	G_4	G_5	L_t	R	L_C	e	Δ	DC	CCR_S	CCR	LW	$R\times LW$	V_{85C}
L_{at}	1																	
L_{et}	-0.27	1																
G_1	0.56*	0.28	1															
G_2	0.65*	0.03	0.89*	1														
G_3	0.65*	0.02	0.87*	1.00*	1													
G_4	0.65*	0.04	0.89*	1.00*	1.00*	1												
G_5	0.56*	0.00	0.56*	0.39	0.38	0.40	1											
L_t	-0.09	-0.08	0.43	0.52*	0.52*	0.52*	-0.18	1										
R	-0.14	0.13	-0.67*	-0.71*	-0.71*	-0.71*	-0.15	-0.88*	1									
L_C	0.08	0.40	0.32	0.09	0.07	0.09	0.11	-0.03	-0.05	1								
e	0.20	-0.24	0.44	0.64*	0.65*	0.64*	-0.17	0.89*	-0.86*	-0.03	1							
Δ	0.07	0.02	0.56*	0.55*	0.55*	0.55*	-0.21	0.82*	-0.78*	0.37	0.80*	1						
DC	0.08	-0.26	0.46	0.55*	0.56*	0.55*	-0.19	0.82*	-0.81*	-0.19	0.81*	0.82*	1					
CCR_S	0.13	-0.19	0.53*	0.60*	0.60*	0.60*	-0.17	0.83*	-0.83*	-0.03	0.83*	0.90*	0.99*	1				
CCR	-0.02	-0.39	0.29	0.43	0.43	0.43	-0.19	0.77*	-0.75*	-0.43	0.72*	0.64*	0.96*	0.90*	1			
LW	-0.02	0.09	-0.45	-0.46	-0.45	-0.46	-0.24	-0.48	0.60*	0.46	-0.36	-0.28	-0.62*	-0.55*	-0.69*	1		
$R\times LW$	-0.15	0.11	-0.70*	-0.73*	-0.72*	-0.73*	-0.22	-0.85*	0.99*	-0.01	-0.81*	-0.72*	-0.79*	-0.79*	-0.73*	0.67*	1	
V_{85C}	-0.36*	0.03	-0.72*	-0.77*	-0.77*	-0.77*	-0.27	-0.45*	0.59*	0.08	-0.41*	-0.52*	-0.65*	-0.66*	-0.60*	0.76*	0.62*	1

*indicates correlation

Table 5.2(b) Correlation matrix of the Operating speed and the geometric variables, of passenger car for Left-turning horizontal curve superimposed with sag

	L_{at}	L_{et}	G_1	G_2	G_3	G_4	G_5	L_V	K	L_t	R	L_C	e	Δ	DC	CCR_S	CCR	LW	$R\times LW$	V_{85C}
L_{at}	1																			
L_{et}	-0.19	1																		
G_1	0.18	-0.52*	1																	
G_2	0.19	-0.51*	0.97*	1																
G_3	0.20	-0.50*	0.95*	0.99*	1															
G_4	0.17	-0.41	0.91*	0.96*	0.99*	1														
G_5	0.24	-0.30	0.86*	0.93*	0.95*	0.98*	1													
L_V	0.19	0.48	-0.15	-0.01	0.07	0.21	0.34	1												
K	-0.27	-0.07	0.27	0.17	0.12	0.06	-0.01	-0.31	1											
L_t	-0.61*	0.30	-0.33	-0.32	-0.29	-0.21	-0.18	0.21	-0.04	1										
R	0.65*	0.04	0.22	0.23	0.24	0.21	0.23	0.08	-0.13	-0.79*	1									
L_C	-0.31	0.58*	-0.46	-0.43	-0.38	-0.26	-0.19	0.53*	-0.09	0.54*	-0.33	1								
e	-0.59*	0.24	-0.32	-0.31	-0.30	-0.26	-0.22	0.11	0.09	0.81*	-0.72*	0.46*	1							
Δ	-0.48	0.35	-0.48	-0.47	-0.43	-0.35	-0.32	0.24	0.01	0.80*	-0.69*	0.85*	0.70*	1						
DC	-0.55*	-0.07	-0.29	-0.31	-0.30	-0.27	-0.30	-0.11	0.16	0.78*	-0.90*	0.45	0.71*	0.83*	1					
CCR_S	-0.52*	0.02	-0.35	-0.36	-0.34	-0.30	-0.32	-0.02	0.14	0.75*	-0.85*	0.60*	0.68*	0.91*	0.98*	1				
CCR	-0.51*	-0.26	-0.04	-0.08	-0.10	-0.11	-0.15	-0.33	0.13	0.72*	-0.81*	-0.02	0.66*	0.47	0.82*	0.70*	1			
LW	-0.28	0.23	-0.17	-0.25	-0.26	-0.21	-0.22	0.04	0.27	0.39	-0.36	0.24	-0.06*	0.30	0.31	0.31	0.21	1		
$R\times LW$	0.60*	0.10	0.17	0.16	0.16	0.13	0.15	0.07	-0.07	-0.77*	0.97*	-0.31	-0.78*	-0.67*	-0.89*	-0.84*	-0.83*	-0.15	1	
V_{85C}	0.30	0.14	0.31*	0.30*	0.26	0.22	0.22	-0.09	0.02	-0.54*	0.67*	-0.47*	-0.51*	-0.68*	-0.74*	-0.77*	-0.42*	-0.17	0.68*	1

*indicates correlation

Table 5.2 (c) Correlation matrix of the Operating speed and the geometric variables, of passenger car for Left-turning horizontal curve superimposed with hog

	L_{at}	L_{et}	G_1	G_2	G_3	G_4	G_5	L_V	K	L_t	R	L_C	e	Δ	DC	CCR_S	CCR	LW	$R\times LW$	V_{85C}
L_{at}	1																			
L_{et}	-0.33	1																		
G_1	0.06	0.03	1																	
G_2	0.23	-0.22	0.82*	1																
G_3	0.41	-0.25	0.63*	0.90*	1															
G_4	0.52*	-0.26	0.42	0.72*	0.94*	1														
G_5	0.65*	-0.45	0.26	0.57*	0.76*	0.85*	1													
L_V	-0.37	0.46	0.28	-0.11	-0.33	-0.48	-0.64*	1												
K	0.17	-0.28	-0.04	0.20	0.33	0.43	0.59*	-0.43	1											
L_t	-0.25	0.12	-0.33	-0.20	-0.26	-0.28	-0.17	-0.23	0.13	1										
R	0.07	-0.02	0.24	0.06	0.08	0.07	-0.06	0.47	-0.19	-0.88*	1									
L_C	0.29	-0.06	0.35	0.47	0.28	0.11	0.26	0.26	0.14	0.12	-0.01	1								
e	-0.19	0.00	0.20	0.41	0.28	0.16	0.23	-0.15	0.45	0.37	-0.41	0.45*	1							
Δ	0.07	-0.03	0.16	0.34	0.14	-0.01	0.16	0.02	0.22	0.63*	-0.57*	0.80*	0.59*	1						
DC	-0.14	-0.03	-0.28	-0.10	-0.13	-0.13	0.01	-0.35	0.26	0.88*	-0.96*	0.07	0.41	0.62*	1					
CCR_S	-0.02	-0.05	-0.08	0.13	0.02	-0.05	0.13	-0.22	0.30	0.79*	-0.86*	0.44	0.55*	0.86*	0.92*	1				
CCR	-0.21	-0.03	-0.53*	-0.44	-0.32	-0.21	-0.17	-0.44	0.11	0.76*	-0.78*	-0.48	0.05	0.09	0.78*	0.48	1			
LW	0.21	-0.10	-0.32	-0.31	-0.29	-0.22	-0.22	0.03	-0.04	0.06	-0.03	-0.10	-0.26	-0.05	0.05	-0.02	0.17	1		
$R\times LW$	0.15	-0.10	0.12	-0.05	-0.03	-0.02	-0.14	0.48	-0.16	-0.80*	0.92*	-0.03	-0.46	-0.53*	-0.86*	-0.78*	-0.66*	0.34	1	
V_{85C}	0.07	-0.12	-0.05	-0.08	0.01	0.07	-0.09	0.20	-0.06	-0.68*	0.61*	-0.22	-0.09	-0.56*	-0.58*	-0.58*	-0.40*	0.02	0.61*	1

*indicates correlation

Table 5.2 (d) Correlation matrix of the Operating speed and the geometric variables, of passenger car for Left-turning horizontal curve superimposed with downgrade

	L_{at}	L_{et}	G_1	G_2	G_3	G_4	G_5	L_t	R	L_C	e	Δ	DC	CCR_S	CCR	LW	$R\times LW$	V_{85C}
L_{at}	1																	
L_{et}	-0.19	1																
G_1	-0.26	-0.14	1															
G_2	-0.51*	-0.15	0.91*	1														
G_3	-0.51*	-0.15	0.91*	1.00*	1													
G_4	-0.51*	-0.15	0.91*	1.00*	1.00*	1												
G_5	-0.60*	0.34	0.45	0.60*	0.60*	0.60*	1											
L_t	-0.31	0.03	-0.09	-0.02	-0.02	-0.02	0.49	1										
R	0.42	0.07	-0.12	-0.22	-0.22	-0.22	-0.61*	-0.92*	1									
L_C	-0.10	-0.19	0.69	0.80*	0.80*	0.80*	0.55*	-0.08	-0.16	1								
e	-0.35	0.09	0.00	0.09	0.09	0.09	0.62*	0.96*	-0.97*	0.09	1							
Δ	-0.36	-0.05	0.21	0.32	0.32	0.32	0.72*	0.90*	-0.91*	0.34	0.93*	1						
DC	-0.39	0.00	-0.03	0.06	0.06	0.06	0.56*	0.99*	-0.94*	-0.02	0.96*	0.93*	1					
CCR_S	-0.40	-0.02	0.06	0.17	0.17	0.17	0.64*	0.97*	-0.96*	0.13	0.98*	0.97*	0.99*	1				
CCR	-0.36	-0.02	-0.11	-0.04	-0.04	-0.04	0.46	0.98*	-0.87	-0.16	0.90*	0.87*	0.98*	0.95*	1			
LW	-0.16	-0.30	0.75	0.63*	0.63*	0.63*	0.10	-0.08	-0.14	0.43	0.01	0.04	-0.08	-0.01	-0.17	1		
$R\times LW$	0.38	-0.05	0.11	-0.03	-0.03	-0.03	-0.55*	-0.93*	0.95*	-0.01	-0.95*	-0.87*	-0.95*	-0.95*	-0.90*	0.16	1	
V_{85C}	0.50*	0.58*	-0.16	-0.34*	-0.34*	-0.34*	-0.33*	-0.55*	0.73*	-0.19	-0.58*	-0.60*	-0.62*	-0.65*	-0.58*	-0.28	0.63*	1

*indicates correlation

Table 5.2(e) Correlation matrix of the Operating speed and the geometric variables, of passenger car for Right-turning horizontal curve superimposed with upgrade

	L_{at}	L_{et}	G_1	G_2	G_3	G_4	G_5	L_t	R	L_C	e	Δ	DC	CCR_S	CCR	LW	$R\times LW$	V_{85C}
L_{at}	1																	
L_{et}	-0.58*	1																
G_1	-0.42	0.58*	1															
G_2	-0.51*	0.56*	0.43	1														
G_3	-0.51*	0.56*	0.43	1.00*	1													
G_4	-0.51*	0.56*	0.43	1.00*	1.00*	1												
G_5	-0.46	0.25	0.26	0.82*	0.82*	0.82*	1											
L_t	-0.12	0.00	-0.46	-0.14	-0.14	-0.14	0.06	1										
R	-0.03	0.12	0.50*	0.21	0.21	0.21	-0.05	-0.95*	1									
L_C	-0.05	0.30	0.16	0.42	0.42	0.42	0.65*	0.22	-0.26	1								
e	0.00	-0.11	-0.54*	-0.16	-0.16	-0.16	0.07	0.97*	-0.98*	0.19	1							
Δ	-0.20	0.12	-0.39	-0.04	-0.04	-0.04	0.16	0.98*	-0.91*	0.37	0.92*	1						
DC	-0.16	0.00	-0.48	-0.14	-0.14	-0.14	0.06	1.00*	-0.95*	0.19	0.97*	0.97*	1					
CCR_S	-0.15	0.03	-0.46	-0.11	-0.11	-0.11	0.11	0.99*	-0.95*	0.28	0.96*	0.99*	1.00*	1				
CCR	-0.19	-0.05	-0.46	-0.18	-0.18	-0.18	-0.01	0.97*	-0.91*	0.01	0.94*	0.91*	0.98*	0.95*	1			
LW	-0.27	0.02	-0.32	-0.02	-0.02	-0.02	0.17	0.71*	-0.66*	-0.13	0.73*	0.63*	0.73*	0.69*	0.78*	1		
$R\times LW$	-0.06	0.12	0.49	0.22	0.22	0.22	0.00	-0.91*	0.98*	-0.30	-0.95*	-0.88*	-0.91*	-0.92*	-0.86*	-0.50*	1	
V_{85C}	0.57*	-0.56*	-0.58*	-0.47*	-0.47*	-0.47*	-0.12	0.02	-0.15	0.16	0.13	-0.02	0.01	0.02	-0.03	-0.05	-0.16	1

*indicates correlation

Table 5.2(f) Correlation matrix of the Operating speed and the geometric variables, of passenger car for Right-turning horizontal curve superimposed with sag

	L_{at}	L_{et}	G_1	G_2	G_3	G_4	G_5	L_V	K	L_t	R	L_C	e	Δ	DC	CCR_S	CCR	LW	$R\times LW$	V_{85C}
L_{at}	1																			
L_{et}	-0.14	1																		
G_1	-0.04	-0.25	1																	
G_2	0.08	-0.28	0.97*	1																
G_3	0.22	-0.24	0.93*	0.98*	1															
G_4	0.23	-0.15	0.90*	0.94*	0.98*	1														
G_5	0.12	-0.15	0.82*	0.89*	0.93*	0.95*	1													
L_V	0.45	0.18	-0.21	-0.02	0.11	0.18	0.36	1												
K	-0.13	-0.13	0.12	0.06	-0.03	-0.09	-0.16	-0.28	1											
L_t	0.44	-0.06	0.29	0.33	0.44	0.52*	0.42	0.24	-0.42	1										
R	-0.08	0.14	-0.70*	-0.65*	-0.67*	-0.69*	-0.55*	0.13	0.01	-0.60*	1									
L_C	0.74	0.14	0.16	0.16	0.30	0.38	0.21	0.25	-0.22	0.60*	-0.41	1								
e	0.41	0.06	0.27	0.36	0.44	0.49	0.48	0.33	-0.50*	0.66*	-0.37	0.52*	1							
Δ	0.58*	0.06	0.40	0.37	0.47	0.55*	0.37	0.11	-0.23	0.74*	-0.67*	0.93*	0.60*	1						
DC	0.07	-0.16	0.76*	0.69*	0.71*	0.74*	0.59*	-0.20	-0.08	0.60*	-0.97*	0.46	0.41	0.73*	1					
CCR_S	0.25	-0.06	0.70*	0.63*	0.68*	0.73*	0.56*	-0.10	-0.10	0.59*	-0.90*	0.68*	0.45	0.87*	0.95*	1				
CCR	-0.36	-0.38	0.43	0.39	0.33	0.30	0.25	-0.39	-0.01	0.38	-0.63*	-0.29	0.20	0.03	0.58*	0.32	1			
LW	-0.37	0.02	0.00	-0.13	-0.18	-0.17	-0.24	-0.48	0.12	0.17	-0.10	-0.11	-0.02	0.02	0.16	0.06	0.34	1		
$R\times LW$	-0.21	0.13	-0.67*	-0.67*	-0.71*	-0.73*	-0.62*	-0.06	0.07	-0.51*	0.92*	-0.44	-0.36	-0.64*	-0.87*	-0.85*	-0.47	0.28	1	
V_{85C}	0.19	0.19	-0.50*	-0.46*	-0.45*	-0.50*	-0.43*	0.11	0.04	-0.42*	0.57*	-0.07	-0.13	-0.31*	-0.65*	-0.53*	-0.50*	-0.28	0.44*	1

*indicates correlation

Table 5.2(g) Correlation matrix of the Operating speed and the geometric variables, of passenger car for Right-turning horizontal curve superimposed with hog

	L_{at}	L_{et}	G_1	G_2	G_3	G_4	G_5	L_V	K	L_t	R	L_C	e	Δ	DC	CCR_S	CCR	LW	$R\times LW$	V_{85C}
L_{at}	1																			
L_{et}	-0.39	1																		
G_1	0.26	-0.28	1																	
G_2	0.10	-0.21	0.87*	1																
G_3	0.04	-0.18	0.83*	0.98*	1															
G_4	0.04	-0.22	0.72*	0.88*	0.94*	1														
G_5	-0.19	-0.24	0.61*	0.75*	0.83*	0.91*	1													
L_V	0.29	-0.08	0.53*	0.34	0.25	0.00	-0.17	1												
K	-0.27	0.09	-0.71*	-0.53*	-0.44	-0.32	-0.11	-0.44	1											
L_t	0.10	-0.25	-0.33	-0.30	-0.29	-0.31	-0.17	-0.09	0.37	1										
R	-0.04	0.17	0.31	0.30	0.29	0.33	0.17	0.06	-0.28	-0.85*	1									
L_C	-0.02	0.31	-0.28	-0.19	-0.27	-0.40	-0.41	0.21	0.37	0.17	-0.06	1								
e	-0.05	-0.25	-0.38	-0.34	-0.36	-0.44	-0.19	-0.08	0.53*	0.71*	-0.73*	0.37	1							
Δ	-0.09	0.19	-0.33	-0.29	-0.31	-0.45	-0.31	0.17	0.46	0.72*	-0.70*	0.65*	0.76*	1						
DC	-0.12	-0.05	-0.14	-0.15	-0.13	-0.23	-0.04	0.13	0.25	0.77*	-0.90*	0.05	0.68*	0.78*	1					
CCR_S	-0.13	0.04	-0.18	-0.17	-0.17	-0.31	-0.13	0.20	0.30	0.73*	-0.86*	0.26	0.73*	0.88*	0.97*	1				
CCR	-0.10	-0.20	-0.09	-0.11	-0.04	-0.04	0.13	-0.05	0.16	0.76*	-0.85*	-0.33	0.47	0.47	0.88*	0.76*	1			
LW	-0.33	0.10	-0.07	0.06	0.08	0.14	0.11	-0.08	-0.06	-0.31	0.09	-0.13	-0.24	-0.30	-0.15	-0.18	-0.07	1		
$R\times LW$	-0.16	0.19	0.25	0.28	0.27	0.31	0.14	0.10	-0.26	-0.87*	0.91*	-0.03	-0.73*	-0.70*	-0.85*	-0.81*	-0.80*	0.47	1	
V_{85C}	-0.02	0.08	-0.18	-0.07	-0.07	0.07	0.08	-0.71*	-0.03	-0.25	0.26	-0.24	-0.25	-0.43*	-0.44*	-0.48*	-0.30*	-0.18	0.09	1

*indicates correlation

Table 5.2(h) Correlation matrix of the Operating speed and the geometric variables, of passenger car for Right-turning horizontal curve superimposed with downgrade

	L_{at}	L_{et}	G_1	G_2	G_3	G_4	G_5	L_t	R	L_C	e	Δ	DC	CCR_S	CCR	LW	$R\times LW$	V_{85C}
L_{at}	1																	
L_{et}	-0.24	1																
G_1	-0.18	-0.42	1															
G_2	0.08	-0.57*	0.64*	1														
G_3	0.11	-0.57*	0.62*	1.00*	1													
G_4	0.09	-0.57*	0.63*	1.00*	1.00*	1												
G_5	-0.19	-0.48	0.77*	0.90*	0.87*	0.89*	1											
L_t	-0.27	-0.13	-0.06	-0.44	-0.44	-0.44	-0.36	1										
R	0.28	-0.14	0.33	0.68*	0.67*	0.68*	0.64*	-0.86*	1									
L_C	0.52*	-0.03	-0.10	-0.03	-0.01	-0.03	-0.26	-0.11	0.06	1								
e	-0.47	0.20	-0.06	-0.58*	-0.59*	-0.58*	-0.39	0.87*	-0.86*	-0.19	1							
Δ	-0.02	-0.02	0.03	-0.48	-0.47	-0.47	-0.51*	0.75*	-0.70*	0.42*	0.67*	1						
DC	-0.37	0.04	0.06	-0.51*	-0.51*	-0.51*	-0.42	0.83*	-0.81*	-0.21	0.80*	0.79*	1					
CCR_S	-0.27	0.07	0.03	-0.55*	-0.55*	-0.55*	-0.50*	0.80*	-0.81*	-0.02	0.78*	0.89*	0.98*	1				
CCR	-0.52*	0.02	0.12	-0.33	-0.34	-0.33	-0.20	0.78*	-0.73*	-0.51*	0.76*	0.51	0.90*	0.80*	1			
LW	-0.15	-0.41	0.72*	0.32	0.30	0.31	0.41	0.17	0.16	0.09	0.06	0.31	0.24	0.24	0.26	1		
$R\times LW$	0.21	-0.23	0.48	0.73*	0.72*	0.72*	0.71*	-0.74*	0.97*	0.05	-0.77*	-0.59*	-0.69*	-0.70*	-0.61*	0.37	1	
V_{85C}	-0.38	0.17	0.13	0.49*	0.48*	0.49*	0.51*	-0.49*	0.43*	-0.07	-0.31*	-0.57*	-0.54*	-0.59*	-0.34*	-0.17	0.35*	1

*indicates correlation

Table 5.3 Operating speed models estimated using the OLS method

Category	Vehicle	V_{85} model	R^2 value
Left Upgrade	Passenger Car	$43.68 - \underset{(0.016)}{2.75G_2} + \underset{(0.018)}{5.94LW}$	0.80
	Loaded Truck	$53.35 - \underset{(0.004)}{4.8G_1}$	0.48
	Empty Truck	$49.41 - \underset{(1.02\text{x}10^{-5})}{0.002CCR}$	0.10
Right Upgrade	Passenger Car	$62.22 + \underset{(0.20)}{0.035L_{at}} - \underset{(0.18)}{1.51G_1}$	0.46
	Loaded Truck	$52.10 - \underset{(0.001)}{4.71G_1}$	0.62
	Empty Truck	$56.48 - \underset{(0.01)}{1.55G_1} - \underset{(0.03)}{0.072\Delta}$	0.63
Left Downgrade	Passenger Car	$49.99 + \underset{(0.008)}{0.06L_{at}} + \underset{(0.0006)}{0.07L_{et}} + \underset{(0.004)}{0.007R \times LW}$	0.93
	Loaded Truck	$43.97 - \underset{(0.01)}{0.096L_{at}} + \underset{(0.055)}{158.13e} - \underset{(0.003)}{0.15\Delta}$	0.75
	Empty Truck	$53.77 - \underset{(0.02)}{0.11L_{at}} + \underset{(0.40)}{0.02L_{et}} - \underset{(0.43)}{0.009R}$	0.61
Right Downgrade	Passenger Car	$73.79 - \underset{(0.012)}{0.06L_{at}} - \underset{(0.003)}{0.029CCR_S}$	0.65
	Loaded Truck	$53.96 - \underset{(0.055)}{0.069L_{et}} + \underset{(0.03)}{1.87G_5}$	0.57
	Empty Truck	$51.461 + \underset{(0.07)}{0.052L_{et}} - \underset{(0.04)}{0.0047CCR}$	0.54
Left Sag	Passenger Car	$74.65 + \underset{(0.81)}{0.096G_1} - \underset{(0.0014)}{0.036CCR_S}$	0.59
	Loaded Truck	$46.44 - \underset{(0.19)}{0.71G_1} - \underset{(0.04)}{0.092L_C}$	0.35
	Empty Truck	$42.9 - \underset{(0.51)}{0.18G_2} + \underset{(9.48\text{x}10^{-7})}{0.015R \times LW}$	0.85
Right Sag	Passenger Car	$72.63 - \underset{(0.006)}{0.76DC}$	0.42
	Loaded Truck	$47.81 - \underset{(0.03)}{0.041L_{et}} - \underset{(0.12)}{0.69G_4}$	0.56
	Empty Truck	$48.867 - \underset{(0.04)}{0.87G_4} + \underset{(0.03)}{0.008R \times LW}$	0.54
Left Hog	Passenger Car	$66.23 - \underset{(0.002)}{0.29L_t}$	0.45
	Loaded Truck	$36.18 - \underset{(0.40)}{0.014L_{at}} - \underset{(0.02)}{1.45G_1} + \underset{(0.16)}{0.18L_t}$	0.45
	Empty Truck	$53.71 + \underset{(0.03)}{0.018L_{at}} - \underset{(0.01)}{106.42e}$	0.70
Right Hog	Passenger Car	$65.41 - \underset{(0.002)}{0.07L_V} - \underset{(0.06)}{0.01CCR_S}$	0.62
	Loaded Truck	$45.40 + \underset{(0.054)}{0.036L_{at}} - \underset{(0.002)}{0.102L_V}$	0.47
	Empty Truck	$49.90 - \underset{(0.27)}{0.52G_4} - \underset{(0.52)}{0.0014CCR}$	0.16

(Values in brackets indicate the *p*-values)

5.3 Weighted Robust Multivariate Linear Regression

The review of the past studies it is clear that no study has considered the selection bias in the variables while developing the operating speed models. However, the description of the data used in some of these studies clearly shows the possible selection bias in the data considered for developing the OSM. Table 5.4 presents the descriptive statistics of the data, highlighting the potential selection bias. Range, mean, and standard deviation of various geometric characteristics indicate that their distributions are

skewed, and there is a scope for selection bias. Table 5.4 shows the data statistics related to a few studies on OSM for the horizontal curves superimposed with vertical alignments. It is evident from the table that some of the data corresponding to a majority of the variables are far from the mean. Also, these data points cannot be excluded from the modeling process because they represent some of the important geometric elements. The bias in the sampled data would further amplify when OSMs are developed after clustering the horizontal curves.

Table 5.4 Statistics of various parameters used in operating speed models for horizontal curves combined with vertical alignment

Author	Parameters	Range	Mean	Std. Dev
Llopis-Castelló et al. (2018c)	R	18.45-1178.36	167.43	228.52
	L_C	32-250	94.5	47.35
	Δ	3.94-159.82	51.57	37.46
	L_{at}	7-1359	194	214
	CCR	41.51-2464.65	618.21	449.34
	G	-11.31to +11.31	-0.04	4.68
Morris and Donnell (2014)	R	163.25-851.2	463.58	183.27
	L_C	80.3-802.6	466.33	188.07
	G_1	-6.3 to +6	-3.03	4.03
	L_{at}	337.1-6240.5	1947.26	1511.69
	$1/e$	0.1-0.5	0.17	0.12
	LW	3.3-3.8	3.59	0.11
	LSW	0-4.6	1.67	1.02
	RSW	0.6-3	2.79	0.56
	Median width	0-304	19.2	67.66
Jacob and Anjaneyulu (2015)	L_{at}	90-700	243	158
	R	24-1573	314	404
	E	-1.9 to +9.6	3.8	3.0
	L_C	28-296	93	63
	G_1	-1.7 to +7.5	3.2	1.7
	LG_1	34-442	118	81
	L_V	65-669	228	122
Gibreel et al. (2001)	R *(sag, hog)*	57-900, 425-1800	N/A	N/A
	Δ	5-40, 5-55		
	E	4.4-5.5, 2.9-6		
	Lt	45-65, 30-75		
	G	≤6, ≤6		
	L_V	80-180, 80-320		
	A	1.15-6, 1-7.10		
	L_O	42.9-186, 5.9-170		
	X	≤150, ≤210		
	LW	3.75, 3.75		
	SW	2, 2		

As mentioned earlier, the present study road stretch contains 175 vertical curves and 253 horizontal curves. Figure 5.3 shows the frequency distribution of some of the critical geometric

variables generally considered for operating speed modeling. It is evident from the figure that, frequencies corresponding to some of the alignment characteristics are very few. Specifically, flat gradients, long tangents, sharp curves are some of the alignment characteristics that are less frequent in the alignment and the sample data used for OSM.

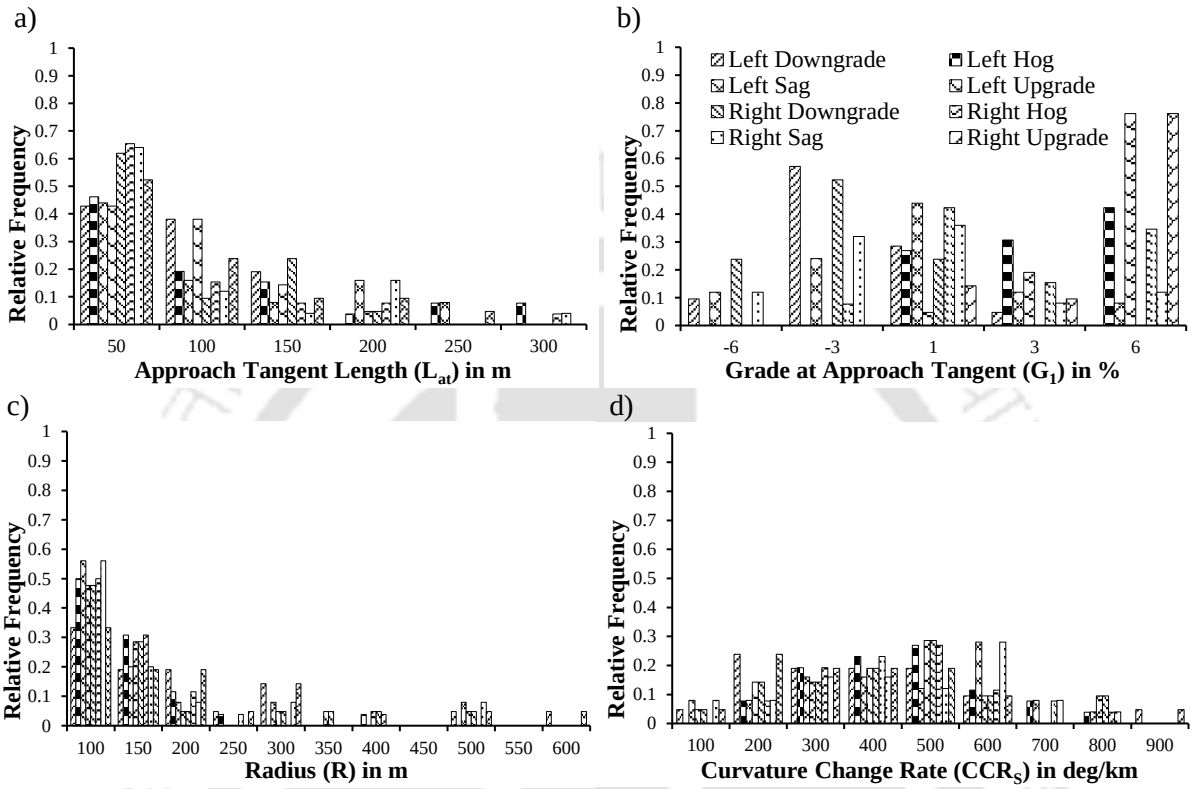

Fig. 5.3 Relative Frequency distribution of a) Approach tangent length b) Grade at Approach Tangent c) Radius d) Curvature Change Rate

Moreover, Figure 5.4 shows that the variables are not uniformly distributed in the speed-geometric variable space. It is visible that the observed operating speed data are over-represented towards a certain range of explanatory variables. In the case of OLS, these over-represented data would govern the regression line, leading to selection bias. For example, in figure, 5.4(a), most of the gradients are greater than 4%, and a few are less than 4%, thereby affecting the parameter estimation. To overcome this selection bias, lower weights are to be given to those over-represented, and higher weights are to be given to the under-represented observations. As a result, all ranges of geometric parameters would be equally represented in the Weighted Least Squares (WLS) method.

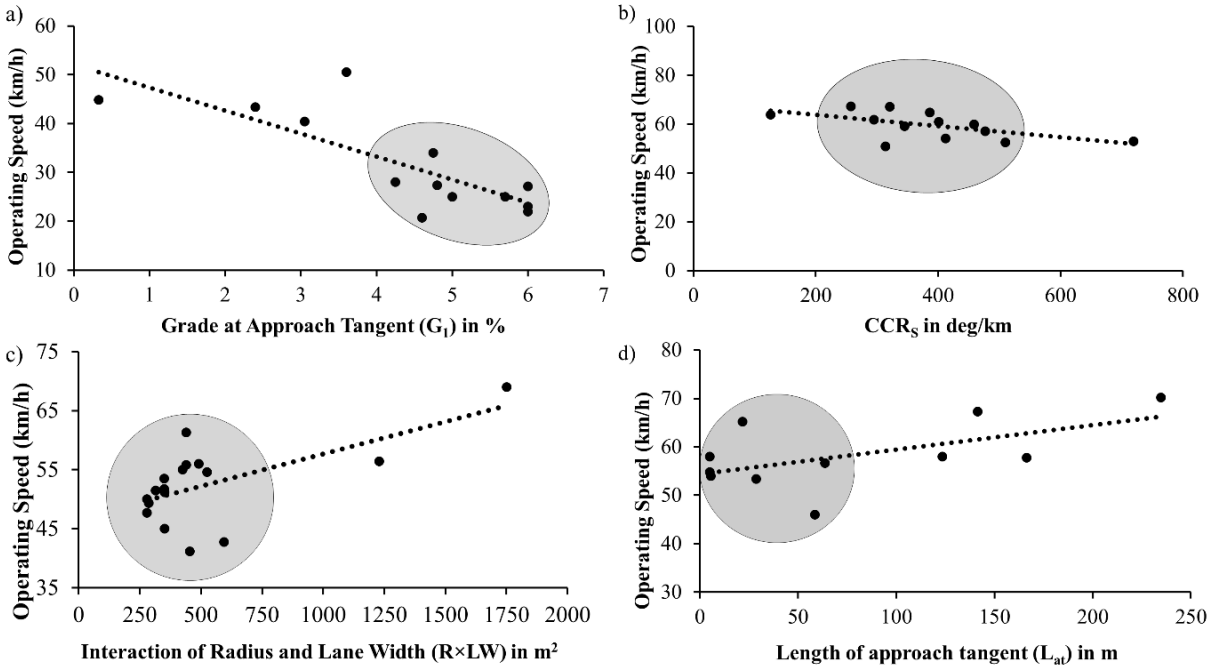

Fig. 5.4 Variation in the operating speed and the dispersion in a few geometric variables corresponding to the curve categories and vehicle type a) right upgrade, loaded truck b) right downgrade, passenger car c) right sag, empty truck d) right upgrade, passenger car.

Apart from the selection bias, heteroscedasticity can also be observed in the data (Figure 5.4). In such circumstances, operating speed modeling using Ordinary Least Square (OLS) technique might lead to erroneous parameter estimation. Heteroscedasticity causes OLS to underestimate standard errors of the coefficients, which means that the t-statistics of the coefficients will be inflated. This, in turn, can increase the probability of rejection of a true null hypothesis (Greer 2012). The coefficient estimates are less accurate due to heteroscedasticity. With lower precision, the coefficient estimates are more likely to be off from the corresponding population parameters. Because of heteroscedasticity, *p*-values are sometimes smaller than they should be (Frost 2019). This issue can lead to an incorrect inference such as a model parameter might become statistically significant when it is not actually. But in the literature, as discussed before, the researchers assume homoscedasticity and unbiasedness and proceed with the OLS regression. To overcome the above-mentioned issues, weighted multivariate linear regression approach was proposed, where two weights were estimated to handle the sampling bias and heteroscedasticity, respectively.

The weight corresponding to sampling bias was estimated based on the proximity of observations in the multi-dimensional observation space. The proposed weight estimation method is a multi-dimensional extension of the weight estimation procedure proposed by Qu et al. (2015) to calibrate the fundamental macroscopic diagram of traffic stream. Qu et al. (2015) have used the one-dimensional Euclidean distance between a pair of points to assign the weights. We extended the procedure for multi-dimension, and the details of the proposed method are as follows.

Let $(x_1, v_1), (x_2, v_2), ..., (x_n, v_n)$ be the observations where v_i is the operating speed and x_i be the vector of geometric parameters. In the case of ordinary least squared regression, the model function $v = f\left(X_i, \hat{\beta}\right)$ is estimated by minimizing the squared deviation:

$$\min_{\hat{\beta}} \sum_{i=1}^{n} \left(v_i - f\left(X_i, \beta\right)\right)^2 \tag{5.1}$$

In this case, the assumption was that all the observations were equally weighted while estimating the model parameters. However, it has already been seen that there is a significant bias in the observation. The weighted linear regression can handle such bias if the weights are properly assigned to the observations. Weighted linear regression minimizes:

$$\min_{\hat{\beta}} \sum_{i=1}^{n} \varpi_i \left(v_i - f\left(X_i, \beta\right)\right)^2 \tag{5.2}$$

where the weights ϖ_i are estimated as follows.

Let $X_i = [x_i^1, x_i^2, ..., x_i^n]^T$ be the *n*-dimensional vector of the geometric variables corresponding to the i^{th} curve in the study area considered in the OSM. The weight corresponding to a particular observation is estimated based on the proximity of the other observations in the *n*-dimensional space. The proximity between a pair of observations x_i and x_j is measured as Euclidean distance $D_{(i),(j)}$ in *n*-dimensional space, as shown in Equation 5.3,

$$D_{(i),(j)} = \sqrt{\sum_{p=1}^{n} \left(x_i^p - x_j^p\right)^2} \tag{5.3}$$

Now, the weight estimation is performed similarly to Qu et al. (2015), as follows;

Step 1: Rank the observations based on the distance from the origin $D_{(i)} = \sqrt{\sum_{p=1}^{n} x_i^{p2}}$. We thus have,

$(v_{(2)}, X_{(2)})$ …, $(v_{(i)}, X_{(i)})$ …, $(v_{(n)}, X_{(n)})$

where $X_{(1)} \leq X_{(2)} \leq \ldots \leq X_{(i)} \leq \ldots \leq X_{(n)}$ and $v_{(i)}$ is the speed observation corresponding to i^{th} geometry.

Step 2: Define (u) as the largest index (i) that corresponds to the same vector as $X_{(1)}$, that is,

$$u := \arg\max\{i = 1,2,\ldots n \mid X_{(i)} = X_{(1)}\} \tag{5.4}$$

Then,

$$\varpi_{(i)} = \frac{D_{(u+1),(1)}}{u}, i = 1,2,\ldots,u \tag{5.5}$$

Step 3: Define $u = u+1$. Define (u) as the largest index (i) that corresponds to the same vector as $X_{(u)}$, that is

$$u := \arg\max\{i = u, u+1, u+2, \ldots n \mid X_{(i)} = X_{(u)}\} \tag{5.6}$$

If $u < n$, set

$$\varpi_{(i)} = \frac{D_{(u+1),(u-1)}}{2(u-u+1)}, i = u,\ u+1, u+2, \ldots, u \tag{5.7}$$

and repeat Step 3. Else,

$$\varpi_{(i)} = \frac{D_{(n),(u-1)}}{n-u+1}, i = u,\ u+1, u+2, \ldots, n \tag{5.8}$$

and stop.

Before proceeding with the weight estimation, all variables were checked for their distribution so that the weighted regression can be carried out. The distribution of sampled data corresponding to various explanatory variables highlights the selection bias. Table 5.5 shows the distribution of geometric parameters considered for modeling the operating speed of Passenger Car. Appendix, Table A-2 shows a similar distribution for empty and loaded trucks. The distribution of approach tangent length in Figure 5.5 (a), corresponding to the left-turning horizontal curves superimposed with a

downward gradient, clearly indicates the selection bias where the representation of longer tangents is relatively low.

Similarly, the flatter grades were underrepresented compared to the steep upgrades in the data, which resulted in a biased operating speed model for the horizontal curves combined with the upgrades. The curves with higher CCR_S were also underrepresented for right-turning curves superimposed with the downgrade and hog curves. But, for the left-turning curves combined with the sag curves, curves with lesser CCR_S were underrepresented. The road alignment passes through mountainous terrain and has a few flat gradients, long tangents, and sharp horizontal curves. The number of such elements would be less, but they are critical in developing the operating speed models. In this scenario, the representation of these features in the randomly sampled data used to develop operating speed models will be lower, resulting in selection bias.

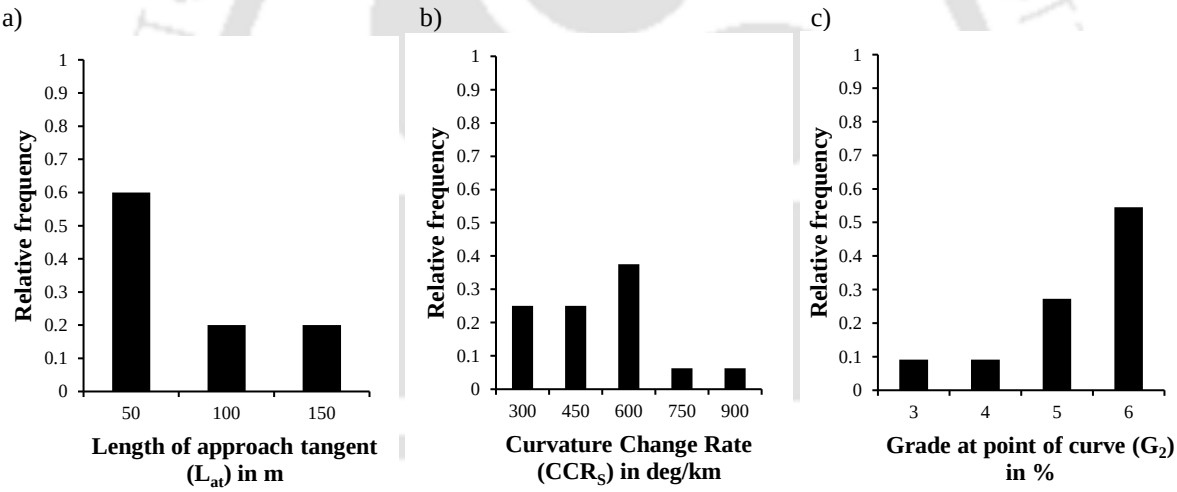

Fig. 5.5 Relative frequency distribution of a) Length of approach tangent for Left downgrade b) Curvature Change Rate for Left sag c) Grade at point of curve for Left upgrade, of Passenger car

Table 5.5 Distribution of geometric parameters considered for modeling the operating speed of Passenger Car

Left-Downgrade		**Left-Hog**		**Left-Sag**		**Left-Upgrade**	
Range of L_{at}	Rel. Freq.	Range of L_t	Rel. Freq.	Range of CCR_S	Rel. Freq.	Range of G_2	Rel. Freq.
0-50	0.6	15-30	0.29	150-300	0.25	2 to 3	0.09
51-100	0.2	31-45	0.47	301-450	0.25	3.1 to 4	0.09
101-150	0.2	46-60	0.24	451-600	0.375	4.1 to 5	0.27
				601-750	0.0625	5.1 to 6	0.54
				751-900	0.0625		
Range of L_{et}	Rel. Freq.			Range of G_1	Rel. Freq.		
0-50	0.6			-5.1 to -7	0.0625		
51-100	0.2			-3.1 to -5	0.25		
101-150	0.2			-1.1 to -3	0.125		
				-1 to 1	0.125		
				1.1 to 3	0.1875		
				3.1 to 5	0.1875		
				5.1 to 7	0.0625		
Range of $R \times LW$	Rel. Freq.						
0-500	0.2						
501-1000	0.4						
1001-1500	0.4						
Right-Downgrade		**Right-Hog**		**Right-Sag**		**Righ-Upgrade**	
Range of L_{at}	Rel. Freq.	Range of L_V	Rel. Freq.	Range of DC	Rel. Freq.	Range of L_{at}	Rel. Freq.
0-50	0.69	50-100	0.69	10-15	0.19	0-50	0.45
51-100	0.15	101-150	0.19	16-20	0.31	51-100	0.18
101-150	0.15	151-200	0.12	21-25	0.43	101-150	0.18
				26-30	0.06	151-200	0.09
						201-250	0.09
Range of CCR_S	Rel. Freq.	Range of CCR_S	Rel. Freq.			Range of G_1	Rel. Freq.
0-150	0.07	150-300	0.25			-1 to 1	0.09
151-300	0.15	301-450	0.5			1.1 to 3	0.09
301-450	0.46	451-600	0.125			3.1 to 5	0.45
451-600	0.23	601-750	0.125			5.1 to 7	0.36
601-750	0.07						

OLS regression assumes that the errors follow a normal distribution and that the extreme values (known as outliers) are rare (Ghosh 2018). However, these values still occur. The main disadvantage of the ordinary least-squares method is its sensitivity to outliers. The outliers significantly influence the fit because squaring the residuals magnifies the effects of these extreme data points. To minimize the influence of outliers, the data can be fitted using robust least-squares regression. The robust regression works under the principle that less weight should be assigned to the observations lying far from the main body of the data and those that are not fitted (well) by the model (Chatterjee and Mächler 1997). The robust regression method formulation considered in this study uses the bisquare weights to the outliers, where the bisquare weights are given by $w_i = \left(1-\left(u_i\right)^2\right)^2$, if $|u_i|<1$, and zero otherwise. The robust regression formulation uses an iteratively reweighted least-squares algorithm (Ghosh 2018), and the procedure is as follows.

i. Initially, the data is fitted by weighted least squares.

ii. The adjusted residuals are computed and standardized. The adjusted residuals are given by

$$r_{adj} = \frac{r_i}{\sqrt{1-h_i}} \tag{5.9}$$

r_i are the usual least-squares residuals, and h_i are *leverages* that adjust the residuals by reducing the weight of high-leverage data points, significantly affecting the least-squares fit. The standardized adjusted residuals are given by

$$u = \frac{r_{adj}}{K.s} \tag{5.10}$$

where K is a tuning constant equal to 4.685, and s is the robust variance given by $MAD/0.6745$, where MAD is the median absolute deviation of the residuals.

iii. The robust weights are computed as a function of u.

5.4 Results and Discussion

This section presents robust weighted least squares modeling results and highlights the need for considering the selection bias for OSM. With the help of literature, this study highlighted sample selection bias in the geometry data used for OSM. When OLS technique was used, many of the important geometric variables were statistically insignificant which can be attributed to the bias in the data. This was evident from the models corresponding to specific curve categories where the geometric variables were not uniform within the actual range. For example, Figure 5.6(a) shows the non-uniformity of the observed data corresponding to the gradient of the approach tangent. OLS models were estimated with and without the geometric variables represented by the data points highlighted using the circle in Figure 5.6. After excluding rare geometry (both flat and higher deflection angles), there was no substantial difference in OLS and Robust Weighted Least Square (RWLS) model statistics. This could be due to the uniformity in the data considered for model estimation. Whereas, with the complete data, statistics have significantly improved in the case of RWLS. This improvement could be because of the lesser weights assigned to the extreme points by the RWLS approach. From the results corresponding to the RWLS model (Table 5.6), it can be noted that the operating speed models show an improved R^2 value compared to the OLS method, signifying the benefit of the proposed method.

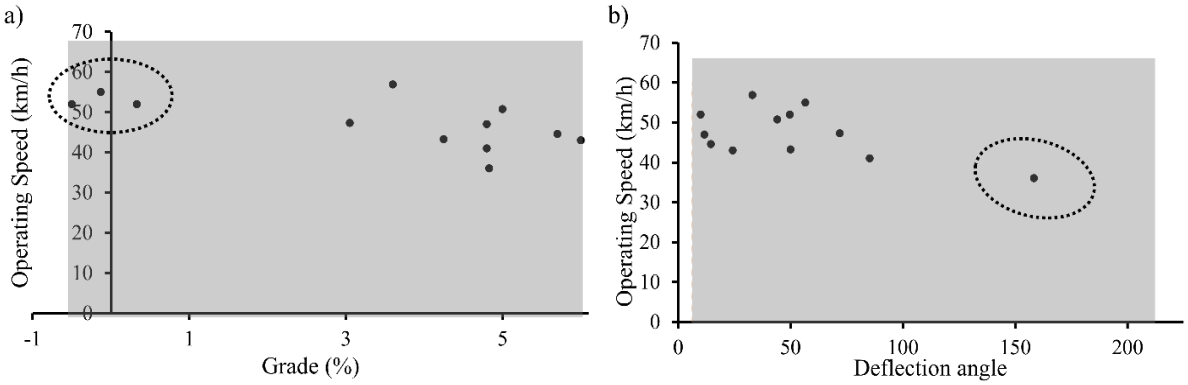

Fig. 5.6 The distribution of grade and deflection angle of the sampled curves over the actual range corresponding to the entire alignment (shaded area)

Table 5.6 Model statistics corresponding to OLS and RWLS, signifying the effect of selection bias

Case	OLS Model	R^2 Value	RWLS Model	R^2 Value
Without the data corresponding to flat gradient & higher deflection angle	70.699-4.05G_1-0.12Δ (0.077) (0.13)	0.52	70.77-3.87G_1-0.14Δ (0.067) (0.09)	0.56
Original data	56.478-1.545G_1-0.072Δ (0.018) (0.038)	0.63	58.413-2.08G_1-0.078Δ (6.3×10^{-7}) (9.12×10^{-8})	0.98

Values in parentheses denote the *p*-value significance level

Appendix, Figure A-2 shows the distribution of all other the critical explanatory variables on the speed-geometric variable plane. The data corresponding to many explanatory variables is biased and contains outliers or influential observations, which can be handled by robust regression analysis.

As the geometric variables influencing the operating speed are not unique across vehicle types, curve types, and turning direction, separate OSM needs to be developed for all the above categories. Table 5.7 shows the results of different OSMs, calibrated, and validated using the field data, for different vehicle types, curve types, and turning directions. The Root Mean Square Error (RMSE) corresponding to all the models range between 2.43 km/h and 11.83 km/h, and the Mean Absolute Percentage Error (MAPE) lies between 6.4% and 25.61%. According to the literature (Dell'Acqua et al. 2013; Esposito et al. 2011; Jacob and Anjaneyulu 2013; Zuriaga et al. 2010), the models with RMSE less than 19.2 km/h are acceptable, and the same criterion is followed in this study.

All the variables are statistically significant at a 5% level of significance (p-value<0.05), which was not the case with the OLS method (Table 5.3). The models explanatory power has also increased significantly as reflected by the average R^2 value of 0.9.

Table 5.7 Operating speed models of different vehicles and for different curve categories

Category	Vehicle	V_{85} Model	R^2 value	R^2_{adj}	RMSE (km/h)	MAPE (%)
Left Upgrade	Passenger Car	$75.42-4.19G_2$	0.62	0.58	7.47	9.83
	Loaded Truck	$57.03-5.73G_1$	0.52	0.47	4.59	11.61
	Empty Truck	$48.34-0.0017CCR$	0.90	0.89	9.34	18.64
Right Upgrade	Passenger Car	$61.82+0.05L_{at}-1.96G_1$	0.98	0.98	8.59	14.29
	Loaded Truck	$48.56-3.85G_1$	0.49	0.45	4.73	12.37
	Empty Truck	$58.41-2.08G_1-0.08\Delta$	0.98	0.98	2.43	10.86
Left Downgrade	Passenger Car	$50.11+0.06L_{at}+0.07L_{et}+0.007R\times LW$	0.92	0.89	11.33	22.57
	Loaded Truck	$38.11-0.06L_{at}+199.49e-0.14\Delta$	0.99	0.98	7.06	13.86
	Empty Truck	$54.43-0.12L_{at}+0.03L_{et}+0.006R$	0.99	0.98	11.2	19.29
Right Downgrade	Passenger Car	$74.45-0.07L_{at}-0.028CCR_S$	0.99	0.99	8.88	12.91
	Loaded Truck	$52.88-0.097L_{et}+0.91G_5$	0.91	0.89	10.24	25.03
	Empty Truck	$54.02+0.025L_{et}-0.052CCR$	0.98	0.98	5.21	6.40
Left Sag	Passenger Car	$77.85+0.31G_1-0.039CCR_S$	0.98	0.98	6.01	9.31
	Loaded Truck	$44.34-0.697G_1-0.065L_C$	0.92	0.91	11.83	18.8
	Empty Truck	$43.12-0.69G_2+0.014R\times LW$	0.78	0.75	4.56	6.78
Right Sag	Passenger Car	$72.68-0.714DC$	0.56	0.53	10.46	16.46
	Loaded Truck	$49.53-0.049L_{et}-0.7G_4$	0.95	0.95	7.57	16.33
	Empty Truck	$37.89+0.016R\times LW$	0.99	0.99	7.36	13.32
Left Hog	Passenger Car	$67.675-0.323L_t$	0.69	0.67	4.40	7.23
	Loaded Truck	$41.83-0.032L_{at}-1.13G_1+0.09L_t$	0.90	0.88	9.07	25.61
	Empty Truck	$55.87+0.016L_{at}-142.85e$	0.98	0.97	6.84	15.09
Right Hog	Passenger Car	$65.36-0.07L_V-0.01CCR_S$	0.99	0.99	9.17	15.35
	Loaded Truck	$46.334+0.038L_{at}-0.12L_V$	0.97	0.97	7.10	17.29
	Empty Truck	$50.83-0.34G_4-0.0023CCR$	0.95	0.95	5.18	10.86

Table 5.7 also shows that, some geometric variables that were not significant in OLS regression became significant when the models were estimated with RWLS. RWLS result reveals that handling the sample selection bias brings out the effect of some important geometric parameters on operating speed, which is otherwise neglected. The OLS estimation was biased towards the over-represented data corresponding to a particular range of values taken by the explanatory variables. With the use of the proposed approach, the modeling bias and heteroscedasticity could be controlled to a certain extent.

5.4.1 Salient Features of the Models

This section presents some improvements in OSM corresponding to the weighted regression modeling (Table 5.7). The implications of the OSM for different vehicle types and curve clusters are described in this section.

The important horizontal alignment characteristics entering into the models are *CCR*, L_{at}, Δ, $R \times LW$, *e*, *R*, L_{et}, L_C, *DC* and L_t. Length of the approach tangent (L_{at}) was found to be significant in the models related to five curve categories and for all three vehicle types. But, L_{at} has a different effect on the passenger cars, empty and loaded trucks. On left-turning curves superimposed with downgrade alignment, L_{at} has positive impact on V_{85C} but negative impact on V_{85T} and V_{85LT}. An increase in the length of L_{at} would encourage the passenger car driver to increase the speed, but not in the case of empty and loaded trucks. Moreover, L_{at} has a relatively higher impact on operating speeds of loaded trucks than the operating speeds of empty trucks. Table 5.7 also reveals that the horizontal alignment characteristics have a dominant effect on the operating speed of all the three vehicle types in case of horizontal curves superimposed with a downward gradient.

The important vertical alignment characteristics entering into the models are G_1, G_2, G_4, G_5 and L_V. Among these variables, gradient at the approach tangent (G_1) is the most common variable affecting the operating speed of the all the vehicle types, across four curve categories. Contrary to earlier findings (Fitzpatrick et al. 2000b), the vertical alignment characteristics (G_1 and G_2) affect the operating speed of passenger cars (on horizontal curves superimposed with upgrades and sag curves). It was also observed that, on right-turning curves superimposed with upgrade, G_1 has the highest negative impact on V_{85LT}, followed by V_{85T} and V_{85C}. Similarly, on right-turning curves superimposed with hog curves, L_V has a higher impact on V_{85LT} than V_{85C}. On left-turning curves superimposed with sag curves, G_1 is positively corelated with V_{85C} and negatively corelated with V_{85LT}, indicating that the passenger cars can accelerate as the downward gradient increases, but loaded trucks are more cautious. Table 5.7 reveals that the vertical alignment variables play a significant role on the operating speeds of the vehicles for left-turning curves superimposed with sag curves and right-turning curves superimposed with hog curves, but not for the opposite turning direction. Such findings support the hypothesis of the present study that the horizontal curves need to clustered based on the turning direction and type of superimposed vertical alignment.

5.4.2 Geometric Design Consistency Evaluation

The difference between the operating speed (V_{85}) and the design speed (V_D) (Lamm et al. 1995) was used to evaluate the geometric design consistency and safety of the subject road stretch. The proposed OSM's performance was assessed by comparing the predicted design consistency using the OLS and RWLS method. Further, the difference in the predicted consistency was tested for any significant difference using the t-test on the mean difference of V_{85} and V_D. The null hypothesis statement for the test is stated as:

H_0: The means of the difference between V_D and V_{85} obtained through OLS and RWLS methods are the same.

Consistency evaluation has been carried out for different vehicle types, turning direction, and superimposed vertical alignment. Table 5.8 shows the test results. It can be observed that, at a 95% confidence level, the mean of the consistency measure shows a statistically significant difference for OLS and RWLS for most of the curve categories. This suggests that for the OLS and RWLS methods, the predicted consistency of the highway geometry is substantially different, showing that the safety assessment may not be reliable if the OSM is not appropriate. It has already been shown (in section 4) that the proposed method outperforms OLS; therefore, design consistency obtained from RWLS would be more reliable.

Table 5.8 Hypothesis test result on the average difference in the operating and design speed

Category	Vehicle	Umiam to Jowai (UJ)			Jowai to Umiam (JU)		
		t stat	p-value	t critical	t stat	p-value	t critical
Left Downgrade	Passenger Car	-1.15	0.25	2.03	-1.12	0.26	2.01
	Empty Truck	0.73	047	2.03	**1.79**	**0.04**	**1.68***
	Loaded Truck	**-3.04**	**0.0045**	**2.03**	0.95	0.34	2.01
Left Hog	Passenger Car	**-5.71**	**<0.001**	**2.03**	**-3.43**	**0.004**	**2.14**
	Empty Truck	**-3.34**	**0.002**	**2.03**	-0.03	0.97	2.14
	Loaded Truck	**3.19**	**0.003**	**2.03**	-0.36	0.72	2.14
Left Sag	Passenger Car	**-11.86**	**<0.001**	**2.06**	**-13.93**	**<0.001**	**2.03**
	Empty Truck	**1.89**	**0.035**	**1.71***	0.15	0.87	2.03
	Loaded	0.88	0.38	2.06	0.38	0.7	2.03
Left Upgrade	Passenger Car	-0.11	0.91	2.02	**-4.68**	**<0.001**	**2.05**
	Empty Truck	**4.76**	**<0.001**	**2.02**	**3.28**	**0.002**	**2.05**
	Loaded Truck	**-3.08**	**0.0039**	**2.02**	**-4.47**	**0.0001**	**2.05**
Right Downgrade	Passenger Car	**-4.12**	**0.0003**	**2.05**	**-4.65**	**<0.001**	**2.02**
	Empty Truck	1.41	0.16	2.05	0.37	0.71	2.02
	Loaded Truck	**-1.725**	**0.04**	**1.70***	**-2.04**	**0.04**	**2.02**
Right Hog	Passenger Car	**-2.01**	**0.03**	**1.76***	**-4.65**	**<0.001**	**2.03**
	Empty Truck	0.73	0.47	2.14	**3.01**	**0.004**	**2.03**
	Loaded Truck	-1.44	0.17	2.14	-1.00	0.32	2.03
Right Sag	Passenger Car	**-11.96**	**<0.001**	**2.03**	**-9.09**	**<0.001**	**2.06**
	Empty Truck	-0.73	0.46	2.03	**2.43**	**0.02**	**2.06**
	Loaded Truck	**2.15**	**0.03**	**2.03**	-0.71	0.48	2.06
Right Upgrade	Passenger Car	**6.33**	**<0.001**	**2.01**	**5.65**	**<0.001**	**2.03**
	Empty Truck	**-3.08**	**0.003**	**2.01**	**-5.85**	**<0.001**	**2.03**
	Loaded Truck	**2.57**	**0.013**	**2.01**	0.04	0.96	2.03

Bold font indicates significance for a two-tailed test; * Indicate that variable is significant for a One-Tailed test

Further, the predicted geometric design consistency using OLS and RWLS was cross-checked with the number of reported crashes. The design consistency analysis carried out based on the OLS method reported 23 unsafe horizontal curves for passenger cars and 1 curve for empty trucks, respectively (Figure 5.7). For RWLS, the number of curves is 28 and 0, respectively, for passenger cars and empty trucks. The geometric design consistency of the curves for loaded trucks in both cases showed safe design, owing to their lower operating speeds. The total number of crashes reported corresponding to the unsafe geometries was 15 and 21, respectively, for OLS and RWLS approaches. The above observation suggests that the OSM developed through the RWLS approach could capture the design inconsistency more accurately.

5.4.3 Sensitivity Analysis

The sensitivity of the OSMs was evaluated for understanding the contribution of different geometric variables in predicting the operating speed. The modulus of the standardized beta coefficient of a

a)

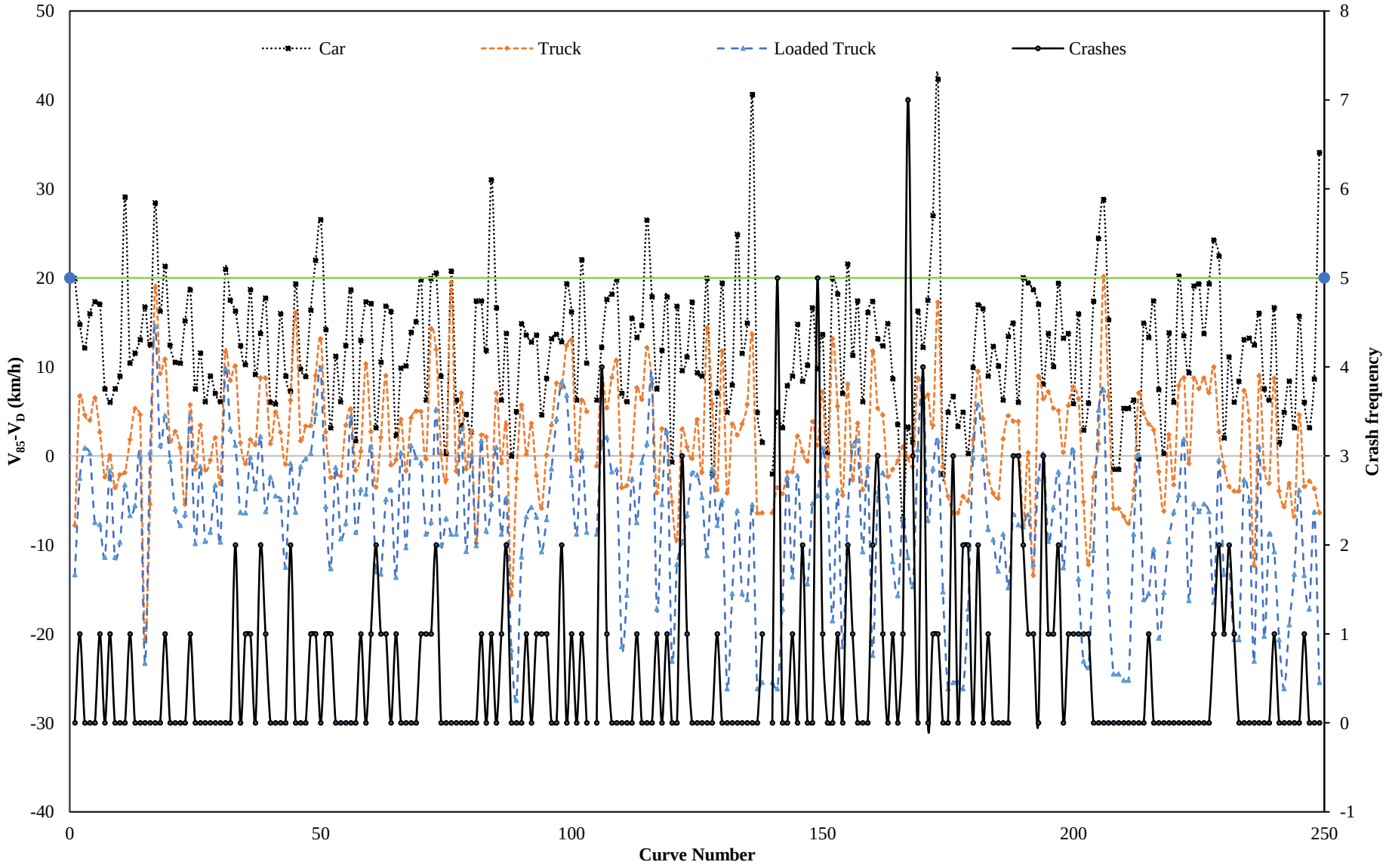

b)

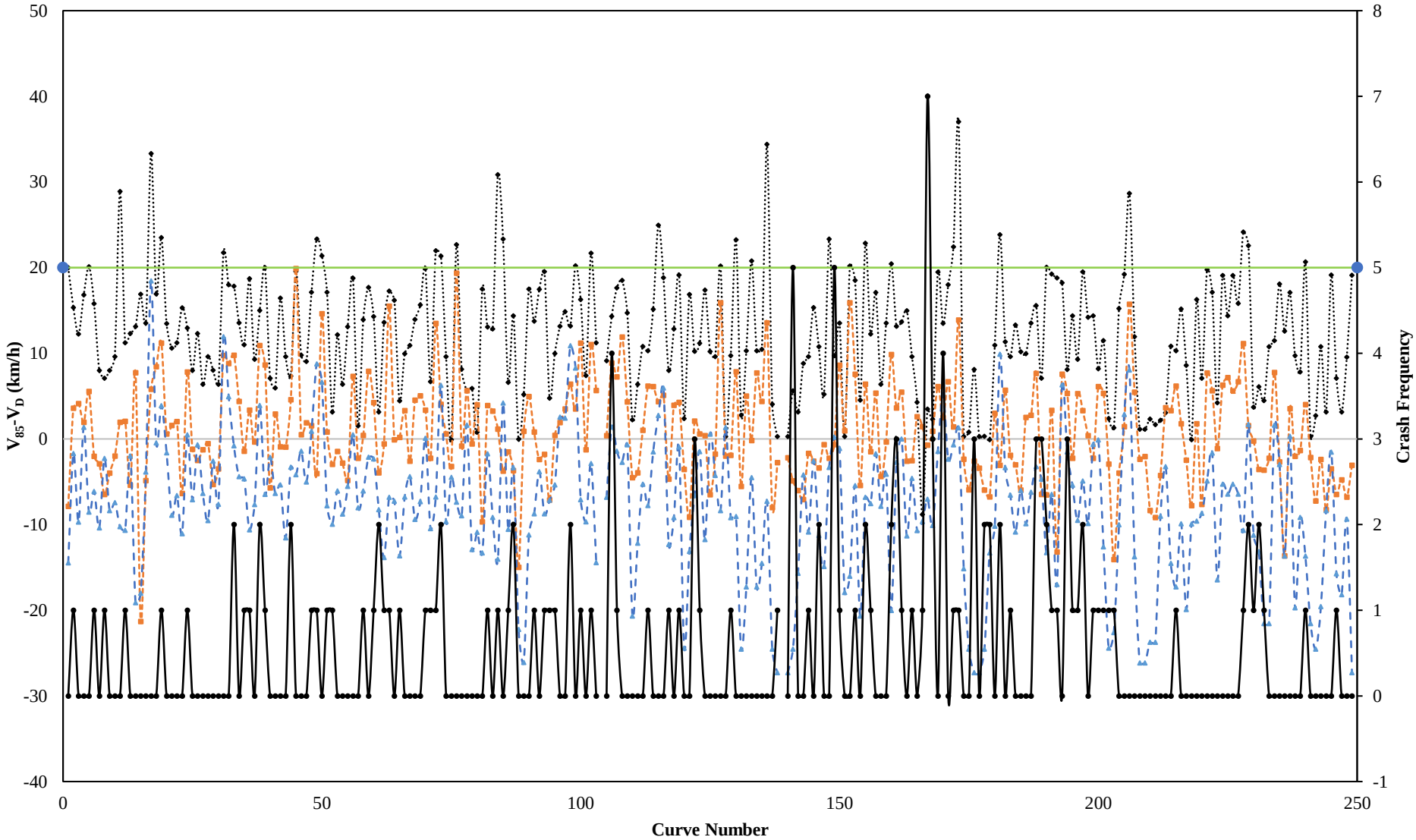

Fig. 5.7 Comparison of the Design Consistency (V_{85}-V_D) and crash frequency; a) OLS; b) RWLS

predictor indicates its sensitivity in estimating the dependent variable. Table 5.9 shows that the operating speed is highly sensitive to the variables highlighted in bold fonts, for the developed models. For example, the OSM for right-upgrade category involves how the L_{at} and G_1 affect the V_{85} of passenger cars. The model shows that with every increase of one standard deviation in L_{at}, the V_{85} rises by 0.346 standard deviations, with the other variable (G_1) is held constant. With an increase of one standard deviation in G_1, V_{85} decreases by 0.41 standard deviations, with L_{at} is held constant. The most sensitive geometric variables are gradient at approach tangent (G_1), curvature change rate (CCR_S & CCR), length of the vertical curve (L_V), length of approach and exit tangents (L_{at} & L_{et}), the interaction of radius with lane width ($R \times LW$). It can also be inferred from the table that the most sensitive variables corresponding to different curve geometries are different, which further supports the need for developing separate OSMs for different curve geometry.

Table 5.9 Operating speed models along with the degree of sensitivity of predictors

Category	Vehicle	β_1	β_2	β_3	Std β_1	Std β_2	Std β_3
Left Upgrade	Passenger Car	***G₂***			-0.81		
	Loaded Truck	***G₁***			-0.903		
	Empty Truck	***CCR***			-0.22		
Right Upgrade	Passenger Car	L_{at}	***G₁***		0.346	-0.41	
	Loaded Truck	***G₁***			-0.645		
	Empty Truck	***G₁***	Δ		-0.539	-0.47	
Left Downgrade	Passenger Car	L_{at}	***Lₑₜ***	$R \times LW$	0.412	0.579	0.502
	Loaded Truck	L_{at}	e	**Δ**	-0.449	0.415	-0.762
	Empty Truck	***Lₐₜ***	L_{et}	R	-0.66	0.17	0.09
Right Downgrade	Passenger Car	L_{at}	***CCRₛ***		-0.52	-0.69	
	Loaded Truck	***Lₑₜ***	G_5		-0.511	0.36	
	Empty Truck	***Lₑₜ***	CCR		0.64	-0.51	
Left Sag	Passenger Car	G_1	***CCRₛ***		0.004	-0.77	
	Loaded Truck	G_1	***L꜀***		-0.24	-0.54	
	Empty Truck	G_2	***R×LW***		-0.07	0.96	
Right Sag	Passenger Car	***DC***			-0.6		
	Loaded Truck	***Lₑₜ***	G_4		-0.54	-0.28	
	Empty Truck	***R×LW***			0.96		
Left Hog	Passenger Car	***Lₜ***			-0.75		
	Loaded Truck	L_{at}	***G₁***	L_t	-0.143	-0.47	0.367
	Empty Truck	L_{at}	***e***		0.5	-0.65	
Right Hog	Passenger Car	***Lᵥ***	CCR_S		-0.729	-0.243	
	Loaded Truck	L_{at}	***Lᵥ***		0.26	-0.70	
	Empty Truck	G_4	***CCR***		-0.23	-0.51	

5.5 Operating Speed Models for Tangent Sections

To carry out the consistency evaluation as per Lamm's criteria II (Lamm et al. 1995), (Section 5.2 of Chapter 2 Literature Review), the tangent section's operating speed needs to be estimated. While collecting the spot speed data of the circular curves, the speed at the approach tangent section was also collected. The speed data were collected at 60m ahead of the transition curve (Gibreel et al. 2001). It was assumed that the drivers would anticipate the effect of the horizontal curve combined with the vertical alignment much ahead of the curve. This is the case for tangents longer than 120m. However, for shorter tangents, the speed was collected from the middle of the tangent. The geometric parameters considered for predicting the speed on a tangent are the geometric characteristics of the previous (variables accompanied by subscript A) and following (variables accompanied by subscript B) horizontal curve of the tangent and the tangent's characteristics. Other researchers observed that a few other geometrical parameters such as the preceding and following also play a significant role.

The number of tangent sections used for modeling in this study was 134 for operating speed of passenger cars, 84 for empty truck, and 140 for loaded trucks. The average length of the tangent sections is 78m and gradient ranges between ±7%. The multiple regression analysis was carried out for modeling the operating speed on tangent sections of passenger cars ($V_{85C,\ Tan}$), empty trucks ($V_{85T,\ Tan}$), loaded trucks ($V_{85LT,\ Tan}$), and shown below.

$$V_{85C,\ Tan} = 55.053+0.043L_{atB}-0.63G_{1B}+0.011R_B+0.012R_A \qquad R^2=0.43 \qquad (5.11)$$

$$V_{85T,\ Tan} = 45.854+0.024L_{atB}-0.59G_{1B}+0.0129R_B+0.01R_A \qquad R^2=0.44 \qquad (5.12)$$

$$V_{85LT,\ Tan} =40.59-1.508G_{3A} \qquad R^2=0.42 \qquad (5.13)$$

The variables are significant at a 95% confidence level but the models' explanatory power is weak. The models could explain that as the length of the approach tangent (L_{atB}), the radius of the preceding (R_A), and the following horizontal curves (R_B) increase, the passenger car's operating speed also increases. Moreover, the speed is inversely dependent on the gradients of the approach tangent (G_{1B}) and the center of the preceding curve (G_{3A}). These geometric variables were also observed on studies by Polus et al. (2000), Gibreel et al. (2001) and Jacob and Anjaneyulu (2013)

One possible reason for these OSMs having a low R^2 value could be the selection bias of the geometric variables. To address this problem, the procedure discussed in the earlier sections was adopted. Weights were assigned to the geometric variables depending on their distribution. Higher weights were given to underrepresented variables and vice-versa. In addition to this, the Robust Weighted Least Square regression was also performed to tackle the outliers and heteroscedasticity. Lesser weights were given to those data lying far from the line of fit and vice-versa. The final models are shown in the equations below. The geometrical variables were found to be significant at a 95% confidence level. The operating speed models of passenger cars ($V_{85Tan,\,C}$) and empty trucks ($V_{85Tan,\,T}$) on tangent were quite reliable, with a high R^2 value of 0.98. The validation of the OSMs was carried out on the remaining 20% data set, and the RMSE and MAPE obtained are low, as shown below.

$$V_{85Tan,\,C} = 56.90+0.038L_{atB}-0.81G_{1B}+0.007R_B+0.011R_A \qquad R^2=0.98 \qquad (5.14)$$
RMSE=5.67km/h MAPE=7.59%

$$V_{85Tan,\,T} = 44.725+0.027L_{atB}-0.57G_{1B}+0.0127R_B+0.011R_A \qquad R^2=0.97 \qquad (5.15)$$
RMSE=5.69km/h MAPE=9.39%

However, the R^2 value did not improve for the operating speed models of loaded trucks ($V_{85Tan,\,LT}$), even with the RWLS method. This could be because the OSM for tangents was developed without segregating the tangents based on the vertical alignment; therefore, the geometry could not be captured adequately to predict the operating speed of the loaded trucks. Hence the tangents are categorized into four groups based on the combination with the vertical alignment – Upgrade, downgrade, sag, and hog curve. The multiple regression analysis was carried out for these categories, and Table 5.10 shows the OSM.

Table 5.10 OSM for loaded truck on tangent, through OLS Regression

Category	Model	R^2 Value
Downgrade	$49.272+1.548G_{5B}-0.0098CCR_{SB}-1.14G_{3A}$	0.55
Upgrade	$40.213-2.39G_{1B}+0.016R_A+0.011R_B$*	0.44
Sag	$35.0967-2.58G_{3A}$	0.71
Hog	$42.233-1.135G_{2B}-0.25DC_A$*	0.58

*p-value>0.05

The models' explainability has not improved despite the categorization, and the R^2 values are low for most cases, and some of the relevant variables are not significant at a 95% confidence level. RWLS was carried out, and Table 5.11 shows the final models. The variables are significant at a 95%

confidence level, with dependable operating speed models of loaded trucks at tangent having high R^2 values.

Table 5.11 OSM for loaded truck on tangent, through RWLS Regression

Category	Model	R^2 value	RMSE (km/h)	MAPE (%)
Downgrade	$46.677+1.27G_{5B}-0.0062CCR_{SB}-1.19G_{3A}$	0.94	7.32	16.44
Upgrade	$43.75-4.002G_{1B}+0.02R_A+0.007R_B$	0.98	6.68	14.26
Sag	$36.529-3.0697G_{3A}$	0.79	8.63	12.1
Hog	$44.885-0.808G_{2B}-0.35DC_A$	0.85	6.94	20.38

The geometrical parameters influencing the operating speed on different categories of tangents were different. The geometry of both the preceding and following curves of the tangent was found to impact the speed at the tangent. The gradient of the elements seems to be playing an essential role in the operating speed of loaded trucks.

The operating speed of loaded trucks on a tangent combined with a downgrade decreases as the grade at the middle of the preceding curve (G_{3A}) and the curvature change rate of the following curve (CCR_{SB}) increases. Whereas, as the exit tangent descending gradient of the following curve (G_{5B}) increases, the speed also increases.

Operating speed models of loaded trucks on tangent combined with an upgrade show that the speed depends on the radius of the preceding (R_A) and the following curve (R_B). Besides these parameters, the grade of the tangent (G_{1B}) is inversely proportional to speed. As the ascending gradient increases, the operating speed decreases.

For tangents combined with a sag curve, the operating speed of the loaded truck was inversely dependent on the grade at the middle of the preceding curve (G_{3A}). Whereas for tangents combined with a hog curve, the speed decreases as the degree of curvature of the preceding curve (DC_A) and the ascending gradient at the starting of the following curve (G_{2B}) increases. With these models, the speed at the approach tangent could now be predicted, which can further be used in evaluating the design consistency.

The RWLS approach has improved the explanatory power of the operating speed models for passenger cars and empty trucks significantly, reflected through higher R^2 value. Besides, the geometric

variables influencing the operating speed of loaded trucks which were insignificant (p-value>0.05) in OLS regression became significant when the models were estimated with RWLS regression.

5.6 Summary and Conclusion

This study analyzed and modeled the impact of sample selection bias, and heteroscedasticity on the OSMs developed for highways passing through mountainous terrain. Bias in the geometry data arises not only due to sampling error but also the nature of alignment. Specifically, for mountainous terrain, one possible reason could be the unavailability of suitable land due to which the road alignment ends up having geometrical elements of exceptional characteristics. In this process, the final alignment could be having a few sharp curves, flat grades, and longer tangents. Flat grades and longer tangents are not common in mountainous terrain. Another reason could be the clustering of curves used to capture the driver's perception of horizontal alignment superimposed with the vertical alignment. To capture the perception differences, the present study clustered the curves into eight categories. As expected, the curve clustering adopted in this study led to selection bias, in the case of specific curve categories.

The RWLS method was used to overcome the possible selection bias in modeling the operating speed of the vehicles. A weight estimation method for performing weighted least squared regression considering the proximity of the geometric variable in the *n*-dimensional space of speed and the geometrical variables was proposed. The RWLS model results indicate that the model performance has significantly improved with RWLS compared to OLS. For confirming the adequacy of the proposed approach, a comparison of design consistency estimated using OSM from OLS and RWLS was performed. It has been observed that there is a statistical difference in the consistency measure estimated using OLS and RWLS methods leading to underrated consistency evaluation. Further, the sensitivity analysis shows that the curve direction and superimposed vertical alignment influence the drivers' behavior. The most sensitive variable that influences drivers' speed choice differs between the curve types. Thus, this study also supports the need to categorize the horizontal curves and subsequently model the operating speed. It is to be noted that the RWLS alone might not solve the operating speed modeling-related issues for mountainous terrain. RWLS would be more effective if the sample data has an adequate representation of the actual range of the explanatory variables. The OSM for tangent

sections was also developed using the speed data collected on approach tangents and the geometry of the preceding and the following curves. The gradient and length of the tangent section, as well as the radius of the preceding and following horizontal curve, were the main geometric variables found to influence the operating speed of the vehicles on tangent sections.

Chapter 6

Geometric Design Consistency Analysis

6.1 General

Lamm et al. (1995) have proposed three different design consistency criteria that have been accepted and used by many researchers worldwide. These criteria were used in the present study to understand the design consistency of the subject highway and compared it with the crash records to see if there exists any agreement. In addition, observed/estimated operating speeds were used for checking the geometric design consistency. Table 6.1 shows Lamm's consistency evaluation criteria (Lamm et al. 1995).

i. Single element – Design inconsistency for a single element was determined based on the absolute difference between the operating speed of the vehicles at middle of the horizontal curve and the corresponding design speed.

ii. Successive elements – This is based on the absolute difference between the operating speeds at the middle of the horizontal curve and the operating speed at approach tangent.

iii. Driving Dynamic Consistency – This has been found based on the difference between the assumed side friction corresponding to the design speed and the demanded side friction corresponding to the operating speed at middle of the horizontal curve.

Table 6.1 Quantitative ranges for safety criteria (SC) I to III for good, fair, and poor design classes

Safety Criterion	Design Class		
	Good (1)	Fair (0)	Poor (-1)
I	$\lvert V_{85} - V_D \rvert \leq 10$	$10 < \lvert V_{85} - V_D \rvert \leq 20$	$\lvert V_{85} - V_D \rvert > 20$
II	$\lvert \Delta V_{85} \rvert \leq 10$	$10 < \lvert \Delta V_{85} \rvert \leq 20$	$\lvert \Delta V_{85} \rvert > 20$
III	$f_{RA} - f_{RD} \geq +0.01$	$-0.04 \leq f_{RA} - f_{RD} < +0.01$	$f_{RA} - f_{RD} < -0.04$

6.1.1 Design Consistency (Safety Criterion I)

The operating speed of the three vehicle types corresponding to all the highway elements was estimated using the developed models. However, the observed operating speeds were used for the elements where the field data were collected. The design consistency evaluation was carried out for the entire length of the road stretch for both the travel directions (Umiam to Jowai and Jowai to Umiam), separately. Figure 6.1 shows the variation in the operating speed and the design speed for the Umiam to Jowai route for various vehicle types. The figure shows that the operating speed is maximum for the passenger cars followed by empty trucks and loaded trucks. A similar trend was observed for the opposite route also.

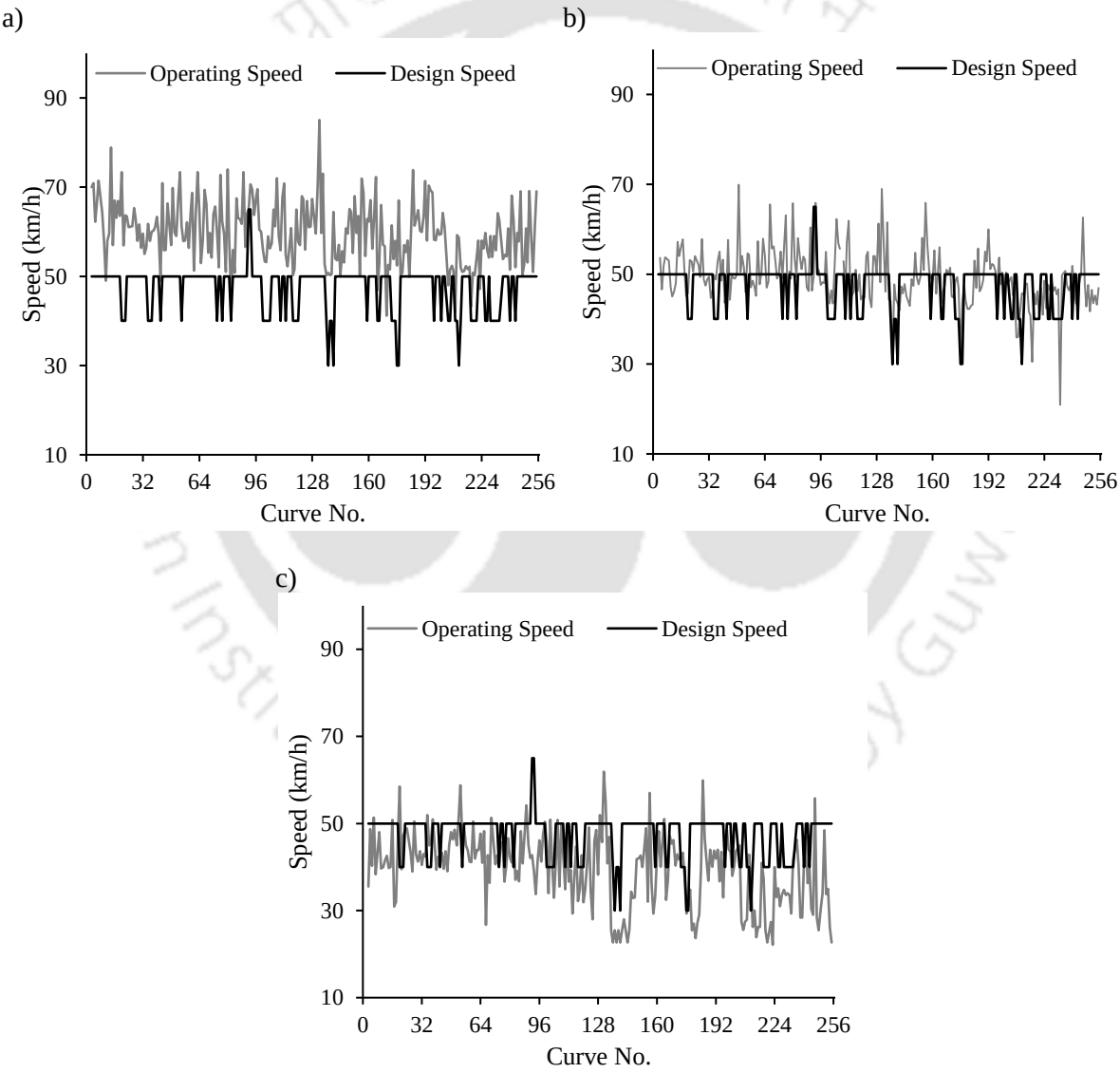

Fig. 6.1 Comparison of the operating and design speeds at the horizontal curves of the alignment of a) passenger car b) empty truck c) loaded truck

These critical speed differences can be evaluated by safety criterion (SC) I. For every single element, safety criterion I determines the speed difference between V_{85} at middle of the curve and V_D of the horizontal curve and according to Table 6.1, a safety criterion factor is assigned, describing the section as good, fair, or poor in design (Lamm et al. 1995).

Figure 6.2 shows the percentage of horizontal curves classified as 'good,' 'fair,' and 'poor' design for the three vehicle categories. These percentages are a measure to quantify the design consistency of the alignment which can be defined as Levels of consistency. Results show that the operating speed of empty trucks seems to be close to the design speed of the horizontal curve, with 86% of the horizontal curves falling in the 'good' design. In contrast, it seems to be deviating for the loaded trucks and even more for passenger cars, with 63% and 41% curves classified as good, respectively. This is due to the type and character of vehicles impacting their operating speed on the horizontal curves. Sixteen percent of the curves fall in the 'poor' design, suggesting that the operating speed of passenger cars is 20km/h higher than the design speed. A high-speed difference, as per this criterion, indicates that the drivers do not follow the speed limit corresponding to the curve and further suggests the need to adopt a higher radius curve or a wider shoulder at these locations. Table 6.2 shows that 94 curves fall under 'poor design' for empty and loaded trucks, resulting in 50 crashes.

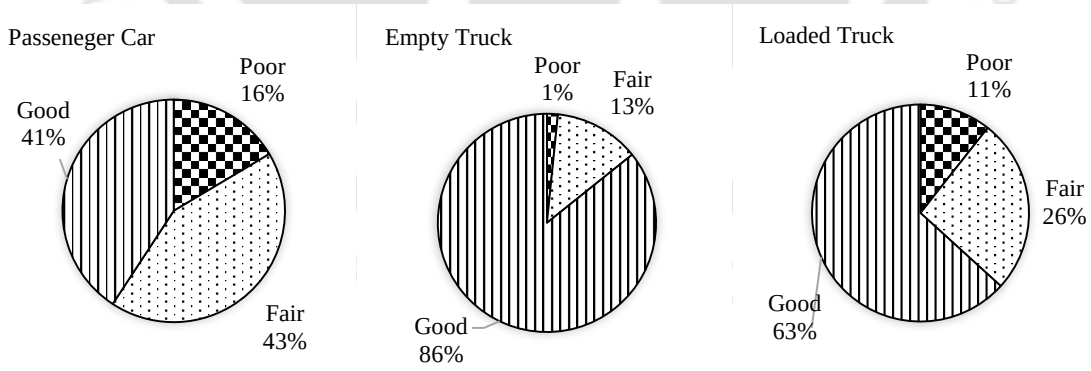

Fig. 6.2 Classification of the curves based on the safety criterion I

The curves were classified by their design speeds, and the number of crashes, and the curves where crashes have occurred. Table 6.2 shows that most crashes (180) occur on curves with a design speed of 50 km/h. As compared to other curves with different design speeds, it was discovered that the curve with a design speed of 30km/h had the highest proportion of crashes (70%). This demonstrates that sections with low design speeds pose safety issues. This can be justified, as there are only 10

horizontal curves with a design speed of 30km/h, but still have 21 total crashes occurring on 7 horizontal curves. This could be due to low design speeds and steeper downward gradients. Table 6.2 also indicates the number of poor designs ($|V_{85} - V_D| > 20$km/h) based on empty and loaded trucks' design speed consistency. Similar results were found for the curves with a design speed of 50 km/h having the highest percentage of crashes (35.71%) due to poor design.

Table 6.2 Number of curves and crashes for different curves based on Design speed

Design Speed, V_D (km/h)	No. of curves (a)	No. of Crashes	No. of curves with crashes (b)	Percentage of curves with crashes (b/a)	Poor Design curves based on V_{85T} & V_{85LT} (c)	Poor design curves with crashes (d)	No. of crashes involving trucks on poor designs	Percentage of crashes on Poor design (d/c)
30	10	21	7	70	0	0	0	-
40	104	52	33	31.7	35	10	18	28.57
50	376	180	113	30.05	56	20	31	35.71
65	4	1	1	25	3	1	1	33.33
Total	494	254	154	-	94	31	50	-

6.1.2 Operating Speed Consistency (Safety Criterion II)

This criterion was developed for evaluating the operating speed consistency in horizontal alignment and is related to the transition between two successive design elements (Lamm et al., 2007). A lower operating speed variation between successive elements represents a consistent design. While safety criterion I compares the operating speed with the design speed for each element, safety criterion II evaluates the operating speed difference between the successive design elements, i.e., the operating speed (V_{85}) on the horizontal curve and the operating speed at the approach tangent (V_{85tan}). Based on this safety criterion, detecting inconsistencies between successive design elements is critical for improving traffic safety. As per safety criterion II, Table 6.1 shows the ranges of differences in operating speeds considered for classifying good, fair, and poor designs.

The operating speeds on the approach tangents, for all the three vehicle types were estimated through the developed models. However, observed operating speed data were used for the tangents where the speed data were collected. The absolute operating speed difference at the tangent and the middle of the curve was calculated for each pair of successive elements, and the safety criterion factor was allotted according to Table 6.1. Figure 6.3 shows the percentage of elements classified as 'good,'

'fair,' and 'poor' design for different vehicle types. The majority of the successive sections have a speed difference of less than 10km/h for all vehicle types, thereby classified as 'good' design. This could be due to the vehicles maintaining consistently higher speeds on both the tangent and the successive curve.

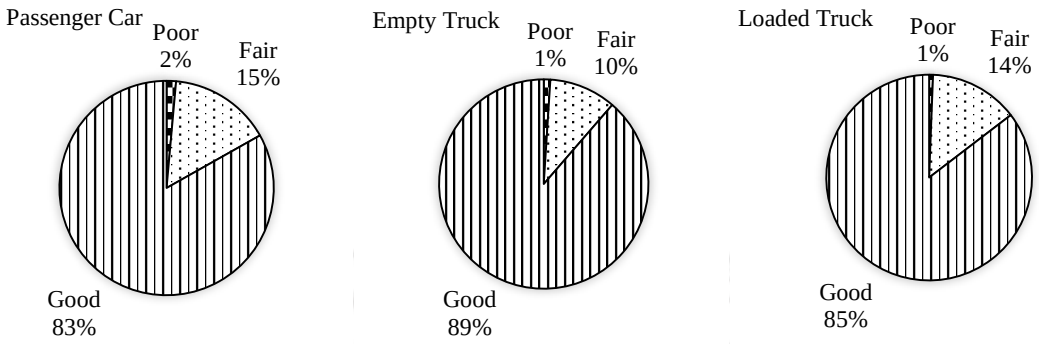

Fig. 6.3 Classification of the curves based on the safety criterion II

6.1.3 Driving Dynamic Consistency (Safety Criterion III)

To ensure safe traffic operation, accounting for vehicle stability in highway design is essential (Gibreel et al. 1999). As the vehicle travels on a horizontal curve, it is subjected to centrifugal force, causing a vehicle to overturn and lateral skid. The centrifugal force is balanced by the side friction between the road surface and the tyres, and the weight component resulting from the superelevation. Previous studies have also shown an increase in the accident rate on the curves with lesser skid resistance (Milton et al. 2008; Piyatrapoomi et al. 2008). Subsequently, highway geometric design clearly emphasizes the need for sufficient transverse friction between the tyres and road surface (in lateral direction), especially on the curved roadway sections. Designers should ensure that the lateral forces are kept within a tolerable range for driver comfort and vehicle stability. Safety criterion III is focused on achieving dynamic driving consistency on the horizontal curves. It compares the assumed side friction (f_{RA}) for curve design based on design speed with the demanded side friction (f_{RD}) for vehicles maneuvering through the curve at the operating speed, and based on the ranges shown in Table 6.1 (Lamm et al. 1995), the curves are categorized.

Side friction assumed (f_{RA}) is given by: $\frac{V_D^{\,2}}{127 * R} - e$ (6.1)

Side friction demanded (f_{RD}) is given by: $\frac{V_{85}^{\,2}}{127 * R} - e$ (6.2)

The rate of superelevation (e) of the horizontal curve varies from 0.025 to 0.1 with an average rate of 0.067. The statistics was shown in Table 3.1 of Chapter 3. For all horizontal curves, the assumed friction (f_{RA}) for curve design and the side friction demanded (f_{RD}) for vehicles maneuvering through the curve at the operating speed level were computed. The difference was calculated, and as per Table 6.1, safety criterion factors were allotted. Figure 6.4 shows the percentage of elements classified as 'good,' 'fair,' and 'poor' for the vehicle categories. According to these safety criteria, most of the horizontal curves fall in the 'poor' category for passenger cars as the operating speed of the passenger car is higher than the design speed. In contrast, most curves are classified as 'fair' and 'good' for empty and loaded trucks, respectively. This implies that with varying vehicle characteristics, the horizontal curves may be categorized differently due to the difference in operating speed.

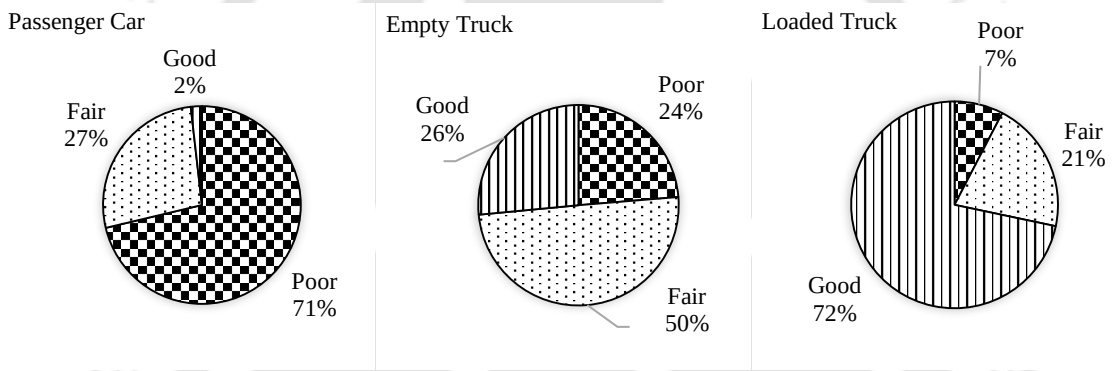

Fig. 6.4 Classification of the curves based on the safety criterion III

Likewise, a previous study by Zilioniene and Vorobjovas (2011) also assessed the horizontal alignment elements according to the three safety criteria. They determined that the design level of the horizontal alignment elements of the study roads according to safety criterion I in 26.7% of cases is fair and in 73.3% of cases is poor. For safety criterion II, 43.3% of the study roads are lower poor design, and in 56.7% of cases the design level is good, that is, the compatibility of curves and tangents on the regional roads is satisfactory. For safety criterion III, the dynamic stability of 7% of the study roads is poor, 80% are satisfactory, and 13% are good.

6.2 Endangerment

This investigation aimed to show the level of agreement between the outcome of the three safety criteria and the actual crash situation. To compare any safety criteria with crash data, the endangerment is

evaluated based on the number of crashes at a particular highway element and as per Table 6.3, defined by Schneider (1999), the curves were categorized.

Table 6.3 Classification of Endangerment (Schneider 1999)

Endangerment	Factor	No. of crashes
Low	1	Not more than 1
Medium	0	Not more than 2
High	-1	More than 2

The endangerment was classified for the passenger cars and trucks separately. Crashes of empty and loaded trucks were combined as they were not separated in the crash report. Table 6.4 shows the number of horizontal curves of the study area falling in various endangerment levels corresponding to passenger car and truck crashes.

Table 6.4 Number of sections in different endangerment levels, corresponding to the crashes involving passenger car and truck

		Endangerment Sections		
Vehicle	Direction	Low	Medium	High
Passenger Car	UJ	248	1	0
	JU	247	1	1
Truck	UJ	223	19	7
	JU	223	12	14

Note: UJ= Umiam to Jowai; JU= Jowai to Umiam

6.3 Analysis of Safety Criteria with the Safety

A relationship between safety criteria I, II, III, and endangerment reveal the level of agreement (Schneider 1999). Evaluating each vehicle type's safety criteria will be compared to the number of crashes involving that vehicle on all the highway sections. For example, when reviewing passenger car safety criteria, passenger cars' crashes are considered the responsible vehicle. Similarly, the safety criteria for empty and loaded trucks require trucks to be the crash's accountable vehicle. Table 6.5 shows the levels of agreement between safety criteria and the different endangerment levels. When a safety criterion reveals good design ("1"), a level of full agreement is reached, if the level of endangerment is low ("1"). However, if a safety criterion falls into the range of poor design ("-1"), a full agreement is reached if the level of endangerment is high ("-1"). The partial agreement arises when the safety criterion reveals good design (factor: "1"), but medium endangerment is observed, i.e., it stills resulted in a crash situation ("0"). A disagreement is defined if the comparison between the individual Safety criteria and endangerment differs by two steps, i.e., from "-1" to "1" or vice versa.

Table 6.5 Level of Agreement between safety criteria and endangerment levels

			Endangerment		
			Low	Medium	High
	Design Class	Factor	1	0	-1
Safety Criteria	Good	1	Full agreement (2)	Partial agreement (1)	Disagreement (0)
	Fair	0	Partial agreement (1)	Full agreement (2)	Partial agreement (1)
	Poor	-1	Disagreement (0)	Partial agreement (1)	Full agreement (2)

For the aggregation of agreement percentages, full agreement is considered as having a weight of "2", partial agreement a weight of "1" and disagreement a weight of "0". The aggregated agreement percentages are evaluated by dividing the actual summation of weighted agreement levels by the maximum agreement possibilities for the observed individual crash and design database. For example, the total level of agreement achieved for passenger car, UJ travel direction was 315, and total possible level of agreement for 249 curves was 498. Therefore, the level of agreement $= \frac{315}{498} \times 100$ = 63.25%. Table 6.6 presents the results of the evaluation conducted for each safety criterion individually corresponding to all the three vehicle types.

Table 6.6 Level of Agreement between each Safety criterion (SC) and endangerment, for all the vehicle type

Vehicle	Direction	SC I (%)	SC II (%)	SC III (%)
Passenger Car	UJ	63.25	**92.51**	15.26
	JU	61.44	**88.41**	16.06
Empty Truck	UJ	87.95	**89.27**	54.21
	JU	83.53	**86.38**	52.40
Loaded Truck	UJ	72.89	**88.25**	81.92
	JU	73.89	**84.95**	75.90

The level of agreement evaluated was similar for a particular safety criterion for both the traveling directions. For both the routes, the level of agreement obtained for safety criterion II was more significant (84-92%) and can be used in the future in making decisions on good, fair, and poor design practices. The level of agreement obtained for safety criterion III is least significant since only 15-16% of the curves show good agreement with the endangerment for passenger cars. Similarly, the safety criterion I also show only 61-63%. Similar investigations were carried out by Beck (1998), Schmidt (1995), Zumkeller (1998) and obtained 74,71, and 68% levels of agreement for SC I, II, and III, respectively. Lamm et al. (2007) mentioned that these results can be considered significant, and the developed safety criteria can, in the future, strongly support the work of traffic-safety officials when

making decisions about good, fair, or poor design practices. Recent studies by Castro et al. (2008) found that highway M-629 in Spain contains alignment inconsistencies with 26% poor designs. Also, Nama et al. (2016) conducted a study on four-lane highway mountainous terrain. They found that about 7% of scenarios under Criterion-I are rated as fair whereas, about 21% under Criterion-II are fair.

6.4 Overall Safety Module

Lamm et al. (2007) reported that the previously mentioned three safety criteria could be combined in an overall safety module for a more concise general description of the safety-evaluation process. According to the classification ranges, safety criteria I to III suggest that roadway sections can have different design safety levels depending on the individual safety criteria. This is because each of the safety criteria reflects a different aspect of highway geometric design safety. For example, the transition section between an independent tangent and a curve can correspond to poor design according to safety criterion II, while safety criterion i in terms of design speed or safety criterion III in terms of assumed side friction, or both, provide suitable values for the observed curved location. As a result, safety criteria I, II, and III will be combined into a safety module for a fast, detailed overview of new or existing alignments or road networks. The overall safety module for a safety criterion is defined as the classification of a criteria based on the cumulative criteria obtained by the average of the factors for all types of safety criteria, i.e., I, II, and III in this case. Table 6.7 shows the classification of the overall safety module.

Table 6.7 Classification of Overall Safety module

Design	Safety Criterion factor	Average value of safety module (x)
Good	1	$x \geq 0.5$
Fair	0	$-0.5 < x < +0.5$
Poor	-1	$x \leq -0.04$

For example, if a particular design element is found to be good design with regards to safety criterion I (factor = 1), fair design with regards to safety criterion II (factor = 0), Fair design with regards to safety criterion III (factor = 0), then the safety module factor is evaluated as the average of the three factors as $x = \frac{1+0+0}{3}$, implying x=0.33. As per Table 6.7, since x<0.5 and x>-0.5, the overall safety

module of that particular curve is classified as fair design. Table 6.8 presents the results of the level of agreement calculated for the overall safety criteria for the different vehicle types.

Table 6.8 Level of agreement for overall safety module and endangerment for various vehicle types

Vehicle	Direction	Level of agreement (%)
Passenger Car	UJ	57.89
	JU	61.44
Empty Truck	UJ	89.27
	JU	86.38
Loaded Truck	UJ	88.25
	JU	84.95

The results depict that the agreement between the overall safety criteria and the endangerment for passenger cars is lesser than that of empty and loaded trucks. The level of agreement between the overall safety criteria and the endangerment obtained for trucks was highest (84-89%).

6.5 Summary and Conclusion

The present chapter evaluated the geometric design consistency based on three safety criteria developed by Lamm et al. (1995). The entire road considered in the study was evaluated to check the design consistency according to the three safety criteria. The operating speed was higher than the design speed for passenger cars and lower for loaded trucks. The majority of the elements were considered 'good' design as per safety criterion I (single element design) for empty trucks, as their operating speed was close to the design speed. Based on safety criterion II (successive element design), most successive sections have a speed difference of less than 10km/h for all the three vehicle types and were classified as 'good' design. But, according to safety criterion III (dynamic driving consistency), the majority of the horizontal curves design falls in the 'poor' category for passenger cars as the operating speed is higher than the design speed. Whereas the majority of the curves are classified as 'fair' and 'good' for empty and loaded trucks, respectively. In other words, safety criterion II shows similar ranges of design consistencies for all the three vehicles considered. While, the design consistency evaluation according to safety criterion I and III yields varying levels of consistency across vehicle categories. The level of agreement between the safety criteria factor for every vehicle type and endangerment (considering the respective vehicle type) was tabulated, and the most significant result obtained was safety criterion II (84-92%) for all the three vehicles considered. Further, the agreement between the overall safety criteria

and the endangerment for trucks was more significant (84-89%) than passenger cars. It is more accurate to use the endangerment by truck for evaluating the design consistency because trucks have a higher proportion in the crash data of the existing alignment. The findings demonstrated that there is a significant relationship between the outcomes of the three safety criteria proposed by Lamm et al. (1995) and the actual crashes rates.

Chapter 7

Conclusion

7.1 Overview

This research has looked into several important aspects of operating speed modeling for two-lane rural highways located on mountainous terrain. The major contributions of this study include clustering of curves and modeling the operating speed for the combined horizontal and vertical alignment. Clustering of the horizontal curves was necessary as it was found that the direction of the horizontal curve and superimposition with the vertical alignment impacted the drivers' perception of the horizontal curve, subsequently affecting their operating speed. To overcome the possibility of selection bias in geometry data due to sampling error and the nature of alignment, the operating speed models were developed using Robust Weighted Least Square (RWLS) approach. The models were then used for predicting the speed, and the design consistency of the entire road stretch considered in the study was evaluated using Lamm et al. (1995) safety criteria. The following sections present the main findings and contributions, and suggestions for future studies.

7.2 Findings and Contributions

The following sections present the two important contributions of this study, namely, the curve clustering and the development of OSM considering the selection bias.

7.2.1 Curve Clustering

Field data indicate a significant difference in the operating speeds of the vehicles while turning left and right on a flat horizontal curve. The effects of curve direction on driver perception were initially tested on flat horizontal curves using the data acquired through the instrumented vehicle equipped with V-BOX. It was found that, for a smaller radius range, the mean difference between the adopted and actual radii is low and the difference increases with the curve radius (R>300m). Moreover, the difference between the two radii is higher for left-turning curves than the right turning for passenger cars, whereas the opposite was observed for the empty trucks. A two-sample t-test confirmed that the difference

between the radius of the chosen path and the actual radius statistically differs for the left and the right-turning curves.

The effect of curve direction and type of superimposed vertical alignment on the driver perception was analysed through the adopted path radius. Drivers tend to follow the design radius of the curve, thereby controlling the speed to negotiate the sharp curves safely, but when the radius of the curve increases beyond 300m, their paths tend to have a larger radius than the actual (difference ranging from 202 to 244m). The difference between the path radius and curve radius was statistically tested for all the curve combinations. The results indicate that the chosen vehicle path significantly depends on the vertical alignment.

The important contributions of this study toward curve clustering are as follows.

1. Speed profile and the path radius reflect the driver perception while the vehicle is traversing a horizontal curve superimposed with vertical alignment.
2. Curve direction and the type of vertical curve/grade were found to be significantly affecting the driver perception, hence can be considered as the criteria for clustering the curves.
3. Curve clustering has helped in capturing the effect of a few important geometric variables on the operating speed which are otherwise have shown poor correlation. Thus, the proposed method can help to build better operating speed models, resulting in better consistency studies.

7.2.2 Operating Speed Modeling

This study highlighted the impact of sample selection bias and heteroscedasticity on the OSMs developed for highways passing through mountainous terrain. Bias in the geometry data arises due to the nature of terrain. One possible reason could be the unavailability of land, due to which the road alignment ends up having geometrical elements of exceptional characteristics. In this process, the final alignment could have a few sharp curves, flat grades, and longer tangents, which are otherwise not common in mountainous terrain. Another reason could be the clustering of curves to minimize the driver's speed choice difference on a specific curve compared to that on a similar curve overlapped with the vertical alignment. The present study clustered the curves into eight categories and this led to selection bias. The RWLS method was then used to overcome the possible selection bias in modelling

the operating speed of the vehicles. The results indicate that the model performance has significantly improved with RWLS compared to OLS.

The important contributions of this study toward OSM in mountainous terrain are summarised as follows.

1. This study proposes a weight estimation method for RWLS that considers the proximity of the geometric variable and the speed in the n-dimensional space.
2. The L_{at} was found to be significant in the models related to five curve categories and for all three vehicle types. For example, on left-turning curves superimposed with downgrade alignment, an increase in the length of L_{at} will encourage the passenger car driver to increase the speed, but not in the case of empty and loaded trucks. Among the vertical alignment characteristics, G_1 is the most common variable affecting the operating speed of the all the vehicle types, across four curve categories. For instance, on right-turning curves superimposed with upgrade, G_1 has the highest negative impact on loaded trucks, followed by empty trucks and passenger cars.
3. It was found that the most sensitive variables corresponding to the OSM of different curve categories were different. This highlights the necessity of curve clustering and the consideration of selection bias through RWLS parameter estimation.

7.3 Design Consistency Findings

The study examined the geometric design consistency using the safety criteria proposed by Lamm et al. (1995) and correlated them with the crash data. The operating speed models for horizontal curves and approach tangents were used for predicting the speed at various geometric elements. The design consistency of the entire route considered in the study was evaluated using the three safety criteria. The results revealed a substantial association between the Lamm et al. (1995) safety criteria and the actual crash data. The important findings from this investigation are summarised as follows.

1. It was found that the consistency measure derived using the OLS and RWLS approaches differ statistically, showing that the safety assessment may not be reliable if the OSM is not appropriate. The predicted geometric design consistency using OLS and RWLS was cross-checked with the number of reported crashes. The observation suggests that the OSM developed through the RWLS approach could capture the design inconsistency more accurately.

2. Safety criterion II shows similar ranges of design consistencies for all the three vehicles considered with more than 80% of the road alignment rated as good design, suggesting compatible operating speed from tangent to the curve. However, the design consistency evaluation yields varying levels of consistency across vehicle categories, according to the results of safety criterion I and III, which evaluates the design of the horizontal curve. This signifies that the design of the horizontal curve may be rated differently based on these two criteria given the difference in operating speed of the vehicles due to their varying characteristics. The percentage of horizontal curves falling in good, fair, and poor designs for these safety criteria, vary according to the vehicle type. For example, under safety criteria I, 41, 86, and 63% of the curves were deemed as good designs for passenger cars, empty and loaded trucks.
3. Safety criterion II shows the highest level of agreement between the endangerment and the consistency, across the vehicle categories. Therefore, this study emphasizes that the successive element design consistency is a better approach for evaluating the consistency.
4. The endangerment of the trucks was showing a better agreement with the overall safety criteria (84-89 percent) than that of passenger cars (57-61 percent). Since trucks have a higher proportion in the crash data, it is more accurate to use the endangerment by truck for evaluating the design consistency for the existing alignment.

The impact of the mountainous road geometry is different on the operating speeds of passenger cars, trucks and loaded trucks. Moreover, the geometric design consistency analysis indicates that the change in operating speed of the vehicles from the tangent to curve, is clearly linked with the crash occurrence. The present study found that such horizontal curves have an operating speed difference of trucks (from tangent to curve) of more than 10km/h, and the crash data also proves that they are unsafe due to high endangerment. As the operating speed is strongly related to the geometric variables, choosing the right design of the geometric variables is crucial to control the operating speed. This is one of the practical applications of the OSMs developed in this study that can help improve the mountainous roads. The OSMs developed in this study can help improve the safety of mountainous roads at their design stage through the geometric design consistency analysis. This study also found that

the consistency assessment based on trucks' operating speed is more relevant than that of passenger cars, for mountainous roads.

7.4 Limitations & Future scope

The limitations & future scope of the study are as follows.

1. The scope of the operating speed models developed in this study is limited to dry road conditions and daytime with a clear sky. A comprehensive analysis can be performed for other weather conditions.
2. This study has not considered the reverse curves while developing the OSM. The proposed method can be extended to develop OSM for the reverse curve superimposed with multiple vertical curves, which are highly complicated. Moreover, sight distance availability was not considered in the present study.
3. This study has assumed that the speed of vehicle remains constant on a given curve and estimated the models based on the speed data collected at the middle of the curve. However, this assumption needs to be verified using the vehicle trajectory data. Further studies in this direction would certainly improve the OSM for mountainous terrain.
4. Test vehicle data were only used to arrive at the hypothesis that vertical alignment and turning direction of the horizontal curve affect the operating speed. Future studies may be carried out for further checking of this hypothesis.
5. Safety criterion III can be further improved considering the load carried by the trucks.
6. Various other approaches for developing OSM by using interaction variables can be considered in future studies. The critical factors contributing to vehicle operating speed on roadways may be examined by estimating a panel mixed generalized ordered probit fractional split (PMGOPFS) model (Eluru et al. 2013; Afghari et al. 2018; Bhowmik et al. 2019).

Appendix

Table A-1. Results of the ANOVA test of the operating speeds corresponding to different vehicle classes

Travel Direction 1				Travel Direction 2			
Curve No.	*F*	*P-value*	*F critical*	Curve No.	*F*	*P-value*	*F critical*
16	56.42	5.54E-20	3.043214	16	56.43	5.54E-20	3.04
37	21.58	3.32E-09	3.041518	37	21.58	3.32E-09	3.04
38	11.96	1.26E-05	3.04199	38	11.96	1.26E-05	3.04
40	25.09	2.19E-10	3.04398	40	25.09	2.19E-10	3.04
42	33.80	2.01E-13	3.039723	42	33.81	2.01E-13	3.04
48	12.81	5.8E-06	3.041056	48	12.81	5.8E-06	3.04
55	15.90	4.06E-07	3.042964	55	15.90	4.06E-07	3.04
65	34.55	1.46E-13	3.042472	65	34.55	1.46E-13	3.04
66	15.76	4.52E-07	3.042472	66	15.77	4.52E-07	3.04
70	15.46	6.04E-07	3.04398	70	15.47	6.04E-07	3.04
71	12.53	0.081952	3.047906	71	12.54	0.081952	3.05
79	12.13	0.121252	3.044771	79	12.13	0.121252	3.04
98	13.28	6.04E-06	3.070512	98	13.28	6.04E-06	3.07
99	7.49	0.000974	3.097698	99	7.50	0.000974	3.10
121	87.04	6.41E-26	3.055558	121	87.04	6.41E-26	3.06
122	23.19	5.47E-09	3.08824	122	23.20	5.47E-09	3.09
123	9.37	0.000179	3.082015	123	9.37	0.000179	3.08
124	52.7	1.29E-16	3.082015	124	52.70	1.29E-16	3.08
126	10.86	5.05E-05	3.081193	126	10.87	5.05E-05	3.08
127	10.87	5.58E-05	3.092217	127	10.88	5.58E-05	3.09
129	19.85	4.16E-08	3.077309	129	19.85	4.16E-08	3.08
131	7.236	0.001068	3.069894	131	7.24	0.001068	3.07
132	52.53	1.8E-18	3.049468	132	52.54	1.8E-18	3.05
136	43.95	3.66E-14	3.094337	136	43.95	3.66E-14	3.09
143	164.49	6.49E-38	3.058928	143	164.50	6.49E-38	3.06
148	94.99	3.4E-24	3.083706	148	95.00	3.4E-24	3.08
150	29.63	7.15E-11	3.085465	150	29.63	7.15E-11	3.09
151	28.40	2.88E-10	3.09887	151	28.41	2.88E-10	3.10
157	10.74	5.53E-05	3.080387	157	10.75	5.53E-05	3.08
158	38.32	9.85E-13	3.09887	158	38.33	9.85E-13	3.10
159	55.34	6.59E-17	3.087296	159	55.34	6.59E-17	3.09
164	21.477	2.72E-08	3.102552	164	21.48	2.72E-08	3.10
165	87.69	3.37E-23	3.082015	165	87.69	3.37E-23	3.08
166	35.50	4.79E-13	3.065296	166	35.50	4.79E-13	3.07
167	46.48	6.94E-15	3.090187	167	46.49	6.94E-15	3.09
168	13.68	4.99E-06	3.079596	168	13.68	4.99E-06	3.08
169	32.62	4.47E-12	3.070512	169	32.62	4.47E-12	3.07
171	18.70	8.81E-08	3.07309	171	18.70	8.81E-08	3.07
172	7.93	0.000564	3.066952	172	7.93	0.000564	3.07
173	25.21	1.03E-09	3.080387	173	25.21	1.03E-09	3.08

Table A-1. Results of the ANOVA test of the operating speeds corresponding to different vehicle classes

Travel Direction 1				Travel Direction 2			
Curve No.	*F*	*P-value*	*F critical*	Curve No.	*F*	*P-value*	*F critical*
174	21.60	1.22E-08	3.078819	174	21.60	1.22E-08	3.08
180	100.64	9.63E-26	3.077309	180	100.64	9.63E-26	3.08
181	92.18	4.75E-25	3.07114	181	92.18	4.75E-25	3.07
182	95.66	1.44E-25	3.071779	182	95.66	1.44E-25	3.07
183	70.39	7.15E-20	3.086371	183	70.40	7.15E-20	3.09
187	27.96	8.62E-11	3.067521	187	27.97	8.62E-11	3.07
188	41.40	2.68E-14	3.074447	188	41.41	2.68E-14	3.07
189	28.14	2.4E-10	3.091191	189	28.15	2.4E-10	3.09
192	15.56	9.18E-07	3.068689	192	15.57	9.18E-07	3.07
193	49.92	6.28E-17	3.063715	193	49.92	6.28E-17	3.06
194	43.66	1.22E-13	3.107891	194	43.67	1.22E-13	3.11
195	41.64	1.46E-14	3.069286	195	41.65	1.46E-14	3.07
200	13.35	7.52E-06	3.090187	200	13.36	7.52E-06	3.09
201	38.96	3.54E-13	3.089203	201	38.96	3.54E-13	3.09
209	56.04	2.75E-17	3.082852	209	56.04	2.75E-17	3.08
221	189.81	3.1E-36	3.079596	221	189.81	3.1E-36	3.08
222	83.70	1.51E-23	3.07114	222	83.70	1.51E-23	3.07
223	183.53	1.11E-34	3.084577	223	183.54	1.11E-34	3.08
231	109.28	3.44E-26	3.084577	231	109.28	3.44E-26	3.08
245	194.60	1.1E-38	3.070512	245	194.61	1.1E-38	3.07

Fig. A-1. Variation of the path radius with the actual radius and the gradient for both left and right turning curves corresponding to sag and hog curves, for a) Passenger car; b) empty truck

a)

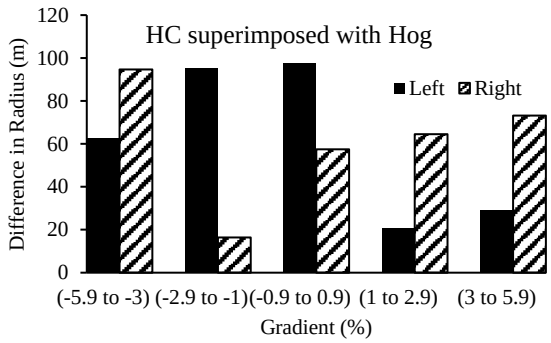

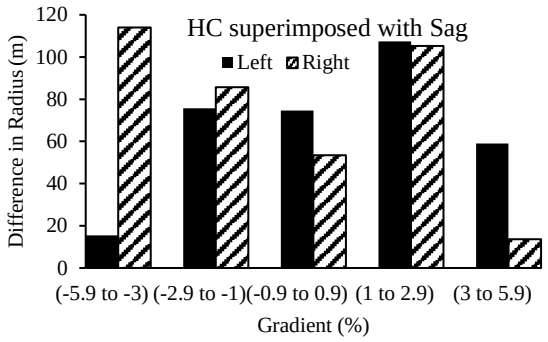

b)

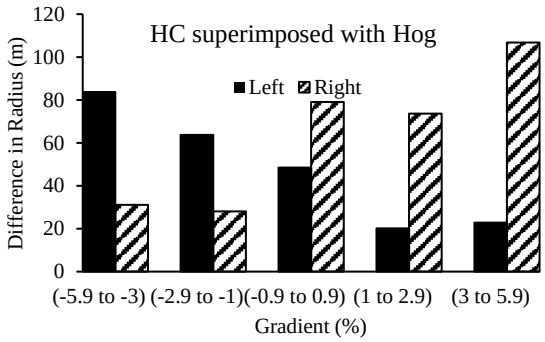

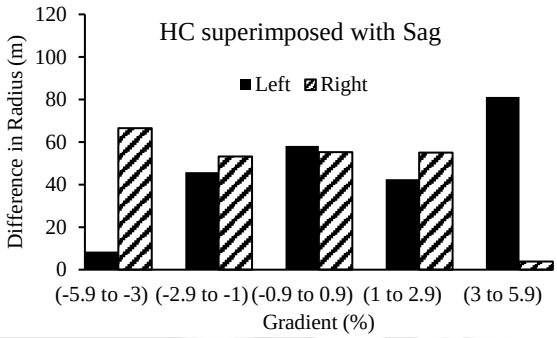

Table A-2 (a). Distribution of Geometric Parameters Considered for Different Curve Categories of Loaded Truck

Loaded/Left/Downgrade		**Loaded /Left/Hog**		**Loaded /Left/Sag**		**Loaded/Left/Upgrade**	
Range of L_{at}	Percentage	Range of L_{at}	Percentage	Range of G_1	Percentage	Range of G_1	Percentage
0-50	0.5	0-50	0.55	-7 to -3	0.26	2 to 3	0.16
51-100	0.25	51-100	0.22	-2.9 to 0	0.26	3.1 to 4	0.08
101-150	0.25	101-150	0.05	0.1 to 3	0.33	4.1 to 5	0.16
		151-200	0.05	3.1 to 7	0.13	5.1 to 6	0.58
		201-250	0.11				
Range of e	Percentage	Range of G_1	Percentage	Range of Lc	Percentage		
0-0.05	0.16	-3 to-1	0.05	0-50	0.33		
0.06-0.07	0.41	-0.9 to 1	0.16	51-100	0.46		
0.08-0.09	0.16	1.1 to 3	0.27	101-150	0.13		
0.10-0.11	0.25	3.1 to 5	0.38	151-200	0.06		
		5.1 to 7	0.11				
Range of Δ	Percentage	Range of Lt	Percentage				
0-50	0.58	15-30	0.38				
51-100	0.33	31-45	0.55				
101-150	0	46-60	0.05				
151-200	0.08						
Loaded/Right/Downgrade		**Loaded/Right/Hog**		**Loaded/Right/Sag**		**Loaded/Right/Upgrade**	
Range of L_{et}	Percentage	Range of L_{at}	Percentage	Range of L_{et}	Percentage	Range of G_1	Percentage
0-50	0.38	0-50	0.63	0-50	0.5	0-2	0.07
51-100	0.46	51-100	0.15	51-100	0.14	2.1 to 4	0.23
101-150	0.15	101-150	0.05	101-150	0.07	4.1 to 6	0.69
		151-200	0.10	151-200	0.14		
		201-250	0	201-250	0.14		
		251-300	0.05				
Range of G_5	Percentage	Range of L_V	Percentage	Range of G_4	Percentage		
-7 to -5	0.38	50-100	0.73	-4to -2	0.42		
-4.9 to -3	0.46	101-150	0.15	-1.9 to 0	0.14		
-2.9 to -1	0.15	151-200	0.10	0.1 to 2	0.21		
				2.1 to 4	0		
				4.1 to 6	0.21		

Table A-2 (b). Distribution of geometric parameters considered for different curve categories of Empty Truck

Truck/Left/Downgrade		**Truck/Left/Hog**		**Truck/Left/Sag**		**Truck/Left/Upgrade**	
Range of L_{at}	Percentage	Range of L_{at}	Percentage	Range of G_2	Percentage	Range of CCR	Percentage
0-50	0.5	0.50	0.46	-7 to -5	0.23	0-500	0.18
51-100	0.33	51-100	0.23	-4.9 to -3	0.17	501-1000	0.18
101-150	0.16	101-150	0.07	-2.9 to -1	0.11	1001-1500	0.45
		151-200	0.07	-0.9 to 1	0.23	1501-2000	0.18
		201-250	0.07	1.1 to 3	0.17		
		251-300	0.07	3.1 to 5	0.05		
Range of L_{et}	Percentage	Range of e	Percentage	Range of R×LW	Percentage		
0-50	0.58	0.02-0.04	0.07	0-500	0.58		
51-100	0.16	0.05-0.06	0.46	501-1000	0.17		
101-150	0.16	0.07-0.08	0.3	1001-1500	0.11		
151-200	0.08	0.09-0.1	0.15	1501-2000	0.11		
Range of R	Percentage						
0-100	0.41						
101-200	0.33						
201-300	0.16						
301-400	0						
401-500	0.08						
Truck/Right/Downgrade		**Truck/Right/Hog**		**Truck/Right/Sag**		**Truck/Right/Upgrade**	
Range of L_{et}	Percentage	Range of G_4	Percentage	Range of R×LW	Percentage	Range of G_1	Percentage
0-50	0.33	-7 to -5	0.07	0-500	0.76	-1 to 1	0.25
51-100	0.53	-4.9 to -3	0.15	501-1000	0.11	1.1 to 3	0
101-150	0.06	-2.9 to -1	0.23	1001-1500	0.05	3.1 to 5	0.58
151-200	0.06	-0.9 to 1	0.23	1501-2000	0.05	5.1 to 7	0.16
		1.1 to 3	0.23				
		3.1 to 5	0.07				
Range of CCR	Percentage	Range of CCR	Percentage			Range of Δ	Percentage
0-500	0.26	0-500	0.15			0-50	0.58
501-1000	0.13	501-1000	0.38			51-100	0.33
1001-1500	0.4	1001-1500	0.15			101-150	0
1501-2000	0.13	1501-2000	0.23			151-200	0.08
2001-2500	0.06	2001-2500	0.07				

Fig A-2. Distribution of Explanatory Variables over the actual range

X-axis: Range of the Variable; Y-axis: Operating speed of the respective vehicle

Type	Passenger Car	Loaded Truck	Empty Truck
Left Upgrade	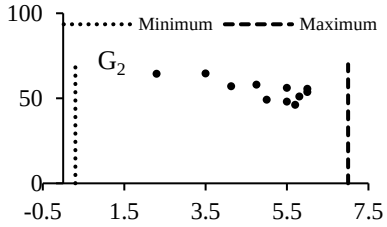	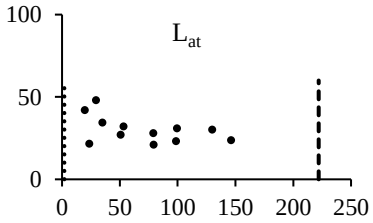	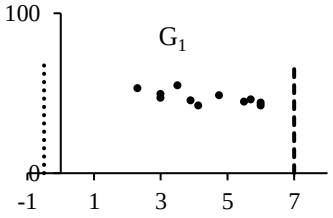
	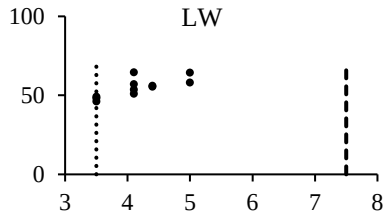	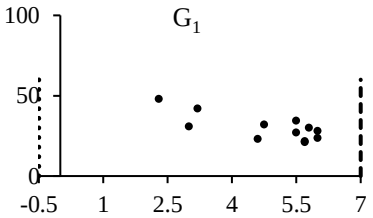	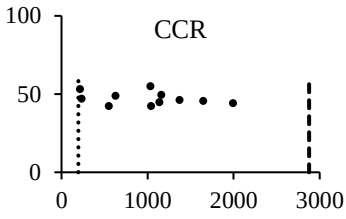
Right Upgrade	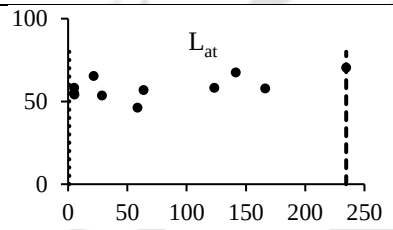	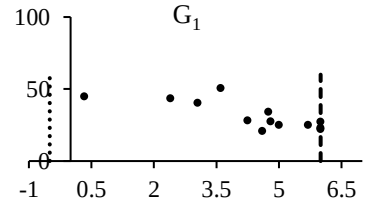	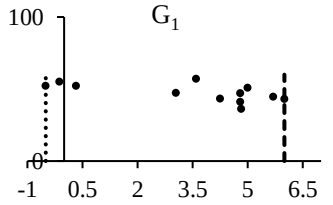
	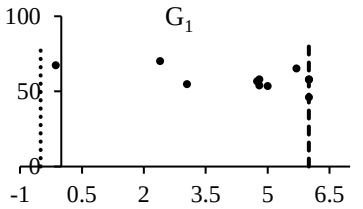	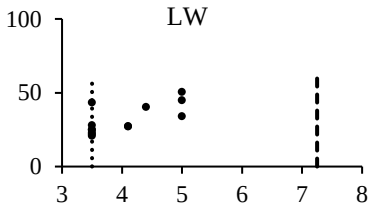	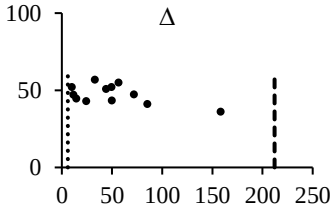

Type	Passenger Car		Loaded Truck	Empty Truck
Left Downgrade	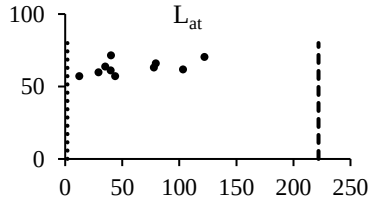	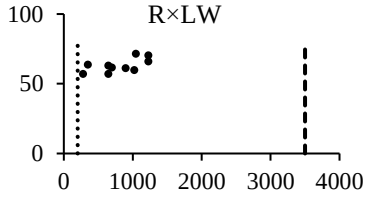	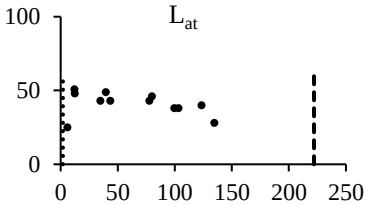	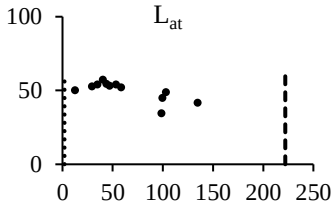
	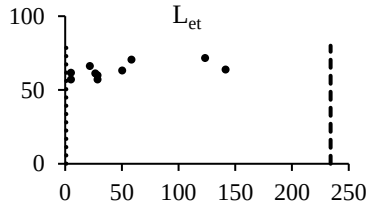		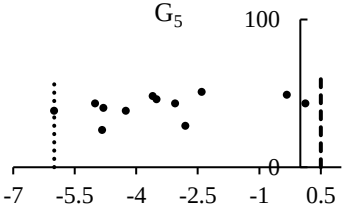	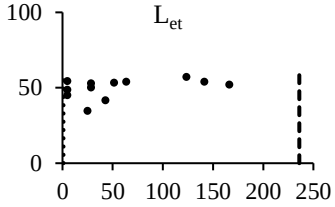
	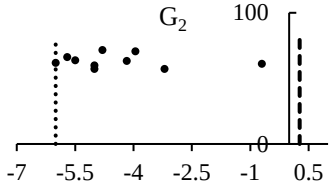		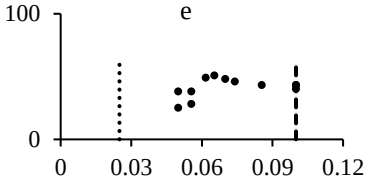	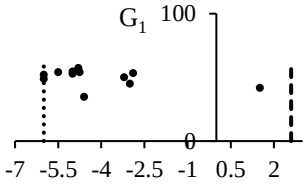
	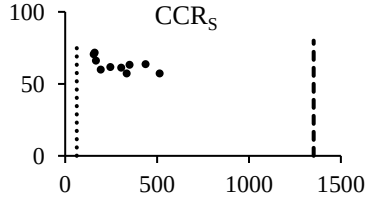		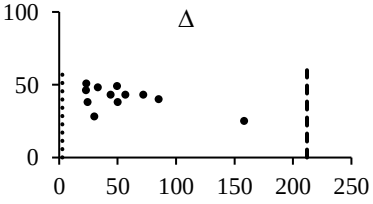	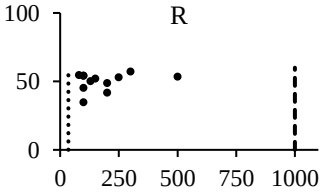

Type	Passenger Car	Loaded Truck	Empty Truck
Right Downgrade	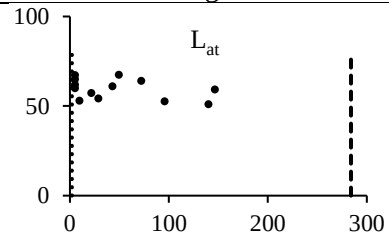	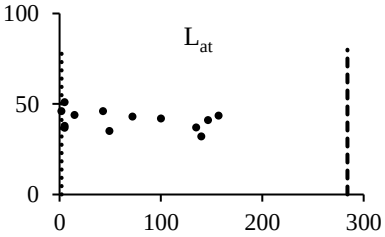	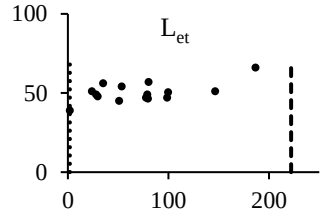
	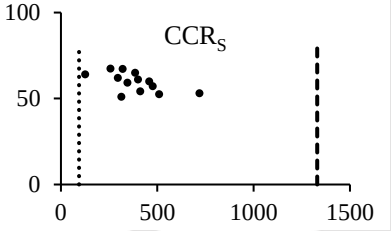	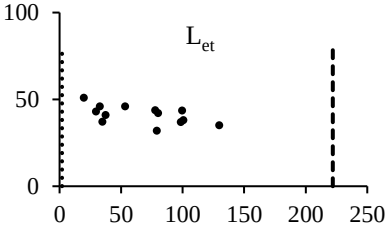	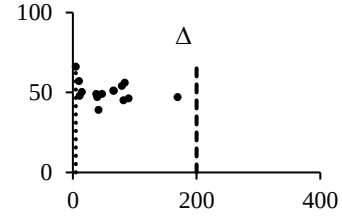
		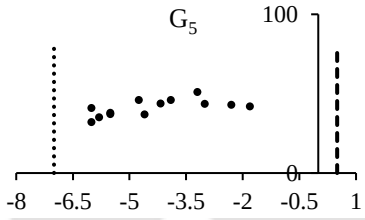	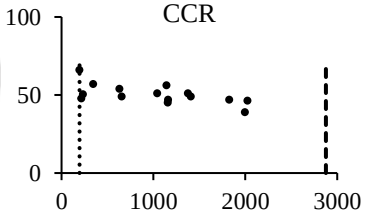

Type	Passenger Car	Loaded Truck	Empty Truck
Left Sag	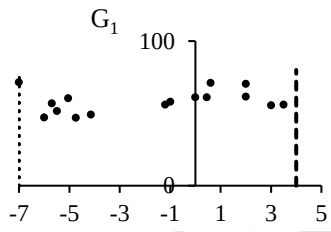	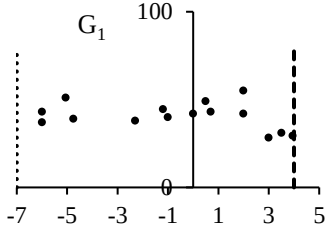	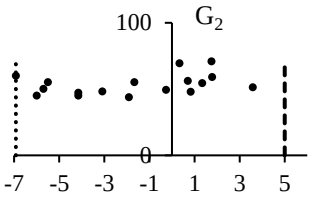
	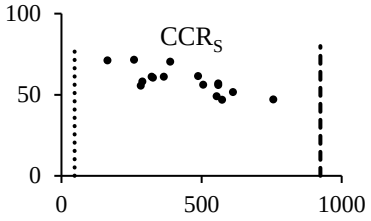	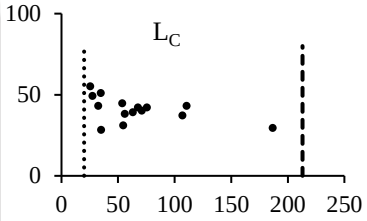	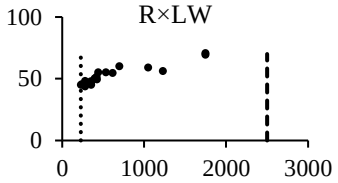
Right Sag	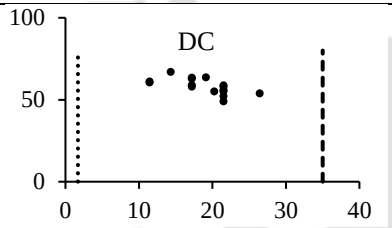	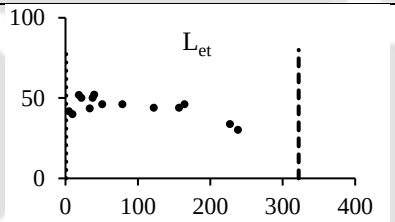	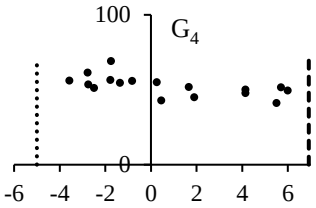
		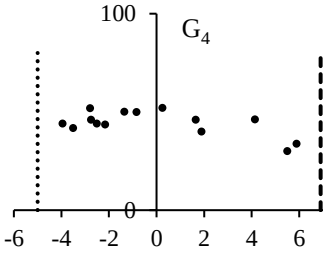	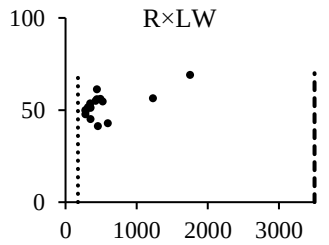

Type	Passenger Car	Loaded Truck	Empty Truck
Left Hog	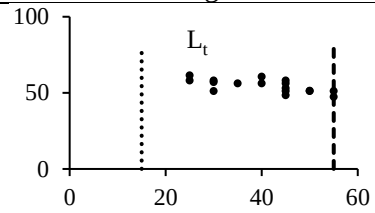	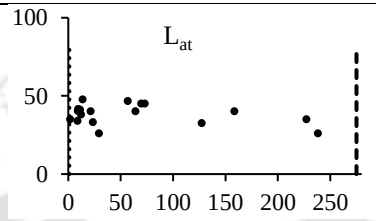 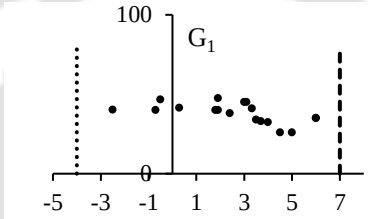 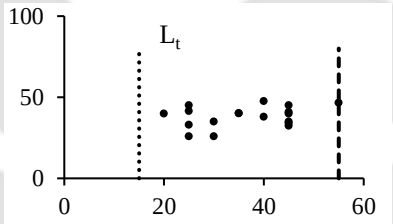	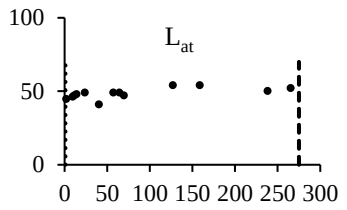 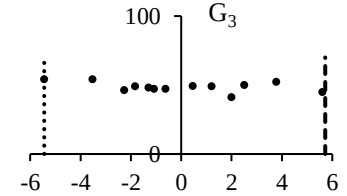 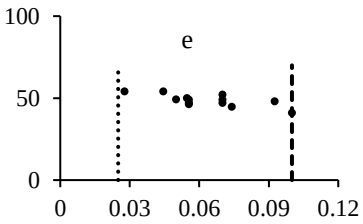

Type	Passenger Car	Loaded Truck	Empty Truck
Right Hog	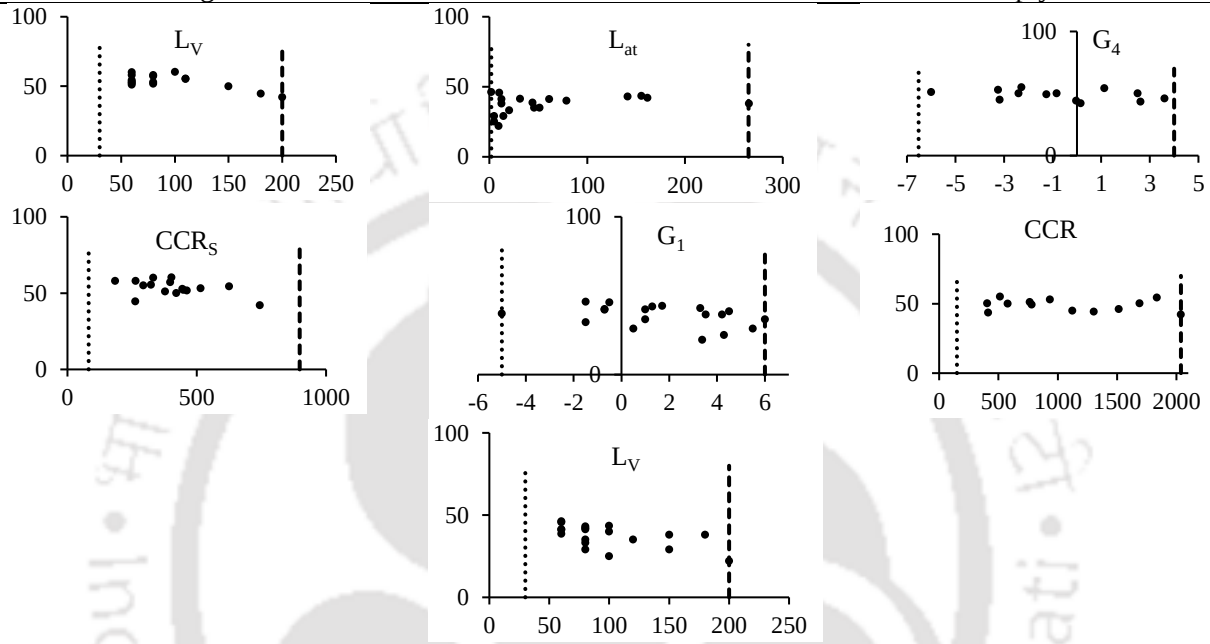		

References

AASHTO. (1994). *A Policy on Geometric Design of Highways and Streets*. American Association of State Highway and Transportation Officials (AASHTO), Washington, DC, US.

AASHTO. (2004). *A Policy on Geometric Design of Highways and Streets*. American Association of State Highway and Transportation Officials (AASHTO), Washington, DC, US.

AASHTO. (2010). *Highway safety manual*. American Association of State Highway and Transportation Officials (AASHTO), Washington, DC, US.

AASHTO. (2011). *A Policy on Geometric Design of Highways and Streets*. American Association of State Highway and Transportation Officials (AASHTO), Washington, DC, US.

AASHTO. (2018). *A Policy on Geometric Design of Highways and Streets*. American Association of State Highway and Transportation Officials (AASHTO), Washington, DC, US.

Abdul-Mawjoud, A. A., and Sofia, G. G. (2008). "Development of models for predicting speed on horizontal curves for two-lane rural highways." *The Arabian Journal for Science and Engineering*, 33(2B), 365–377.

Adolini-Minnicino, M., and Elefteriadou, L. (2004). "Speed prediction models for trucks on two-lane rural highways." *In 83rd Annual Meeting of the Transportation Research Board. Washington, DC*.

Afghari, A. P., Haque, M. M., and Washington, S. (2018). "Applying fractional split model to examine the effects of roadway geometric and traffic characteristics on speeding behavior." *Traffic Injury Prevention*, Taylor & Francis, 19(8), 860–866.

Akoglu, H. (2018). "User's guide to correlation coefficients." *Turkish Journal of Emergency Medicine*, 18(August), 91–93.

Al-Masaeid, H. R., Hamed, M., Aboul-Ela, M., and Ghannam, A. G. (1995). "Consistency of Horizontal Alignment for Different Vehicle Classes." *Transportation Research Record*, Transportation Research Board, Washington, D.C., 1500, 178–183.

Alexander, G. (1986). *Driver Expectancy in Highway Design and Traffic Operations*. U.S. Department of Transportation, Federal Highway Administration Office of Traffic Operations.

Anderson, I. B., Bauer, K. M., Harwood, D. W., and Fitzpatrick, K. (1999). "Relationship To Safety of Geometric Design Consistency Measures for Rural Two-Lane Highways." *Transportation Research Record*, Transportation Research Board, Washington, D.C., 1658, 43–51.

Andueza, P. J. (2000). "Mathematical models of vehicular speed on mountain roads." *Transportation Research Record*, Transportation Research Board, Washington, D.C, 1701, 104–110.

Antonio Martín-Jiménez, J., Zazo, S., Arranz Justel, J. J., Rodríguez-Gonzálvez, P., and González-Aguilera, D. (2018). "Road safety evaluation through automatic extraction of road horizontal alignments from Mobile LiDAR System and inductive reasoning based on a decision tree." *ISPRS Journal of Photogrammetry and Remote Sensing*, Elsevier Ltd, 146(May), 334–346.

Beck, A. (1998). "Analysis and Evaluation of Relationships between Traffic Safety and Highway Design on Two-Lane Rural Roads." (Doctoral dissertation, Master Thesis, Institute for Highway and Railroad Engineering, University of Karlsruhe (TH), Germany).

Ben-Bassat, T., and Shinar, D. (2011). "Effect of shoulder width, guardrail and roadway geometry on driver perception and behavior." *Accident Analysis and Prevention*, Elsevier Ltd, 43(6), 2142–2152.

Bhowmik, T., Yasmin, S., and Eluru, N. (2019). "A multilevel generalized ordered probit fractional

split model for analyzing vehicle speed." *Analytic Methods in Accident Research*, Elsevier Ltd, 21(July 2018), 13–31.

Bidulka, S., Sayed, T., and Hassan, Y. (2002). "Influence of vertical alignment on horizontal curve perception. Phase I: Examining the hypothesis." *Transportation Research Record*, Transportation Research Board, Washington, D.C., 1796, 12–23.

Boroujerdian, A. M., Seyedabrishami, E., and Akbarpour, H. (2016). "Analysis of Geometric Design Impacts on Vehicle Operating Speed on Two-Lane Rural Roads." *Procedia Engineering*, 1144–1151.

Cafiso, S., and La Cava, G. (2009). "Driving performance, alignment consistency, and road safety." *Transportation Research Record*, Transportation Research Board, Washington, D.C., 2102, 1–8.

Cafiso, S., La Cava, G., Heger, R., Lamm, R., and PIARC, W. R. A.-. (2003). "Integrating human factor evaluation in the design process of roads - A way to improve safety standards for rural roads." *Proceedings of the 22nd PIARC World Road Congress (CD-ROM)*, Durban, South Africa, 19–25.

Cafiso, S., Di Graziano, A., and La Cava, G. (2005). "Actual Driving Data Analysis for Design Consistency Evaluation." *Transportation Research Record*, Transportation Research Board, Washington, D.C., 1912, 19–30.

Cafiso, S., Di Graziano, A., La Cava, G., Lamm, R., and Heger, R. (2004). "In Field Data Collection for Driving Behaviour Analysis using the DIVAS Instrumented Car." *14th International Congress of the Italian Society of Highway Infrastructure*, Florence, Italy.

Cafiso, S., Di Graziano, A., Di Silvestro, G., La Cava, G., and Persaud, B. (2010). "Development of comprehensive accident models for two-lane rural highways using exposure, geometry, consistency and context variables." *Accident Analysis and Prevention*, Elsevier Ltd, 42(4), 1072–1079.

Camacho-Torregrosa, F. J., Pérez-Zuriaga, A. M., Campoy-Ungría, J. M., and García-García, A. (2013). "New geometric design consistency model based on operating speed profiles for road safety evaluation." *Accident Analysis and Prevention*, Elsevier Ltd, 61, 33–42.

Castro, M., Pardillo-Mayora, J. M., and Jurado, R. (2013). "Development of a Local Operating Speed Model for Consistency Analysis Integrating Laser, GPS and GIS for Measuring Vehicles Speed." *Baltic Journal of Road and Bridge Engineering*, 8(4), 281–288.

Castro, M., Sánchez, J. A., Vaquero, C. M., Iglesias, L., and Rodríguez-Solano, R. (2008). "Automated GIS-Based System for Speed Estimation and Highway Safety Evaluation." *Journal of Computing in Civil Engineering*, 22(5), 325–331.

Castro, M., Sánchez, J. F., Sánchez, J. A., and Iglesias, L. (2011). "Operating Speed and Speed Differential for Highway Design Consistency." *Journal of Transportation Engineering*, 137(11), 837–840.

Chatterjee, S., and Mächler, M. (1997). "Robust regression: A weighted least squares approach." *Communications in Statistics - Theory and Methods*, 26(6), 1381–1394.

Chatterjee, S., and Mitra, S. (2019). "Safety Assessment of Two-Lane Highway using a Combined Proactive and Reactive Approach : Case Study from Indian National Highways." *Transportation Research Record*, SAGE Publications Sage CA: Los Angeles, CA, 2673(7), 709–721.

Chen, F., Wang, M., and Duan, L. (2014). "Letting Drivers Know What is Going on in Traffic." *Advances in Intelligent Vehicles*, Elsevier, 291–318.

Choudhari, T., and Maji, A. (2019). "Effect of Horizontal Curve Geometry on the Maximum Speed Reduction : A Driving Simulator - Based Study." *Transportation in Developing Economies*,

Springer International Publishing, 8, 1–8.

Colonna, P., Berloco, N., Intini, P., Perruccio, A., and Ranieri, V. (2016). "Evaluating skidding risk of a road layout for all types of vehicles." *Transportation Research Record*, SAGE Publications Sage CA: Los Angeles, CA, 2591, 94–102.

Dell'Acqua, G., Russo, F., and Mauro, R. (2013). "Validation procedure for predictive functions of driver behaviour on two-lane rural roads." *European Transport - Trasporti Europei*, (53), 1–13.

Dhahir, B., and Hassan, Y. (2019a). "Using horizontal curve speed reduction extracted from the naturalistic driving study to predict curve collision frequency." *Accident Analysis and Prevention*, Elsevier Ltd, 123(Feb), 190–199.

Dhahir, B., and Hassan, Y. (2019b). "Modeling Speed and Comfort Threshold on Horizontal Curves of Rural Two-Lane Highways Using Naturalistic Driving Data." *Journal of Transportation Engineering, Part A: Systems*, 145(6), 04019025.

Donnell, E., Ni, Y., Adolini, M., and Elefteriadou, L. (2001). "Speed Prediction Models for Trucks on Two-Lane Rural Highways." *Transportation Research Record*, Transportation Research Board, Washington, D.C., 1751, 44–55.

Donnell, E., Wood, J., Himes, S., and Torbic, D. (2016). "Use of side friction in horizontal curve design: A margin of safety assessment." *Transportation Research Record*, 2588, 172–180.

Easa, S. M., and He, W. (2006). "Modeling Driver Visual Demand on Three-Dimensional Highway Alignments." *Journal of Transportation Engineering*, 132(5), 357–365.

Eluru, N., Chakour, V., Chamberlain, M., and Miranda-Moreno, L. F. (2013). "Modeling vehicle operating speed on urban roads in Montreal: A panel mixed ordered probit fractional split model." *Accident Analysis and Prevention*, Elsevier Ltd, 59, 125–134.

Esposito, T., Mauro, R., Russo, F., and Dell'Acqua, G. (2011). "Speed prediction models for sustainable road safety management." *Procedia - Social and Behavioral Sciences*, 20, 568–576.

Fink L, K., Krammes A, R., Fink, K. L., and Krammes, R. A. (1995). "Tangent length and sight distance effects on accident rates at horizontal curves on rural two-lane highways." *Transportation Research Record*, Transportation Research Board, Washington, D.C., 1500, 162–168.

Fitzpatrick, K. (2000). *Evaluation of design consistency methods for two-lane rural highways, executive summary*. (No. FHWA-RD-99-173). United States. Federal Highway Administration., Mclean, Va.

Fitzpatrick, K., Carlson, P., Brewer, M., and Wooldridge, M. D. (2003). "Design speed, operating speed, and posted speed limit practices." *82nd Annual Meeting of the Transportation Research Board*, Washington, DC, 1–20.

Fitzpatrick, K., Carlson, P. J., Wooldridge, M. D., and Brewer, M. A. (2000a). *Design factors that affect driver speed on suburban arterials*. (No. FHWA/TX-00/1769-3). Texas Transportation Institute, Austin, Texas.

Fitzpatrick, K., Elefteriadou, L., Harwood, D. W., Collins, J. M., McFadden, J., Anderson, I. B., Krammes, R. A., Nelson, I., Parma, K. D., Bauer, K. M., and Passetti, K. (2000b). *Speed Prediction for Two-Lane Rural Highways*. (No. FHWA-RD-99-171). United States. Federal Highway Administration, Mclean, Va.

Fitzpatrick, K., Krammes, R. A., and Fambro, D. B. (1997). "Design speed, operating speed and posted speed relationships." *ITE Journal (Institute of Transportation Engineers)*, 67(2), 52–59.

Fitzpatrick, K., Miaou, S.-P., Brewer, M., Carlson, P., and Wooldridge, M. D. (2005). "Exploration of the Relationships between Operating Speed and Roadway Features on Tangent Sections."

Journal of Transportation Engineering, 131(4), 261–269.

Fitzpatrick, K., Parham, A. H., and Brewer, M. A. (2002). *Treatments for Two-Lane Highways in Texas*. (No. FHWA/TX-02/4048-2). Texas Transportation Institute, College Station, Texas.

Fitzpatrick, K., Wooldridge, M. D., Tsimhoni, O., Collins, J. M., Green, P., Bauer, K. M., Parma, K. D., Koppa, R., Harwood, D. W., Anderson, I. B., Krammes A, R., and Poggioli, B. (2000c). *Alternative design consistency rating methods for two-lane rural highways*. (No. FHWA-RD-99-172) Federal Highway Administration, Mclean, Va.

Frost, J. (2019). *Regression analysis: An intuitive guide for using and interpreting linear models*. Statisics By Jim Publishing.

Furedy, J. J., Heslegrave, R. J., and Scher, H. (1992). "T-wave amplitude utility revisited: some physiological and psychophysiological considerations." *Biological Psychology*, 33(2–3), 241–248.

Garach, L., Calvo, F., Pasadas, M., and Oña, J. De. (2014). "Proposal of a New Global Model of Consistency : Application in Two-Lane Rural Highways in Spain." *Journal of Transportation Engineering*, 140(8), 04014030.

Garach, L., de Oña, J., López, G., and Baena, L. (2016). "Development of safety performance functions for Spanish two-lane rural highways on flat terrain." *Accident Analysis and Prevention*, Elsevier Ltd, 95, 250–265.

García, A. G., Llopis-Castello, D., Camacho-Torregrosa, F. J., and Perez-Zuriaga, A. M. (2013). "New consistency index based on inertial operating speed." *Transportation research record*, Transportation Research Board, Washington, D.C., 2391, 105–112.

Ghosh, P. (2018). *Numerical, Symbolic And Statistical Computing For Chemical Engineers Using Matlab*. PHI Learning Pvt. Ltd.

Gibreel, G. M., Easa, S. M., and El-Dimeery, I. A. (2001). "Prediction of Operating Speed on Three-Dimensional Highway Alignments." *Journal of Transportation Engineering*, 127(1), 21–30.

Gibreel, G. M., Easa, S. M., Hassan, Y., and El-Dimeery, I. A. (1999). "State of the art of highway geometric design consistency." *Journal of Transportation Engineering*, 125(4), 305–313.

Gong, H. (2007). "Operating Speed Prediction Models Four-Lane Non-Freeway Highways." (Doctoral dissertation, University of Kentucky, Lexington).

Gong, H., and Stamatiadis, N. (2008). "Operating speed prediction models for horizontal curves on rural four-lane highways." *Transportation Research Record*, Transportation Research Board, Washington, D.C., 2075, 1–7.

Greer, M. (2012). *Electricity marginal cost pricing: applications in eliciting demand responses*. Elsevier.

Harwood, D. W. (2003). *Review of Truck Characteristics as Factors in Roadway Design*. Transportation Research Board, Washington, D.C., (NCHRP505).

Hasan, M., Sayed, T., and Hassan, Y. (2005). "Influence of vertical alignment on horizontal curve perception: effect of spirals and position of vertical curve." *Canadian Journal of Civil Engineering*, 32(1), 204–212.

Hassan, Y. (2004). "Highway design consistency: Refining the state of knowledge and practice." *Transportation Research Record*, Transportation Research Board, Washington, D.C., 1881, 63–71.

Hassan, Y., and Easa, S. M. (2003). "Effect of Vertical Alignment on Driver Perception of Horizontal Curves." *Journal of Transportation Engineering*, 129(4), 399–407.

Hassan, Y., Easa, S. M., and Halim, A. O. A. El. (1997). "Design Considerations For Combined Highway Alignments." *Journal of Transportation Engineering*, 123(1), 60–68.

Hassan, Y., Gibreel, G., and Easa, S. M. (2000). "Evaluation of Highway Consistency and Safety: Practical Application." *Journal of Transportation Engineering*, 126(3), 193–201.

Hassan, Y., and Sarhan, M. (2011). "Modeling Operating Speed." *Transportation Research Circular*, Federal Highway Administration, Transportation Research Board, Washington, DC.

Hassan, Y., Sayed, T., and Bidulka, S. (2002). "Influence of Vertical Alignment on Horizontal Curve Perception: Phase II: Modeling Perceived Radius." *Transportation Research Record*, Transportation Research Board, Washington, D.C., 1796, 24–34.

Hassan, Y., Sayed, T., and Tabernero, V. (2001). "Establishing practical approach for design consistency evaluation." *Journal of Transportation Engineering*, 127(4), 295–302.

HCM. (2000). "Highway capacity manual." Transportation Research Board, National Research Council, Washington, DC.

Heger, R. (1995). "Driving Behavior and Driver Mental Workload As Criteria of Highway Geometric Design Quality." *International Symposium on Highway Geometric Design Practices*, Boston, 1918–1933.

Hirsh, M. (1987). "Probabilistic approach to consistency in geometric design." *Journal of Transportation Engineering*, 113(3), 268–276.

Hou, Y., Sun, C., and Edara, P. (2012). "Statistical test for 85th and 15th percentile speeds with asymptotic distribution of sample quantiles." *Transportation Research Record*, Transportation Research Board, Washington, D.C., 2279, 47–53.

IRC 52. (2001). "Recommendations about the Alignment Survey and Geometric design of Hill Roads (Second Rev.)." The Indian Roads Congress, New Delhi: IRC.

IRC SP 48. (1998). "Hill road manual." The Indian Roads Congress, New Delhi: IRC.

IRC SP 73. (2015). "Manual of specifications & standards for two laning of highways with paved shoulder." The Indian Roads Congress, New Delhi: IRC.

Islam, M. N., and Seneviratne, P. N. (1994). "Evaluation of design consistency of two-lane highways." *Institute of Transportation Engineers*, Institute of Transportation Engineers, 64(2), 28–31.

Jacob, A., and Anjaneyulu, M. V. L. R. (2013). "Operating Speed of Different Classes of Vehicles at Horizontal Curves on Two-Lane Rural Highways." *Journal of Transportation Engineering*, 139(3), 287–294.

Jacob, A., and Anjaneyulu, M. V. L. R. (2015). "Geometric Design Consistency and Safety Evaluation of Combined Curves on Two-Lane Rural Highways." *3rd Conference of Transportation Researchers Group of India (CTRG-2015)*, Kolkata, India.

Joshi, A. K., Joshi, C., Singh, M., and Singh, V. (2014). "Road traffic accidents in hilly regions of northern India: What has to be done?" *World Journal of Emergency Medicine*, 5(2), 112.

Kowler, E. (2011). "Eye movements: The past 25 years." *Vision Research*, Elsevier B.V., 51(13), 1457–1483.

Krammes, R. A., Brakett, R. Q., Shaffer, M. A., Ottesen, J. L., Anderson, I. B., Fink, K. L., Collins, K. M., Pendleton, O. J., and Messer, C. J. (1995). *Horizontal alignment design consistency for rural two-lane highways*. (FHWA-RD-94-034). United States. Federal Highway Administration, Mclean, Va.

Lamm, R., Beck, A., Ruscher, T., Mailaender, T., Cafiso, S., and Lacava, G. (2007). *How to make Two-Lane Rural Roads Safer*. WIT, Southampton, UK.

Lamm, R., and Choueiri, E. M. (1987). "Recommendations for Evaluating Horizontal Design Consistency Based on Investigations in the State of New York." *Transport Research Record*, Transportation Research Board, Washington, D.C., 1122, 69–78.

Lamm, R., Choueiri, E. M., Hayward, J. C., and Paluri, A. (1988). "Possible design procedure to promote design consistency in highway geometric design on two-lane rural roads." *Transportation Research Record*, Transportation Research Board, Washington, D.C., 1195, 111–122.

Lamm, R., Guenther, A. K., and Choueiri, E. M. (1995). "Safety module for highway geometric design." *Transportation Research Record*, Transportation Research Board, Washington, D.C., 1512, 7–15.

Lamm, R., Hayward, J. C., and Cargin, J. G. (1986). "Comparison of Different Procedures for Evaluating Speed Consistency." *Transportation Research Record*, Transportation Research Board, Washington, D.C., 1100, 10–20.

Lamm, R., Psarianos, B., and Mailaender, T. (1999). *Highway design and traffic safety engineering handbook*. McGraw-Hill, 1999, New York.

Leisch, J. E. (1977). "Dynamics of highway design for safety." *Transportation*, 6(1), 71–83.

Leisch, J. E., and Leisch, J. P. (1977). "New concept in design speed applications, as a control in achieving consistent highway design." *Transportation Research Record*, Transportation Research Board, Washington, D.C., 631, 4–14.

Liu, J., Wang, X., and Yang, X. (2017). "Safety Evaluation of Combined Alignments of Freeway: a Driving Simulator Study." *Proc., 14th World Conf. on Transport Research (WCTR).*, Elsevier, Amsterdam, Netherlands.

Llopis-Castelló, D., Bella, F., Camacho-Torregrosa, F. J., and García, A. (2018a). "New Consistency Model Based on Inertial Operating Speed Profiles for Road Safety Evaluation." *Journal of Transportation Engineering, Part A: Systems*, 144(4), 04018006.

Llopis-Castelló, D., Camacho-Torregrosa, F. J., and García, A. (2018b). "Development of a global inertial consistency model to assess road safety on Spanish two-lane rural roads." *Accident Analysis and Prevention*, Elsevier Ltd, 119, 138–148.

Llopis-Castelló, D., Findley, D. J., Camacho-Torregrosa, F. J., and García, A. (2019). "Calibration of inertial consistency models on North Carolina two-lane rural roads." *Accident Analysis and Prevention*, Elsevier Ltd, 127, 236–245.

Llopis-Castelló, D., González-Hernández, B., Pérez-Zuriaga, A. M., and García, A. (2018c). "Speed Prediction Models for Trucks on Horizontal Curves of Two-Lane Rural Roads." *Transportation Research Record*, Transportation Research Board, Washington, D.C., 2672(17), 72–82.

Lobo, A. (2017). "Operating Speed Modeling in Two-Lane Highways." (Doctoral dissertation, Universidade do Porto, Portugal).

Maji, A., Sil, G., and Tyagi, A. (2018). "85th and 98th Percentile Speed Prediction Models of Car, Light, and Heavy Commercial Vehicles for Four-Lane Divided Rural Highways." *Journal of Transportation Engineering, Part A: Systems*, 144(5), 04018009.

Malaghan, V., and Pawar, D. S. (2020). "Operating Speed Differential Model for Heavy Vehicles using GPS Driving Data." *Transportation Research Procedia*, Elsevier B.V., 48(2019), 3706–3716.

Malaghan, V., Pawar, D. S., and Dia, H. (2020a). "Modeling Operating Speed Using Continuous

Speed Profiles on Two-Lane Rural Highways in India." *Journal of Transportation Engineering, Part A: Systems*, 146(11), 04020124.

Malaghan, V., Pawar, D. S., and Dia, H. (2020b). "Speed prediction models for heavy passenger vehicles on rural highways based on an instrumented vehicle study." *Transportation Letters*, Taylor & Francis, 1–10.

Malaghan, V., Pawar, D. S., and Dia, H. (2021). "Exploring Maximum and Minimum Operating Speed Positions on Road Geometric Elements Using Continuous Speed Data." *Journal of Transportation Engineering, Part A: Systems*, 147(8), 04021039.

Mcfadden, J., and Elefteriadou, L. (2000). "Evaluating horizontal alignment design consistency of two-lane rural highways: Development of new procedure." *Transportation Research Record*, Transportation Research Board, Washington, D.C., 1737, 9–17.

McFadden, J., and Elefteriadou, L. (1997). "Formulation and Validation of Operating Speed-Based Design Consistency Models by Bootstrapping." *Transportation Research Record*, Transportation Research Board, Washington, D.C., 1579, 97–103.

Messer, C. J. (1980). "Methodology for Evaluating Geometric Design." *Transportation Research Record*, Transportation Research Board, Washington, D.C., (757), 7–14.

Milton, J. C., Shankar, V. N., and Mannering, F. L. (2008). "Highway accident severities and the mixed logit model: An exploratory empirical analysis." *Accident Analysis and Prevention*, Elsevier Ltd, 40(1), 260–266.

Misaghi, P., and Hassan, Y. (2005). "Modeling Operating Speed and Speed Differential on Two-Lane Rural Roads." *Journal of Transportation Engineering*, 131(6), 408–418.

Montella, A., Colantuoni, L., and Lamberti, R. (2008). "Crash Prediction Models for Rural Motorways." *Transportation Research Record*, Transportation Research Board, Washington, D.C., 2083, 180–189.

Montella, A., and Imbriani, L. L. (2015). "Safety performance functions incorporating design consistency variables." *Accident Analysis and Prevention*, Elsevier, 74, 133–144.

Montella, A., Pariota, L., Galante, F., Imbriani, L., and Mauriello, F. (2014). "Prediction of Drivers' Speed Behavior on Rural Motorways Based on an Instrumented Vehicle Study." *Transportation Research Record*, Transportation Research Board, Washington, D.C., 2434, 52–62.

Morris, C. M., and Donnell, E. T. (2014). "Passenger car and truck operating speed models on multilane highways with combinations of horizontal curves and steep grades." *Journal of Transportation Engineering*, 140(11), 04014058:1–10.

MoRTH. (2019a). *Basic Road Statistics of India*. Ministry of Road Transport and Highways, New Delhi.

MoRTH. (2019b). *Road Accidents in India*. Ministry of Road Transport and Highways, New Delhi.

Nama, S., Maurya, A. K., Maji, A., Edara, P., and Sahu, P. K. (2016). "Vehicle Speed Characteristics and Alignment Design Consistency for Mountainous Roads." *Transportation in Developing Economies*, Springer International Publishing, 2(2), 23.

Ng, J. C. ., and Sayed, T. (2004). "Effect of geometric design consistency on road safety." *Canadian Journal of Civil Engineering*, 31(2), 218–227.

Piyatrapoomi, N., Weligamage, J., Arun, K., and Jonathan, B. (2008). "Identifying relationship between skid resistance and road crashes using probability-based approach." *Proceedings of the 2nd International Safer Roads Conference*, Safe Roads Organisation, United Kingdom, 1–12.

Poe, C. M., and Mason, J. (2000). "Analyzing influence of geometric design on operating speeds

along low-speed urban streets mixed-model approach." *Transportation Research Record*, Transportation Research Board, Washington, D.C., 1737, 18–25.

Polus, A., Fitzpatrick, K., and Fambro, D. B. (2000). "Predicting Operating Speeds on Tangent Sections of Two-Lane Rural Highways." *Transportation Research Record*, Transportation Research Board, Washington, D.C., 1737, 50–57.

Polus, A., and Mattar-Habib, C. (2004). "New Consistency Model for Rural Highways and Its Relationship to Safety." *Journal of Transportation Engineering*, 130(3), 286–293.

Qu, X., Wang, S., and Zhang, J. (2015). "On the fundamental diagram for freeway traffic: A novel calibration approach for single-regime models." *Transportation Research Part B: Methodological*, Elsevier Ltd, 73, 91–102.

Richl, L., and Sayed, T. (2005). "Effect of speed prediction models and perceived radius on design consistency." *Canadian Journal of Civil Engineering*, 32(2), 388–399.

Rosey, F., and Auberlet, J. M. (2012). "Trajectory variability: Road geometry difficulty indicator." *Safety Science*, Elsevier Ltd, 50(9), 1818–1828.

Russo, F., Biancardo, S. A., and Busiello, M. (2016). "Operating speed as a key factor in studying the driver behaviour in a rural context." *Transport*, Taylor & Francis, 31(2), 260–270.

Said, D., Hassan, Y., and Abd El Halim, A. O. (2006). "Methodology for analysing vehicle trajectory and relation to geometric design of highways." *Advances in Transportation Studies*, (10), 55–72.

Said, D., Hassan, Y., and Abd El Halim, A. O. (2007). "Quantification and Utilization of Driver Path in Improving the Design of Highway Horizontal Curves." *Presented at the 86th Annual Meeting of the Transportation Research Board*, Washington, D.C.

Schmidt, G. (1995). "Analyses and Evaluation of Roadway Sections with Respect to Three Safety Criteria." (Doctoral dissertation, Master Thesis, Institute for Highway and Railroad Engineering, University of Karlsruhe (TH), Germany).

Schneider, B. (1999). "Development of a Superior Safety Module for the Evaluation of the Danger of Two-Lane Rural Roads in Tune with the Actual Accident Situation." (Doctoral dissertation, Master Thesis, Institute for Highway and Railroad Engineering, University of Karlsruhe (TH), Germany).

Schurr, K., Spargo, B., Huff, R., and Pesti, G. (2005). "Predicted 95th Percentile Speeds on Curved Alignments Approaching a Stop." *Transportation Research Record*, Transportation Research Board, Washington, D.C., 1912, 1–10.

Shankar, A. R., Anjaneyulu, M., and Sowmya, N. (2013). "Consistency evaluation of horizontal curves on rural highways." *Journal of The Indian Roads Congress*, 73(4), 91–99.

Smith, B. L., and Lamm, R. (1994). "Coordination of horizontal and vertical alignment with regard to highway esthetics." *Transportation Research Record*, Transportation Research Board, Washington, D.C., 1445, 73–85.

Taylor, J. I., and Thompson, H. T. (1977). *Identification of hazardous location by kernel density*. (No. FHWA-RD-77-83) Federal Highway Administration, Washington, DC.

Thiessen, A., El-Basyouny, K., and Gargoum, S. (2017). "Operating Speed Models for Tangent Segments on Urban Roads." *Transportation Research Record*, 2618(1), 91–99.

TRB Operational Effects of Geometrics Committee and others. (2011). *Modeling Operating Speed: Synthesis Report*. *TRB E-Circular 151*, Washington DC, USA.

W.H.O. (2018). *Global status report on road safety 2018*. (WHO/NMH/NVI/1820) Licence: CC BY-NC-SA 30 IGO, World Health Organization, Geneva, Switzerland.

Wang, X., and Wang, X. (2018). "Speed change behavior on combined horizontal and vertical curves: driving simulator-based analysis." *Accident Analysis and Prevention*, Elsevier Ltd, 119, 215–224.

Wang, X., Yu, R., and Wang, X. (2014). "A speed study of mountainous freeway combined alignment." *Proceedings of the 14th COTA International Conference of Transportation Professionals*, American Society of Civil Engineers, Changsha, China, 2257–2265.

Wilches, F. J., Burbano, J. L. A., and Sierra, E. E. C. (2020). "Vehicle operating speeds in southwestern Colombia: An important database for the future implementation of optimization models for geometric design of roads in mountain topography." *Data in Brief*, Elsevier Ltd, 32, 106210.

Wooldridge, M. D., Fitzpatrick, K., Harwood, D. W., Potts, I. B., Elefteriadou, L., and Torbic, J. D. (2003). *Geometric design consistency on high-speed rural two-lane roadways, Rep. 502*. National Corporative Highway Research Program, Transport Research Board, Washington, D.C.

Wooldridge, M. D., Fitzpatrick, K., Koppa, R., and Bauer, K. (2000). "Effects of horizontal curvature on driver visual demand." *Transportation Research Record*, Transportation Research Board, Washington, D.C., (1737), 71–77.

Wu, K.-F., Donnell, E. T., Himes, S. C., and Sasidharan, L. (2013a). "Exploring the Association between Traffic Safety and Geometric Design Consistency Based on Vehicle Speed Metrics." *Journal of Transportation Engineering*, 139(7), 738–748.

Wu, X., Wang, X., Lin, H., District, J., He, Y., Advanced, N., Simulator, D., City, I., and Yang, L. (2013b). "Evaluating Alignment Consistency for Mountainous Expressway in Design Stage : A Driving Simulator-Based Approach." *Proceedings of the 92nd Annual Meeting of the Transportation Research Board*, Washington, D.C., 1–20.

Xu, J., Lin, W., and Shao, Y. (2017). "New design method for horizontal alignment of complex mountain highways based on 'trajectory-speed' collaborative decision." *Advances in Mechanical Engineering*, 9(4), 1–18.

Xu, J., Luo, X., and Shao, Y. M. (2018). "Vehicle trajectory at curved sections of two-lane mountain roads: a field study under natural driving conditions." *European Transport Research Review*, Springer, 10(1), 1–16.

Yan, Y., Li, G., Tang, J., and Guo, Z. (2017). "A Novel Approach for Operating Speed Continuous Predication Based on Alignment Space Comprehensive Index." *Journal of Advanced Transportation*, 2017, 1–14.

Zilioniene, D., and Vorobjovas, V. (2011). "Correspondence of horizontal and vertical alignment with safe driving conditions on low-volume roads." *Transportation Research Record*, Transportation Research Board, Washington, D.C., 2203, 49–56.

Zumkeller, K. (1998). "Analysis and Evaluation of Possible Relationships between Traffic Safety, Road Design and Road Equipment with Road Markings, Traffic Control Devices and Guardrails." (Doctoral dissertation, Master Thesis, Institute for Highway and Railroad Engineering, University of Karlsruhe (TH), Germany).

Zuriaga, A. M. P., García, A. G., Torregrosa, F. J. C., and D'Attoma, P. (2010). "Modeling operating speed and deceleration on two-lane rural roads with global positioning system data." *Transportation Research Record*, Transportation Research Board, Washington, D.C., 2171, 11–20.

Papers and Conferences

Journals

- Shallam, R. D. K., Venthuruthiyil, S. P., Chunchu, M., & Siddagangaiah, A. K. (2019). Empirical Analysis of Operating Speed Performance on Undivided Hilly Roads. *Journal of Transportation Engineering, Part A: Systems, 145*(8), 04019034.

- Shallam, R. D. K., Venthuruthiyil, S. P., Chunchu, M., Siddagangaiah, A. K. (2021). Operating Speed Modeling for The Rural Highways Passing Through Hilly Terrain, *Journal of Transportation Engineering, Part A: Systems, 147*(5), 04021015

- Balusu, S. P. K., Iraganaboina, N. C., Shallam, R. D. K., & Chunchu, M. (2017). Speed-profile-based road segmentation for accident occurrence modelling for hilly terrains. *International journal of injury control and safety promotion, 24*(4), 444-451.

- Shallam, R. D. K., Chunchu, M., Siddagangaiah, A. K. Assessment of the Safety and Consistency of a Two-Lane Rural Highway passing through Hilly Terrain. (To be submitted)

Conferences

- Shallam R. D. K., Venthuruthiyil, S. P., Chunchu, M., & Siddagangaiah, A. K. (2018). Impact of the Direction of the Horizontal Curves on the Operating Speed Performance of the Vehicles on Hilly Terrain. *International Symposium of Transport Simulation (ISTS'18) and the International Workshop on Traffic Data Collection and its Standardization (IWTDCS'18)*, Ehime, Japan.

- Shallam, R. D. K., Chunchu, M., & Siddagangaiah, A. K. (2017). Applicability of the existing speed-models for the Indian highways passing through hilly terrain. *National Conference on Civil, Geo-tech & Transport Research*, NERIST, Arunachal Pradesh